Combined In Vitro and In Silico Investigation into the Interplay between Ceramides and the Skin Barrier Function

Dissertation

der Mathematisch-Naturwissenschaftlichen Fakultät

der Eberhard Karls Universität Tübingen

zur Erlangung des Grades eines

Doktors der Naturwissenschaften

(Dr. rer. nat.)

vorgelegt von

Moritz Reuter

aus Fürth

Tübingen

2025

Gedruckt mit Genehmigung der Mathematisch-Naturwissenschaftlichen Fakultät der Eberhard Karls Universität Tübingen.

Tag der mündlichen Qualifikation:	28.11.2025
Dekan:	Prof. Dr. Thilo Stehle
1. Berichterstatter/-in:	Prof. Dr. Dominique Lunter
2. Berichterstatter/-in:	Prof. Dr. Rolf Daniels

Danksagung

Ohne die vielen Menschen, welchen ich hier danken möchte, wäre diese Arbeit nicht möglich gewesen.

Meinen vollen, herzlichen Dank möchte ich meiner Betreuerin Professor Dominique Lunter aussprechen. Ich glaube nicht, dass ich für meine Arbeit eine bessere Betreuung hätte haben können, als die, die ich von ihr bekommen habe. Wo immer ich es brauchte, bekam ich von ihr die richtige Anleitung und ansonsten die vollkommene Freiheit in meiner Arbeit. Ich hatte das Privileg, von ihr nicht nur die Möglichkeit für eine Promotion zu erhalten, sondern das Forschungsthema auch wirklich zu meiner Promotion zu machen. Ich habe mich immer gut aufgehoben gefühlt, und ich danke ihr für all die Möglichkeiten, das Vertrauen und den Respekt, welche ich von ihr in meiner Promotionszeit erfahren habe. Ich freue mich auf die zukünftige Zusammenarbeit!

Ein großes Danke auch an Professor Rolf Daniels für die Begutachtung der Arbeit, die hilfreichen Anmerkungen in den Seminaren, und dafür, dass Sie damals meine Email herausgefischt und weitergeleitet haben. Ansonsten wäre das alles nicht möglich gewesen!

A very special thanks to Professor Guoping Lian of the University of Surrey, who gave me the opportunity to visit his lab, the UoS and the United Kingdom to learn about molecular dynamics simulations of the skin lipids. I am immensely grateful for his guidance, my stay and the memories I was able to make there! Without his cooperation, this work would not have been possible.

Einen besonderen Dank möchte ich an alle meine ehemaligen und aktuellen Kollegen (aber eigentlich doch Freunde) bei uns am Lehrstuhl richten. Ich glaube nicht, dass ich meine Zeit auf der Arbeit als so erfüllend und aufbauend erlebt hätte, wenn sie nicht dabei gewesen wären. Ich bin so dankbar dafür, wie herzlich ich am Anfang aufgenommen wurde, und ohne sie würde sich der Lehrstuhl nicht wie das Zuhause anfühlen, das er ja doch irgendwie geworden ist.

Vielen Dank an Klaus, Irina, Boguslawa, Ingrid und Tanja, die den Lehrstuhl zusammenhalten und die Arbeit bei uns ja überhaupt erst möglich machen. Einen besonderen Dank auch noch einmal an Klaus, den Atlas, auf dem doch die gesamte technische Welt der Pharmazeutischen Technologie Tübingen ruht.

A big thank you to Edwin, Jia, Alice, Yuanjing and Caitlin for warmly welcoming me during my stay in Guildford and making me feel a little bit more at home abroad. Thank you so much and I wish you all the best!

Meinen Eltern möchte ich für alles danken, was sie über die Jahre hinweg für mich getan haben: Für all ihre Unterstützung, sei sie emotional oder finanziell, und für ihr Vertrauen in mich.

Meinen letzten Dank möchte ich mir für Esther, meine Frau, aufbewahren: Ohne deine lieben Worte, deine ständigen Ermutigungen, deine Wertschätzung und deine Unterstützung, kurz gesagt, ohne dich, würde es nicht nur diese Arbeit nicht geben, sondern auch nicht mich, wie ich bin. Ich danke dir für den Weg, den wir zusammen gegangen sind, und den Weg, den wir in Zukunft noch gemeinsam nehmen werden. Und für alles.

„Ich will immer mehr lernen, das Notwendige an den Dingen als das Schöne zu sehen – so werde ich einer von denen sein, welche die Dinge schön machen.“

Friedrich Nietzsche

Table of Contents

Abbreviations

%	Percent
Å	Ångström
ACF	Autocorrelation function
AD	Atopic dermatitis
APL	Area per lipid
C20	PEG-20 cetyl ether
C8	Octyl-linked silica (column)
CER	Ceramides
COM	Center of mass
cm	Centimeter
D	Diffusion coefficient
EO	Esterified ω-hydroxyacyl (ceramides)
FA	Fatty acid
FFA	Free fatty acids
G	Gibbs Free Energy
HLB	Hydrophilic-lipophilic balance
HPMC	Hydroxypropyl methylcellulose
HPTLC	High-performance thin layer chromatography
IL-4	Interleukin-4
IL-6	Interleukin-6
IS	Internal standard
K	Degrees Kelvin
LC-MS	Liquid chromatography–mass spectrometry
LCB	Long-chained base
LOO	Leave-one-out (cross-validation)
LOQ	Limit of quantification
LPP	Long periodicity phase
MD	Molecular dynamics

µl	Microliter
MRM	Multiple reaction monitoring
MS/MS	Tandem mass spectrometry
MS^n	n-stage tandem mass spectrometry
NPT	Isothermal-isobaric ensemble (Number of atoms, pressure and temperature constant)
NVT	Canonical ensemble (Number of atoms, volume and temperature constant)
ns	Nanosecond
nm	Nanometer
PEG	Polyethylene Glycol
PLS	Partial least squares
PMcF	Potential of mean constraint force
Q^2	Predictive ability (cross-validated R^2)
R^2	Coefficient of determination
RC	Reaction coordinate
S_z	Lipid order parameter
s	Second
S100	PEG-100 stearyl ether
S2	PEG-2 stearyl ether
S20	PEG-20 stearyl ether
SC	Stratum corneum
SEM	Standard error of the mean
SLS	Sodium lauryl sulfate
SPP	Short periodicity phase
TEWL	Transepidermal Water Loss
TLC	Thin layer chromatography
TNF-α	Tumor necrosis factor alpha
UHPLC-MS	Ultra-high-performance liquid chromatography–mass spectrometry
UV	Ultraviolet (radiation)

Zusammenfassung

Die Erforschung der Barrierefunktion des menschlichen Stratum Corneums (SC) ist von hoher Relevanz für die Entwicklung topischer Arzneimittel sowie Kosmetika. In diesem Bereich der Forschung wurde sich in den letzten Jahren vermehrt auf die Ceramide als Bestandteile der interzellulären Lipidmatrix des SC fokussiert, da die Rolle dieser vielfältigen Lipidfamilie für die Aufrechterhaltung der Hautbarriere bisher nur unvollständig bekannt ist. Diese Arbeit nähert sich dieser Thematik auf zwei Wegen: Zum einen wurde im Rahmen dieses Projektes die Wechselwirkung von pharmazeutisch verwendeten Emulgatoren auf die Ceramide des menschlichen SC in einer Humanstudie untersucht, welche durch Massenspektrometrie-gekoppelte Flüssigchromatographie (LC-MS) im Detail analysiert wurden. Die erfolgte Detailanalyse der Ceramide wurde als Basis einer Regressionsanalyse verwendet, welche in der Lage war, einzelne Ceramidklassen, Kettenlängen sowie individuelle Ceramide mit ihren jeweils spezifischen Effekten auf die Hautbarriere zu assoziieren. Die Analyse ergab, dass einige Ceramidklassen mit einer geschädigten Hautbarriere assoziiert sind, was insbesondere für Sphingosin-basierte Ceramide galt. Umgekehrt waren einige Ceramidklassen mit einer intakten Hautbarriere assoziiert, was wiederum insbesondere für Phytosphingosin-basierte Ceramidklassen der Fall war. Im zweiten Teil der Arbeit wurde versucht, die gefundenen Zusammenhänge zwischen Ceramidklasse und Hautpermeabilität in Molekulardynamik-Simulationen (MD-Simulationen) zu replizieren und genauer zu untersuchen. In dieser Studie wurden SC-Lipidmembranen simuliert, welche jeweils eine Sphingosin-basierte Ceramidklasse sowie eine Phytosphingosin-basierte Ceramidklasse enthielten, und ihre Wasserpermeabilität sowie Struktur analysiert. Die Ergebnisse der Permeabilitätsmessungen deckten sich mit den Ergebnissen der Humanstudie und zeigten einen signifikanten Unterschied in der Wasserdurchlässigkeit der Membranen. Diese Permeabilitätsunterschiede konnten mit Unterschieden in der Membranstruktur in Verbindung gebracht werden, welche insbesondere die Geometrie der Ceramidkopfgruppen als auch die Wasserstoffbrückenbindungen der Membranen betreffen.

Summary

Research into the barrier function of the human stratum corneum (SC) is of high relevance for the development of topical drugs and cosmetics. In recent years, research in this area has increasingly focused on ceramides as vital components of the intercellular lipid matrix of the SC, as the role of this diverse lipid family in maintaining the skin barrier function is still not fully understood. This work approaches the topic in two ways: In the first part of this project, the interaction of pharmaceutically used emulsifiers on the ceramides of the human SC was investigated in a human study, the effects of which were analyzed in detail using liquid chromatography coupled with mass spectrometry (LC-MS). This detailed analysis of the ceramides in the SC was then used as the basis for a regression analysis, which was able to associate individual ceramide classes, chain lengths, and individual ceramides with specific effects on the skin barrier. The analysis revealed that some ceramide classes, in particular sphingosine-based ceramides, are associated with a damaged skin barrier. Conversely, some ceramide classes, in particular phytosphingosine-based ceramide classes, were associated with an intact skin barrier. In the second part of the project, the established correlations between ceramide class and skin permeability were investigated using molecular dynamics simulations (MD simulations). In this study, SC lipid membranes containing a sphingosine-based ceramide class and a phytosphingosine-based ceramide class were simulated, and their water permeability and structure were analyzed. The results of the permeability measurements were consistent with the results of the human study and showed a significant difference in the water permeability of the membranes. These permeability differences could be linked to differences in membrane structure, particularly affecting the geometry of the ceramide head groups and the hydrogen bonds of the membranes.

Publications and Contributions

1. Reuter, M.; Schoenfelder, H.; Gaiser, A.; Volc, S.; Lunter, D. Emulsifier-induced changes to the human skin barrier – Connection to ceramide profiles and assessment as a skin lesion model. Skin Pharmacology and Physiology 2025.
DOI: 10.1159/000545234.

Contributions:
M.R.: LC-MS method development and validation, LC-MS sample preparation and measurements, statistical analysis, data curation, and writing – original draft. H.S.: study organization, sample administration, skin health measurements, data curation, and writing – review and editing. A.G.: tape stripping and data curation, and writing – review and editing. S.V.: study supervision and writing – review and editing. D.L.: conceptualization, methodology, study organization and supervision, resources, and writing – review and editing.

2. Reuter, M.; Joseph, E.; Lian, G.; Lunter, D. J. Presence of Different Ceramide Species Modulates Barrier Function and Structure of Stratum Corneum Lipid Membranes: Insights from Molecular Dynamics Simulations. Molecular Pharmaceutics 2025. DOI: 10.1021/acs.molpharmaceut.5c00580.

Contributions:
M.R.: MD simulations setup and analysis, data curation, statistical analysis, and writing – original draft. E.J.: MD simulations analysis and writing – review and editing. G.L.: Conceptualization, methodology, resources, and writing – review and editing. D.L.: Conceptualization, methodology, resources, and writing – review and editing.

Acknowledgements for Support

The author acknowledges support by the High Performance and Cloud Computing Group at the Zentrum für Datenverarbeitung of the University of Tübingen, the state of Baden-Württemberg through bwHPC and the German Research Foundation (DFG) through grant no INST 37/1159-1 FUGG.

The research stay at the University of Surrey was kindly supported by the Boehringer Ingelheim Fonds (BIF) with a travel grant.

1 Introduction

1.1 The Human Skin and the Stratum Corneum

The human skin is, as for every vertebrate animal, the outermost protective organ of our body, serving not only as a physical and mechanical, but also as a chemical barrier shielding the organism from the environment [1, 2]. Importantly, our skin barrier works both ways: While protecting the body from being exposed to exogenous, potentially noxious chemicals and microorganisms, the skin is also crucial for regulating the organism's homeostasis and keeping it in equilibrium, as it serves as a barrier to the uncontrolled loss of water and heat from the body to the environment [2-5]. The anatomy of the skin reflects these important duties in its three-layered structure: Starting from the bottom, the hypodermis, or subcutaneous fat tissue, serves as the base for the rest of the skin layers sitting on top of it [6, 7]. While not being considered part of the so-called "true" skin, or cutis, the hypodermis nonetheless contains neurons detecting pressure and touch and serves as a thermal insulation for the body [6]. Moving closer to the skin surface, the subcutaneous tissue smoothly transitions to the dermis: The dermis, being the central layer of the skin located between the hypodermis and epidermis, consists of flexible, yet firm connective tissue of elastin and collagen fibers and is highly vascularized [6, 8]. This vascularization also enables this skin layer to house sebaceous glands as well as sweat glands and hair follicles, being able to sustain the metabolism of these structures. Interestingly, the vascularization of the dermis provides nutrients and oxygen not only to the dermis, but also to the epidermis on top of it: As an avascular tissue, the part of the epidermis containing living cells is dependent on the diffusion of nutrients and oxygen from the deeper skin layers [6, 8]. These bottom layers of the epidermis, which contain living cells undergoing mitosis and differentiating, are collectively called the viable epidermis, while the top layers, which are mostly composed of dead, cornified cells, are collectively called the stratum corneum (SC) [1-3]. Both parts of the epidermis are crucial for the tissue to sustain its main purpose to serve as the main barrier of the body against xenobiotics, microorganisms, UV radiation and water loss from within [9]: From the base of the viable epidermis, the stratum basale, keratinocytes differentiate themselves from the epidermal stem cells located there and rise towards the skin surface, all the while differentiating from the base keratinocytes to the fully differentiated, fully cornified corneocytes found in the

SC. From there, the corneocytes are then renewed in regular intervals, shedding the uppermost layers in a process called desquamation while continuously replenishing the deeper layers of the SC with newly differentiated corneocytes [1, 2, 9-11]. As such, the SC is in a permanent state of continuous renewal, while the underlying viable epidermis serves as the replenishment layer for it, ensuring the integrity of the skin's most vital barrier.

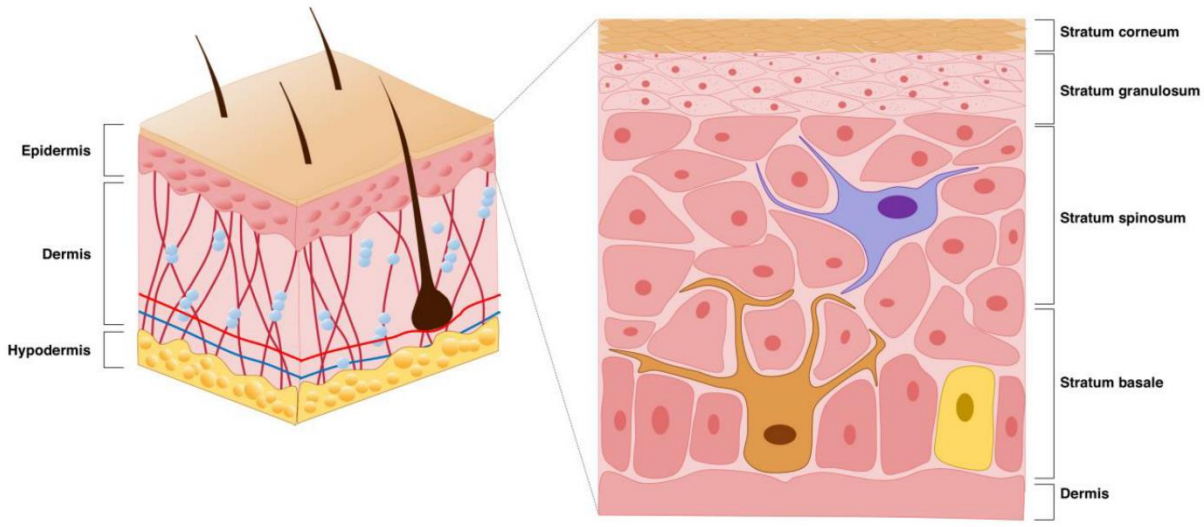

Figure 1: Schematic of the three main layers of the skin as well as the different layers of the epidermis, with the SC as the uppermost layer of the skin. Figure taken from Brito et al. [11].

1.2 The SC as a Permeability Barrier

The significance of the integrity of the SC for the barrier function of the skin can hardly be overstated, as it represents the main obstacle against uncontrolled ingress of xenobiotics and egress of water from the organism [1, 4, 8, 9, 12]. This is due to its extraordinary barrier properties, which in turn are a function of its specialized morphology: The SC is commonly referred to as exhibiting a so-called "brick-and-mortar" structure, being comprised of the keratin-filled corneocytes ("bricks"), which are embedded in a lamellar, continuous lipid matrix ("mortar") [1, 2]. The corneocytes and the lipid matrix act synergistically to form an especially effective diffusion barrier: The spatial arrangement of the solid corneocytes forms winding, so-called "tortuous" paths between them, blocking the straight diffusion path across the SC, and therefore forcing intercellular diffusing molecules to "take a detour" around the corneocytes, resulting in

a much longer diffusion distance needed to cross the SC [13-16]. The degree of tortuosity τ of the SC can be mathematically described as the ratio between the actual distance traveled by the diffusing molecule along the tortuous path to cross the SC and the theoretical shortest distance needed to cross the SC, which is simply the SC's thickness. The actual value for τ differs in physiological SC depending on the skin condition as well as the physicochemical properties of the permeant, with studies in the literature spanning a range of tortuosity values from around 1.6 to 12 [14, 17-19].

By diffusing around the corneocytes, permeating substances are forced to travel through the extracellular lipid matrix, which forms a continuous phase throughout the entire SC [4, 20-22]. The lipids in this matrix are arranged in a highly ordered fashion, forming repetitive lamellar structures which are described by their vertical repetition distance, the so-called short periodicity phase (SPP) and the long periodicity phase (LPP) [3, 12, 22-24]. From there, these periodic lamellar structures can be further categorized by the density of their lateral lipid packing, from the highly ordered, densest orthorhombic packing to the intermediate hexagonal and least ordered fluid packing orders [25, 26]. The high degree of order of these liquid crystalline domains is crucial to hinder and therefore slow the diffusion of traversing molecules, while also acting as a solubility barrier for hydrophilic molecules due to the lipophilic nature of these domains [22, 25, 27]. Combining the aforementioned tortuosity of the available intercellular diffusion pathways with the liquid crystalline intercellular lipid matrix results in an exceptionally low permeability for chemicals trying to cross the skin barrier in either direction [28-30]. Nonetheless, pathologies affecting the skin have the potential to cause disruptions of this important barrier, especially when interfering with the physiological balance of the SC lipids, which in turn may cause structural changes in the SC [31-37].

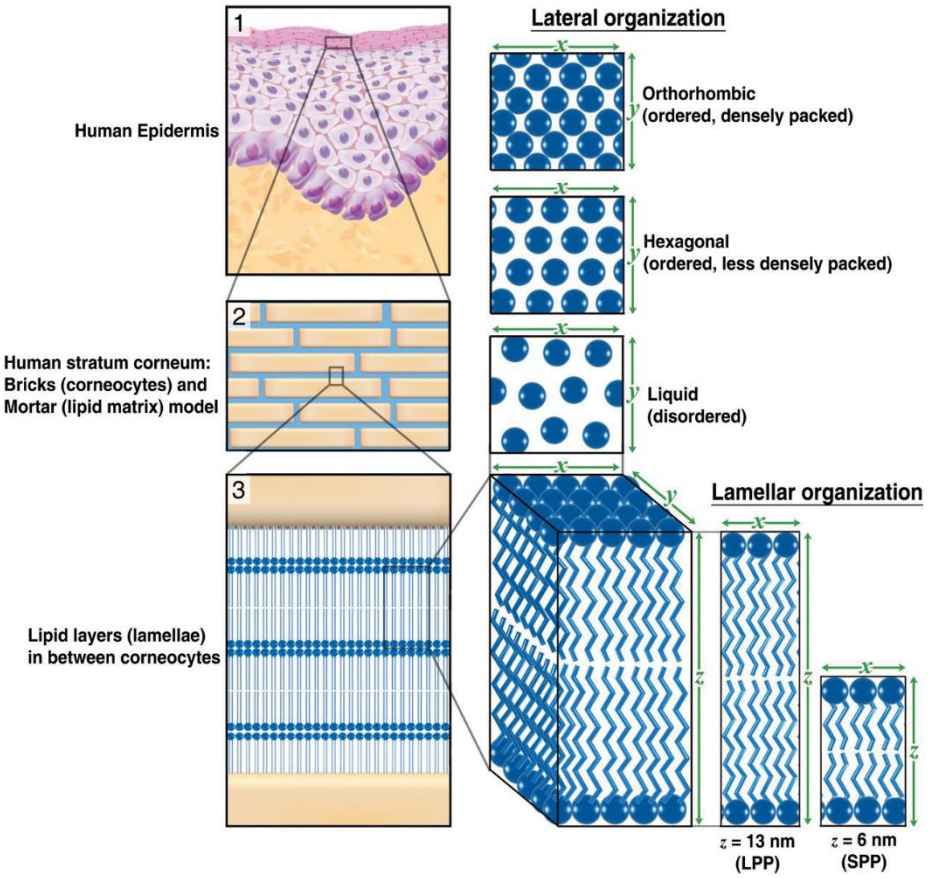

Figure *2:* Overview of the SC brick-and-mortar structure as well as the structure and organization of the lipid lamellae. The ordered structure of the SC lipids is of high importance for the SC barrier, as they hinder diffusion of any permeants through the intercellular path between the corneocytes. Figure taken from Janssens et al. [31].

1.3 Lipid Classes in the SC Lipid Matrix

The lipid matrix of the SC is comprised of three main lipid classes, which are cholesterol, free fatty acids, and the ceramides, found in equimolar amounts [10, 38]. Due to their different molecular weight, this translates to a relative mass ratio in which the ceramides are the most abundant fraction of the lipid matrix with more than 50 percent by mass, while the free fatty acids and cholesterol contribute to 15-25 percent and 25-35 percent by mass respectively. Despite the fact that our knowledge of the relative ratios of these lipid classes of the SC matrix has not changed significantly for more than 40 years [10, 39, 40], the intra-class varieties of these main lipids as well as their respective function and role in the SC have only gradually been discovered since then and are still not fully understood [38, 41-43].

Taking a closer look at these three main lipid classes, cholesterol is in more than one way an outlier: Firstly, it offers the least degree of intra-class structural variety, as it is predominantly found in its unmodified form in the SC, with only a small degree of cholesteryl esters such as cholesterol sulphate present [40, 44]. More importantly, cholesterol shows the most unusual phase behavior out of all the lipids present in the SC: Cholesterol molecules are known to separate from the other SC lipids to form crystalline cholesterol-rich domains, which in turn show distinctively different physicochemical properties from the rest of the SC lipid domains where the SC lipids can freely mix [45-47]. In these structures of mixed lipid leaflets, cholesterol acts to fluidize the system, lowering the phase transition temperature of the lipid mixture while increasing the permeability of the lipid matrix correspondingly, acting not dissimilar to a penetration enhancer as one would find in pharmaceutical or cosmetic formulations [47, 48].

On the other hand, the presence of free fatty acids serves to stabilize the SC lipid leaflets in which they associate in with other lipids and lower the permeability of the lipid matrix [45, 46, 49]. Yet, it is important to note that the extent of this effect is actually strongly dependent on the structure of the fatty acids in the membrane, as the chain length of the fatty acids significantly affects the properties of the lipid lamellae they are found in: Elevated levels of fatty acids with longer carbon chains, of which the most prevalent in the human SC are lignoceric acid (24 carbon atoms) and hexacosanoic acid (26 carbon atoms), but which can go up to 30 or even 34 carbon atoms in the SC [41], are associated with a lower permeability as well as a higher phase transition temperature of the skin lipid matrix. Conversely, higher levels of shorter chain free fatty

acids, containing less than 20 carbon atoms, are associated with a higher permeability of the lipid matrix, lower phase transition temperature and a correspondingly impaired skin barrier function [33, 50, 51]. While these effects were studied and described in detail in simulation and *in vitro* studies and thus may appear to be of a more theoretical nature [45, 50], they are indeed observed in clinical studies: Shifts in the relative ratios of short- and long-chained fatty acids are typical for patients suffering from inflammatory skin diseases such as psoriasis or atopic dermatitis, which are, among other symptoms, associated with an impaired skin barrier as well as a shift towards shorter-chain free fatty acids in the SC, highlighting the significance of changes in the SC lipid profile [12, 33].

The structural variety of the SC lipids grows even larger when focusing on the ceramides as the most abundant lipid class constituting the SC lipids. Ceramides, in general, are classified as sphingolipids: This is due to their general structure, which is based on a sphingosine-derived lipid molecule, which in the ceramide structure is called the long-chained base (LCB). This LCB moiety is linked with an amide bond to a fatty acid (FA), which in turn can be hydroxylated or even further esterified, forming a single molecule with a polar headgroup and two lipid tails [52, 53]. Due to the modular nature of the ceramide structure, the structural variety of individual, structurally discrete ceramide species is staggering: Ceramides can vary by FA moiety chain length, LCB chain length as well as by the hydroxylation and saturation pattern of their headgroups, resulting in more than 3000 ceramide species having been found in the human SC [42, 43]. But ceramides are not unique to the skin: They are found in a host of other tissues and organs, from the brain to the liver as well as in the blood [54]. Yet intriguingly, no other tissue in the human body can match the SC in the variety of the ceramide species, with many ceramide families found only in the SC [36].

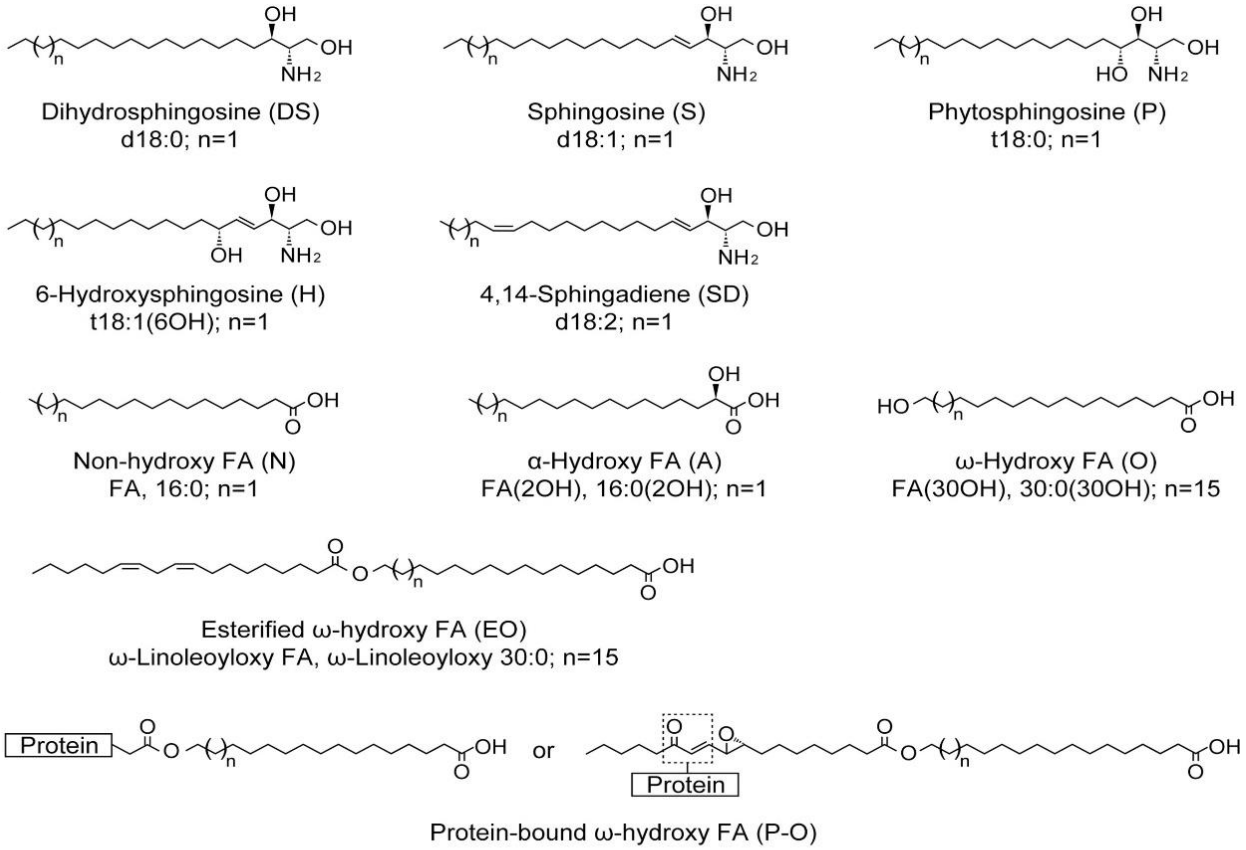

LCBs \ FAs	Non-hydroxy (N)	α-Hydroxy (A)	ω-Hydroxy (O)	Esterified ω-hydroxy (EO)	Protein-bound ω-hydroxy (P-O)
Dihydro-sphingosine (DS)	NDS	ADS	ODS	EODS	P-ODS
Sphingosine (S)	NS	AS	OS	EOS	P-OS
Phytosphingosine (P)	NP	AP	OP	EOP	P-OP
6-Hydroxy-sphingosine (H)	NH	AH	OH	EOH	P-OH
4,14-Sphingadiene (SD)	NSD	ASD	OSD	EOSD	P-OSD

Figure 3*:* Overview of common LCB and FA moieties of ceramides in the human SC. Ceramides are formed via an amide bond linkage between the carboxyl group of the FA and the amine of the LCB, resulting in a wide variety of structures.
Figure modified from Suzuki et al. [43].

1.4 Ceramides and the Skin Barrier

Ceramides are able to influence and modulate the skin lipid barrier in a variety of ways: Analogous to the free fatty acids, the chain length of the ceramides' fatty acid moieties influences the permeability and structure of the lipid lamellae, with the same effect of higher chain lengths being associated with a better skin barrier function and vice versa [55-60]. But, in contrast to the free fatty acids, the headgroup of the ceramide species is also significant for the structure and permeability of the lamellae: Higher abundances of ceramide species with certain headgroups, such as sphingosine-based ceramide species, are suspected to be associated with a higher permeability of the lipid matrix and therefore an impaired skin barrier, while elevated levels of other ceramides, such as those with phytosphingosine-based headgroups, are associated with a lower permeability and therefore better skin barrier function [61-63]. Similar to the effects of the chain length of free fatty acids as well as the ceramide chain length, these particular effects are also not only limited to experimental *in silico* and *in vivo* studies, but were actually found in clinical studies on healthy subjects as well as patients with inflammatory skin diseases: The skin of patients suffering from psoriasis [37, 52, 62, 64] and atopic dermatitis [34, 65, 66] show characteristic changes in the ceramide profile, which are even specific to the disease. As expected, these alterations to the ceramide ratios are most prevalent in the lesional sites of the disease, where the skin is in its most damaged state and the skin barrier is correspondingly the lowest [34, 66, 67]. Note that for AD, the total level of ceramides present in the SC lipid matrix stays the same between the patients' healthy, unaffected skin and the lesional skin areas [34]. This implies that not the mere presence of ceramides in the physiological amounts is important for maintaining the skin barrier function, but indeed the types of ceramides present in the skin are. The etiology of the observed changes to the ceramide profile characteristic for these diseases is linked to the effect of inflammatory cytokines such as IL-4, IL-6 and TNF-α, which directly influence the skin's ceramide synthesis [68, 69].

Focusing on the actual changes in the ceramide profile, the relative abundances of the sphingosine-based ceramide class NS to other ceramide classes are of great interest, as it is indeed found more abundantly in lesional skin of both psoriasis and atopic dermatitis patients [34, 62, 66], which is thought to be a result of disturbed corneocyte differentiation [36]. Comparing the amount of this ceramide with the abundance of ceramides with decreasing prevalence in skin affected with AD or psoriasis, such as

the phytosphingosine-based ceramide class NP or the hydroxysphingosine-based ceramide class NH, has with some success been investigated for the possible use as a biomarker of these diseases, with the ratio of ceramide NP to ceramide NS in particular having been found to correlate well with changes in the skin barrier integrity [62, 70].

But inflammatory skin diseases are not the only trigger of decreased barrier function of the skin, as exposure to organic solvents or surfactants is also linked to an impaired skin barrier: Skin treatment with certain solvents capable of solubilizing the skin lipids, such as chloroform and methanol in combination, results in a marked decrease of barrier function together with a significant decrease in the overall lipid levels [71, 72]. This is in contrast to the typical skin damage caused by surfactants such as detergents used for cleaning or emulsifiers as found in a multitude of pharmaceutical and cosmetic dermal products: These substances, especially of the anionic variety such as sodium lauryl sulfate (SLS), are able to cause significant impairment to the skin barrier while the lipid levels of the skin are not decreased across the board [39, 73, 74]. While it is thought that solutions containing harsh surfactants in higher concentration can preferentially solubilize certain lipid classes of the SC [75, 76], these results are not conclusive and also dependent on the surfactant type, concentration and application time [49]. Furthermore, the depletion of certain lipid classes by surfactants has only been investigated for the main lipid classes of the SC as well as for a few ceramide classes with low resolution, so detailed effects of pharmaceutically used emulsifiers on the ceramide profile of the human skin are still unclear.

1.5 Skin Lipid Analysis with Coupled Liquid Chromatography–Mass Spectrometry

To quantify and detect changes in the skin lipid profile, a variety of analytic methods have been developed over time: Early studies into the structure and composition of the SC obtained their results using thin layer chromatography (TLC) [39, 77] as well as infrared spectroscopy [78, 79], allowing for insights into qualitative as well as quantitative changes in the skin lipid composition and packing despite having only limited resolution. Thin layer chromatography, as well as its variation of high-performance thin layer chromatography (HPTLC), are usually able to chromatographically separate the main SC lipid classes as well as a few of the subclasses of the ceramides, but usually

are unable to resolve changes in the lipid chain length [38, 39]. As such, more sophisticated and more sensitive analytical methods for the analysis of skin lipids have been developed, the current gold standard of which can be considered to be ultra-high-performance liquid chromatography coupled to mass spectrometry (UHPLC-MS, in this work: LC-MS) [80]. The basic idea behind the LC-MS concept is the combination of a column chromatography setup, which enables separation of chemically very similar substances with high chromatographic resolution, with a mass spectrometer setup, which enables very sensitive and specific detection of the analytes separated by the LC step [81]. The specificity of the detection step can be further increased by the use of tandem mass spectrometry, which is often abbreviated as MS/MS or MS^n [82-84]. In tandem mass spectrometry, the instrument does not directly analyze the ionized molecule species, but uses them as precursor ions to fragment in a collision cell: This process of fragmentation results in characteristic product ions, which are specific to certain functional groups and structural elements of the molecules.

The resulting high specificity and sensitivity of the LC-MS and LC-MS/MS methodologies not only enabled more detailed investigations into the composition of the skin lipids, especially in regards to the chain length distributions of free fatty acids and ceramides [41-43, 85], but also made possible the discovery of previously undetected ceramide classes in the human skin, adding to the knowledge base of the SC lipidome [42, 86]. The more widespread adoption of these methods also made possible their use to profile the lipidome of healthy and diseased skin with altered skin barrier characteristics, enabling their use in the clinical and pharmaceutical context. Nonetheless, it is important to note the limitations of the method: While the results of the LC-MS methodology return very detailed information about the lipid composition of the skin sites analyzed, they provide no information about the lateral packing of the lipids, their order state or their repeat distance, which are of course all just as important as the composition of the SC lipids to obtain an accurate picture of the skin state [12]. To address this problem, other sophisticated analysis methods such as Raman spectroscopy [87, 88], x-ray [89] or neutron scattering [90, 91] are available, which can close the blind spots in the analysis of just the lipid composition, but demand specialized instruments and know-how. Another limitation of the use of LC-MS methodology to understand how the SC lipids affect the skin barrier function is the inherently phenomenological nature of the measurement: While changes in the lipid composition of the

samples can be quantified and correlated with known changes in the skin barrier function, skin lipid analysis with LC-MS in itself does not provide insights into the underlying mechanisms which describe how the skin barrier function is modulated by the presence of different kinds of lipid species in the skin. To actually be able to gain insight into the fundamental, molecular workings of how, for example, different ceramide species influence the permeability of the skin lipid matrix, molecular simulations of the system in question are a valuable resource.

1.6 Molecular Dynamics Simulations of the Skin

The basic premise of molecular dynamics (MD) simulations is one of simplification: While one aims to simulate and therefore reproduce real physicochemical phenomena of real molecular systems, the representation of the molecules present in the systems is achieved as a particle simulation of all the atoms in the system, in which the movement and forces on each particular, spherical atom are derived using purely classical dynamics instead of the more realistic, but also orders of magnitude more complex combination of classical and quantum mechanics [92, 93]. In practice, this means that all the forces commonly associated and relevant to the movement and behavior of individual atoms, forces stemming from covalent bonds as well as intermolecular forces, are calculated using classical, optimized approximations for bond geometries as harmonic potentials between spheres as well as using, among others, Lennard-Jones potentials and Coulomb interactions for the calculation of nonbonded forces [94, 95]. While the resulting models of the system are in this sense simplified and limited in scope, e.g. forming and breaking of covalent bonds cannot be represented accurately, this “universe as balls and springs” [96] of MD simulation has proven to be of great use and surprising accuracy in the description and modeling of the real molecular world. In particular, MD simulations are able to offer access to the physicochemical and biophysical processes which happen on molecular scales in biological systems, and which are experimentally almost unavailable to researchers [97]. As an added bonus, due to the flexibility and versatility of the *in silico* methods, the results of changes or modifications to known systems can be calculated and predicted, which in turn can enhance and multiply the insights gained from experiments. As such, this methodology has also found use in the modeling and investigation of phenomena related to the SC lipid matrix, as the pharmaceutically and physiologically relevant processes of the

permeation of drugs, other xenobiotics or even just water through the skin can be understood as a dynamic process on a molecular scale [98-101]. But even though MD simulations are based on simplified calculations to speed up the simulation process, the simulation of even just a small area of the entire stratum depth would lead to unfeasibly big computational loads to simulate over a timeframe of just a few nanoseconds. Thus, the simulated models of the SC lipid matrix often span over just a few lipid layers, which can be bilayers (as depicted in Figure 4) or multilayers, and which can further be immersed in simulated water or in a more realistic, water-sparse environment [102-104]. Using these models, studies on the permeability of organic solvents, drug molecules and water have been conducted, which found in general good agreement to experimental results and in turn serve as comparison to future studies [105-107]. But while the permeation of various chemicals has been studied intensely, factors influencing the permeability of the skin lipids, the skin lipid barrier, have been studied to a lesser extent: These kinds of studies often focus on the modes of action of chemical permeation enhancers such as propylene glycol which are able to modulate the skin barrier, yielding valuable information on how the skin barrier can be altered and which parameters influence its integrity [108-110]. Nonetheless, these investigations study the effect of extrinsic substances on the human skin barrier, not how intrinsic changes in the composition of the skin lipids may affect the barrier. On this topic, research using MD models has mostly been focused on the impact of lipid chain length on the barrier properties, the simulations of which were able to link longer chain lengths to thicker, less permeable lipid membranes, which explained the experimental and clinical findings [58, 107, 111, 112]. On the other hand, investigations into the influence of different ceramide classes on the structure and permeability of skin lipid membranes are scarce: A few studies relating to this topic investigate the influence of the ultra-long chain ceramide EOS in its role in the formation of the LPP from the SPP [107, 113]. While this effect is indeed very relevant for the overall permeability of the SC lipid matrix, as the LPP and the SPP show distinctly different permeabilities, these studies do not address the effect of different ceramide species on the lipid leaflets themselves. Studies into the effects of different ceramide species on structural parameters are available, but these studies often do not report permeabilities of the models [114-116]. Regarding the permeabilities, there exist studies reporting those of SC lipid model layers containing either ceramide NS [99, 102, 105] or Ceramide NP [104], but the studies

in question used slightly different force fields describing the behavior of the molecules in their simulations and also used different methods to obtain the permeabilities, complicating a direct comparison. Thus, the question whether the skin barrier impairment associated with shifts in the ceramide classes, as seen in experimental investigations and clinical studies of inflammatory skin diseases, can be mechanistically explained by MD simulations is still open.

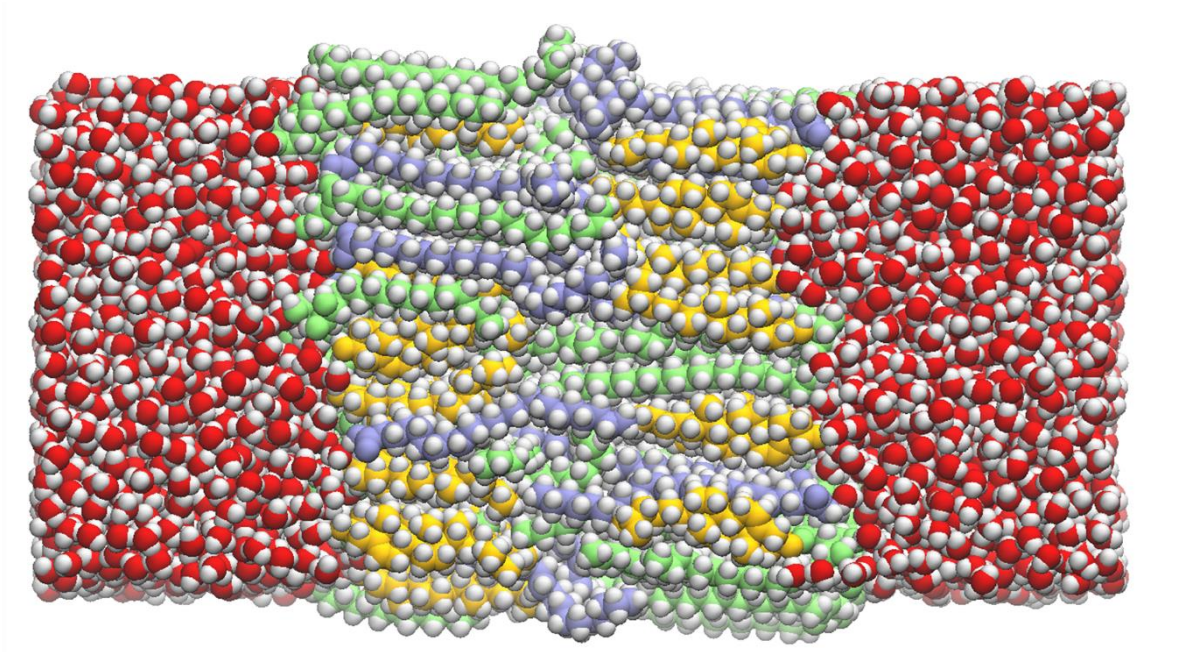

Figure 4*:* Snapshot of a membrane MD simulation depicting an SC lipid bilayer membrane surrounded by water. As depicted in this shot, atoms are represented by uniform spheres, whose interactions with each other, be they non-bonded or bonded, dispersive or ionic, are approximated and calculated using classical mechanics.
Color Legend: Cholesterols in orange, ceramides in lime, fatty acids in ice blue, bulk water in red, hydrogens in white for clarity. Figure modified from the supplementary material of [101].

2 Objectives

The overall goal of the research project was to gain deeper insight into the nature of the interplay between the ceramides of the human SC and its barrier function, with a special focus on skin damage suffered from surfactant treatment. The first aim of the project was to develop, validate and implement an LC-MS method to be able to analyze the ceramides of the SC sampled by tape stripping. The desired capabilities of this method included the quantification of the most common ceramide species found in the human SC combined with a limited runtime, as to enable rapid, yet accurate analysis of a large number of samples.

Using this method, the effect of pharmaceutically used emulsifiers on the ceramide content and profile of the SC of human volunteers were to be investigated, focusing on multiple aims: Firstly, this included a general assessment of the skin tolerability of the emulsifiers, for which measurements of various skin condition parameters such as the barrier function were included in the study design. In addition, the total ceramide content as well as the abundances of the individual ceramides were to be determined from tape strips taken from the treatment sites and connected to the skin condition parameters, as to be able to derive connections between a specific emulsifier, its effect on the skin condition parameters and the associated changes to the ceramide content and profile.

The next goal of the project was to investigate a mechanistic explanation for the *in vivo* connections found between the presence of certain ceramide species in the SC and the skin barrier, for which MD simulations of SC lipid bilayers were employed. The objective of the simulations was therefore to compare the lipid bilayers containing different ceramides in regards to their structure and permeability, as to be able to draw conclusions regarding possible connections of these membrane features.

3 Results & Discussion

3.1 Development of an LC-MS Method for Ceramides in Human Skin

To be able to accurately measure and track changes in the ceramide profile of the SC, a comprehensive LC-MS method was developed to analyze the most common ceramide species in human skin from extracted SC tape stripping samples. The ceramide species included in the method (see Table 1) were chosen based on their relative abundance in the SC lipid matrix, and comprise the 10 most abundant ceramide families in the human SC [41, 42]. The range of ceramide chain lengths to be analyzed was also based on the chain lengths distribution of the ceramides in the human SC: For non-EO ceramide classes, ceramide species with a fatty acid chain length between 20 and 28 carbon atoms were included in the method, the range in which around 95 percent of chain length distribution of these classes can be found, while for EO ceramide classes, to account for the longer chain lengths, the measurement range was shifted to molecules with 28 to 35 carbon atoms in the esterified fatty acid chain. An exception to this rule was made for the ceramide species AS16, which, due to its exceptionally high abundance in comparison with other ceramide species of its class, was also included in the method.

To chromatographically separate the ceramides for analysis, an existing UHPLC method provided by the instrument supplier was adapted to obtain optimal separation of the ceramides by slight modifications of the gradient curve as well as to minimize sample carryover of the analytes by increasing the duration of the rinsing step. The resulting LC method utilized a flow rate of 0.4 ml/min with a binary gradient of an ammonium formate solution with a concentration of 10 micromole per liter of water as the aqueous eluent as well as an organic eluent of an equivolume mixture of isopropyl alcohol and acetonitrile, containing formic acid with a concentration of 0.1% by volume. The total method duration was 20 minutes and separation of the analytes was performed on reversed-phase C8 column with a particle size of 3 µm.

Detection of the individual ceramide species after the chromatographic separation was achieved using Multiple Reaction Monitoring mass spectrometry (MRM-MS). MS detection using MRM was chosen for its high specificity, as the individual ceramide

species are not quantified as whole ionized molecules, but instead from the obtained product ions after a fragmentation step, in which the precursor ceramide ions are fragmented in a collision cell at a specified energy. Previous works on the mass spectrometric characterization of ceramides showed the resulting product ions of the fragmented ceramide species to be characteristic of the LCB found in the ceramide species, allowing a very specific and precise measurement of each individual ceramide species in the sample [42, 82, 83]. To accurately determine the concentrations of the ceramides in the extracted tape stripping samples, a quantitative measurement was achieved using a combination of internal standards (IS) to neutralize possible matrix effects as well as calibration curves of standard solutions of the different ceramide classes for the final quantification. Deuterated ceramide species NS16, NS24 as well as EOS26 were added to each sample as internal standard substances to detect and neutralize effects which might have distorted the accurate quantification of the analytes. After normalization to the known internal standard concentrations, the concentration of each ceramide species in the sample was calculated using calibration curves of a standard solution corresponding to its ceramide class. This method was chosen to accommodate the differing ionization efficiency and the following change in the signal response ratio of the different ceramide headgroup varieties. An exception to this is the ceramide class EOH, for which, as a suitable analytical standard substance was unavailable at the time of measurement, the calibration curve of the related ceramide class AH was used for quantification. In Table 1, the values for the limit of quantification (LOQ) as well as the goodness-of-fit parameter for the calibration curve R^2 as obtained from the method validation can be found. The LC-MS method as described here was subsequently used for ceramide quantification from tape stripping samples in the investigation described in the following chapter.

Table 1: Overview of the ceramide classes included in the LC-MS method, their limits of quantification as well as the goodness-of-fit parameter R^2 of the standard curves.

Ceramide Class	LOQ (ng/mL)	R^2 of Calibration Curve
NS	0.030	>0.999
AS	0.119	>0.999
NP	0.119	0.998
AP	0.298	0.997
NH	0.119	>0.999
AH	0.238	0.992
NDS	0.298	0.999
EOS	0.001	0.996
EOP	0.030	0.998
EOH	0.238*	0.992*

3.2 Investigation into Effects of Emulsifiers on Human Skin Ceramides and Molecular Characterization of Surfactant-Induced Skin Damage

This chapter summarizes the findings of the article "Emulsifier-Induced Changes to the Human Skin Barrier: Connection to Ceramide Profiles and Assessment as a Skin Lesion Model" by Reuter, Schoenfelder, Gaiser, Volc and Lunter, published in Skin Pharmacol Physiol (2025) 38 (3): 79–91 [117]. The entire article can be found in Annex 1 of this work.

This work details the findings of a systematic study into the macroscopic and molecular impacts of pharmaceutically used emulsifiers on the human skin, and involved two main threads of investigation: Firstly, this work investigated and compared changes to

the skin condition caused by the dermal application of a range of pharmaceutically used emulsifiers (See Table 2), comprising a harsh anionic emulsifier, sodium lauryl sulfate, as well as multiple non-ionic emulsifiers. The non-ionic emulsifiers used in the study constituted mostly polyoxyethylene fatty alcohol ethers with HLB values ranging from lipophilic (S2 with an HLB value of 4.9) to very hydrophilic (S100 with a value of 18.8), with the addition of the polymeric emulsifier hydroxypropyl methylcellulose (HPMC). The emulsifiers were then either dissolved or dispersed in ultrapure water and the resulting treatments applied on the forearms of 12 human volunteers. The treatment sites were then incubated for 4 hours, as to simulate the application of a pharmaceutical or cosmetic leave-on formulation with these emulsifiers present. To act as a reference treatment to the emulsifiers, pure water was applied and incubated in the same way on the same forearm as the other treatments. After the incubation time and cleaning of the application sites, the pertaining sites on the volunteers' forearms were then measured in regards to four parameters, namely the pH value, the erythema index, the skin hydration and the TEWL value to assess the skin condition after treatment. Following the skin condition measurements, the SC of all treatment sites was sampled by tape stripping, the obtained tapes extracted and the extracted ceramides in the obtained lipid solutions measured using the LC-MS method described in the previous chapter.

Table 2: Overview of the emulsifiers used for skin treatment in this study. The asterisk denotes the lack of an HLB value given by the supplier.

Emulsifier	Abbreviation	HLB Value	Classification
Sodium lauryl sulfate	SLS	40	Anionic
PEG-20 cetyl ether	C20	15.7	Nonionic
PEG-2 stearyl ether	S2	4.9	Nonionic
PEG-20 stearyl ether	S20	15.3	Nonionic
PEG-100 stearyl ether	S100	18.8	Nonionic
Hydroxypropyl methylcellulose	HPMC	*	Nonionic (Polymer)

Graphs of the data obtained from the skin condition measurements after treatment can be found in Figure 5. As can be seen in this figure, no statistically significant effect of the non-ionic emulsifiers on any of the measured parameters was detected, implying that their prolonged contact with the skin affected it no different than just ultrapure

water. The solution of the anionic sodium lauryl sulfate was the only treatment found to significantly affect the skin condition, namely the skin hydration and TEWL: In both measurements, clear signs of surfactant-induced skin damage could be identified, characterized by a lowered ability of the skin to hold onto water, which is quantified by the capacitance measurement determining the skin hydration, as well as an impaired skin barrier function, identified by an increased loss of water throughout the epidermis.

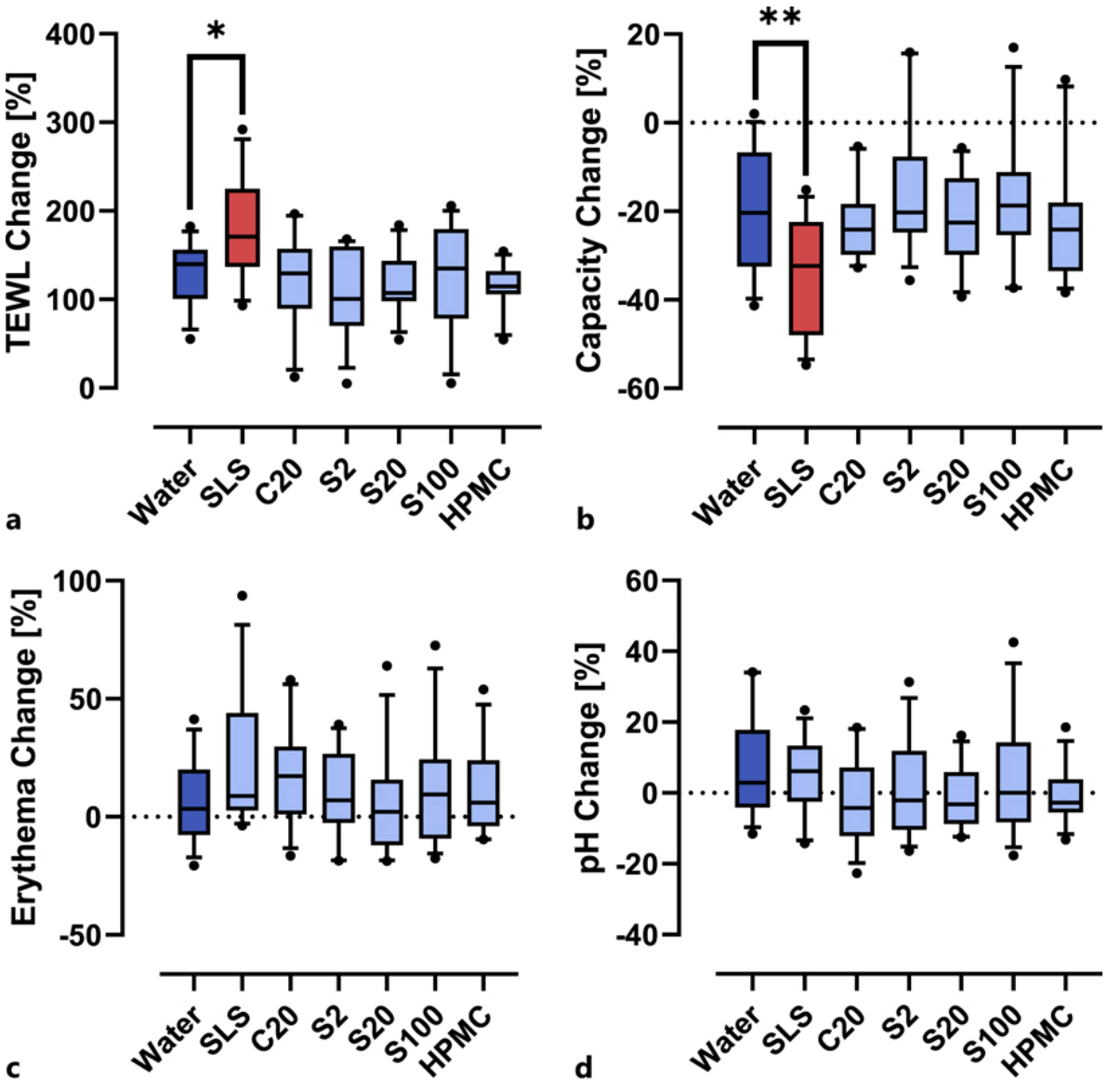

Figure 5: Skin parameters obtained from the treatment sites: (a) TEWL change before/after treatment (b) Skin hydration measured by capacitance change before/after treatment (c) Erythema change before/after treatment (d) skin pH change before/after treatment. The boxed line represents the median, the box the interquartile range. Whiskers are drawn from the 10th to the 90th percentile, n=12. Significant differences are further indicated by the number of asterisks as such: *$p < 0.05$; **$p < 0.01$.

Yet curiously, this impairment to the skin condition caused by the SLS treatment did not translate into a significantly different total ceramide content of the skin: For SLS, as for all emulsifiers assessed in the investigation, the total ceramide content of the treatment sites, as quantified by tape stripping and the subsequent LC-MS analysis, did not significantly change when compared to the skin sites treated with ultrapure water, as can be seen in Figure 6. These results suggested that for emulsifier-treated skin, an impaired skin condition might not be connected to a change in the total abundance of ceramides in the skin, which concluded the first part of the investigation and naturally lead to the main question of the second part of the study: The objective of which was to analyze the nature by which, if not the total ceramide content, then individual ceramide species may potentially influence the skin barrier function when challenged by surfactant treatment.

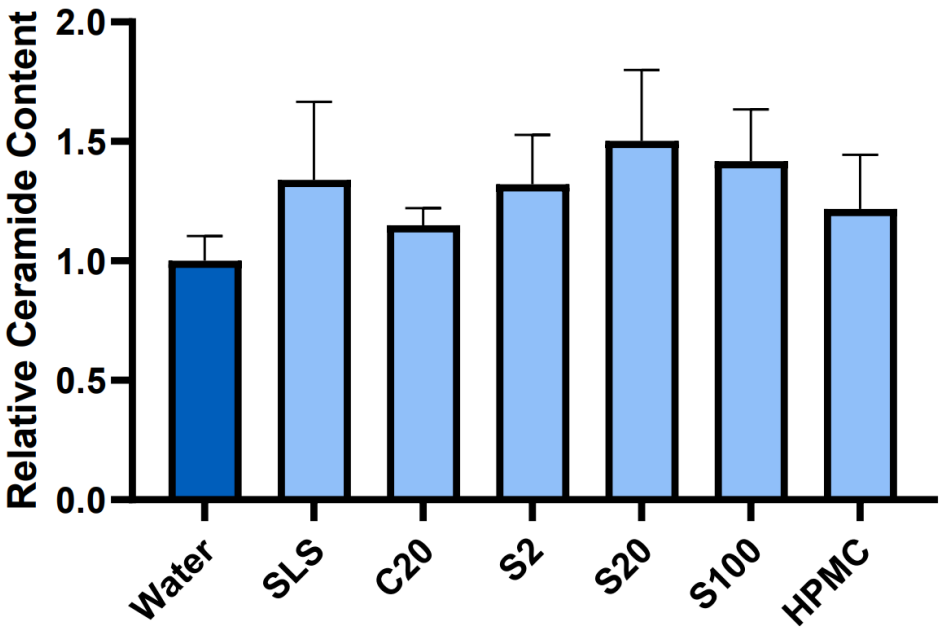

Figure 6: Total ceramide content of the treatment sites relative to water. No statistically significant difference is observed. Mean ± SEM, n=12.

To connect the fluctuations of each individual ceramide species with the measured change of the TEWL as the macroscopic parameter for the skin barrier function, regression modeling was employed: The goal of the modeling approach was to build a statistical model describing how a collection of predictor variables (changes in the concentration of each ceramide species measured in the SC of the treatment sites) may

influence a single dependent variable (the skin barrier function, TEWL). Such a regression model, given an acceptable fit of the model to the data, would make it possible to draw conclusions about the influence of each individual ceramide species in the SC on the skin barrier function by examining the corresponding regression coefficient assigned to it by the model. The regression modeling was performed using a Partial Least Squares (PLS) algorithm [118, 119], which based its model on the differences in concentration of the individual ceramide species between the SLS- and water-treated skin sites as the predictor variable matrix and the difference between the TEWL values for each volunteer obtained after treatment as the response vector. Validation of the model was performed using Leave-One-Out (LOO) cross-validation to detect possible overfitting of the model to the data and to ensure accurate results from the analysis of the model parameters. In the course of the study, a similar regression analysis using the differences between the ceramide concentrations in skin sites treated with the nonionic emulsifier C20 and water was explored, but the resulting model suffered from very noticeable overfitting and a lack of predictive properties, therefore being discarded from further analysis. On the other hand, the SLS-based model showed a good fit to the data (R^2 of 0.67) as well as good predictive properties (Q^2 from cross-validation of 0.44), implying a successful model fit. For better interpretation of the relationships between the concentration of individual ceramide species and the skin barrier function of the treated skin sites, the regression coefficients obtained from the model were graphed as seen in Figure 7.

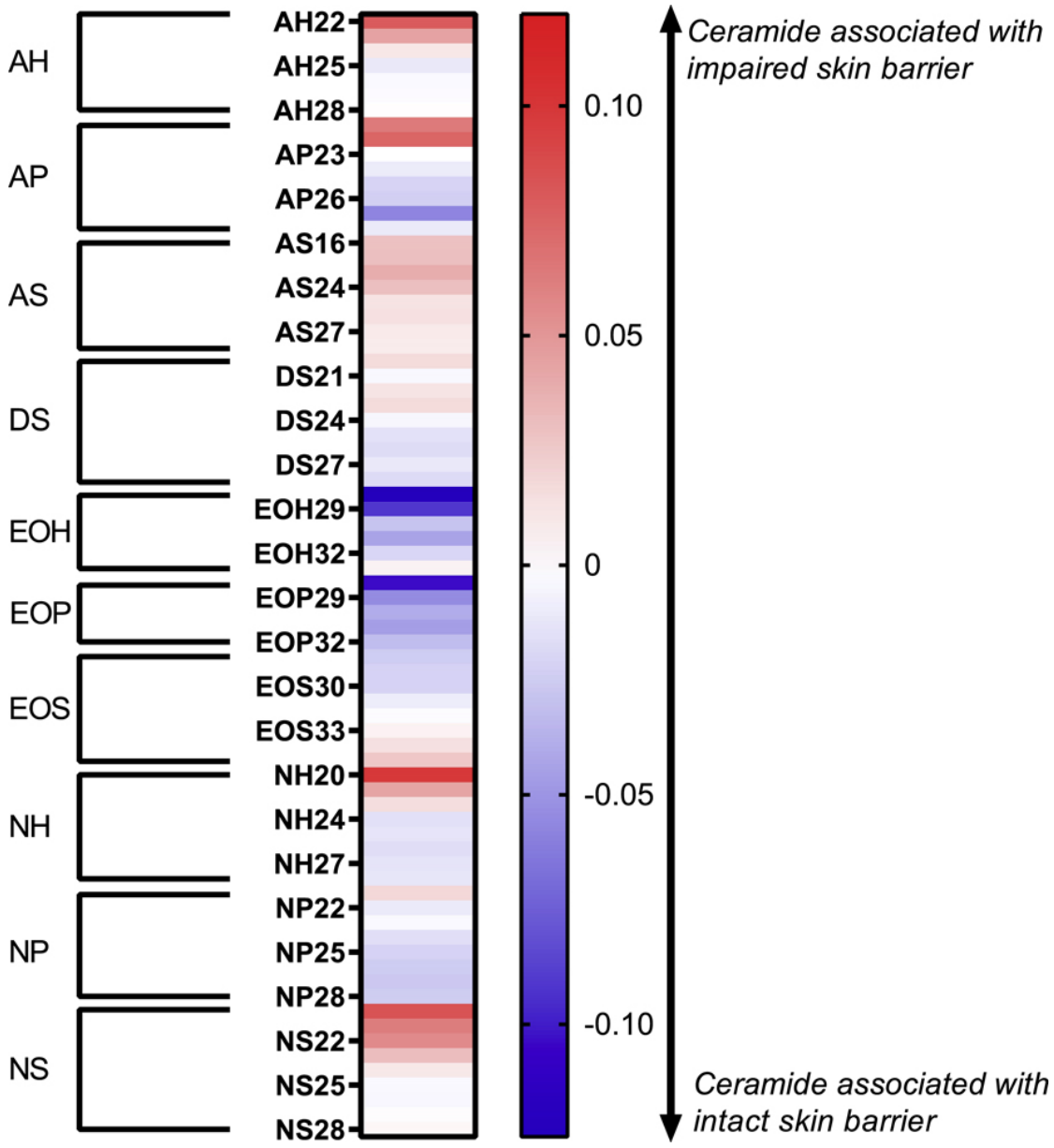

Figure 7: Heatmap of the individual correlation coefficients between the measured ceramide species and the TEWL values.

Closer analysis of the relationships revealed distinct patterns in the association of certain ceramides with an altered skin barrier function: In regards to the ceramide classes, higher abundances of ceramides containing sphingosine as their LCB moiety, such as ceramides NS or AS, were more prominently found in skin with a lower barrier function, possibly implying an association between an impaired skin barrier and the presence of these ceramides. On the other hand, presence of ceramides with certain other LCB varieties, such as phytosphingosine as found in ceramide families NP and AP, were in turn associated with an intact skin barrier, showing negative correlations between their

concentration in the skin and the TEWL. Further, the analysis demonstrated that not only the type of ceramide headgroup affected the impact of the ceramide species on the skin barrier function, but also the ceramide chain length: For ceramides without esterified omega-hydroxylated fatty acid moieties, the chain length of the fatty acid moiety directly correlated with the skin barrier function of the treatment site, with longer chain lengths therefore being associated with a lower TEWL value. However, the ceramides with esterified omega-hydroxylated fatty acid moieties showed the opposite effect: Despite the presence of all ceramide classes belonging to this group (EOS, EOP and EOH) in general being associated with an intact skin barrier, this effect noticeably waned with longer chain lengths toward a more negative effect.

In general, the results of the regression modeling and overall investigation into the effects of changes in the ceramide profile of the SC yielded new insights on the effect of surfactants on the skin: Importantly, the assumption that surfactant treatment influences skin ceramides uniformly proved to be inaccurate. On the contrary, different ceramide species, with their different headgroup structure and chain length, seemed to play different roles in maintaining the integrity of the skin barrier, with the elevated presence of some ceramides even seeming to have a negative effect on the skin barrier function. This finding is crucial to note in the context of research on the effects of emulsifier treatment on the skin health in general: As demonstrated, just a casual glance at the effect of a treatment on the total ceramide content of the skin is insufficient to accurately assess the full scope of possible emulsifier-induced changes in its ceramide profile. Yet importantly, these insights regarding the link between changes in the ceramide profile of the SC and the barrier function of the skin are not limited to surfactant-induced skin damage: Indeed, very similar relationships and correlations between certain ceramide classes and impaired skin health have been observed in clinical studies investigating the skin of patients with inflammatory skin diseases [31, 34, 62, 66]. Comparing the results of this analysis with literature descriptions of the changes to the ceramide profile in the skin of patients with these conditions, it becomes apparent that the shifts in the ceramide profile induced by harsh surfactant treatment are very similar to those found in the lesional skin of atopic dermatitis patients when compared to non-lesional skin. Hence, certain shifts in the ceramide profile may be common to a variety of different causes to the impairment of the skin barrier, be it psoriasis, atopic dermatitis or surfactant treatment of healthy skin. This in turn could

be utilized in future studies developing possible treatments for the disease-related skin conditions, as the skin of healthy volunteers treated with an appropriately harsh surfactant may serve as a disease model for lesional atopic dermatitis skin, reducing the need for patient enrollment in clinical studies.

3.3 Molecular Dynamics Investigation on the Role and Influence of Different Ceramide Classes on the Permeability of SC Lipid Membranes

This chapter summarizes the findings of the article "Presence of Different Ceramide Species Modulates Barrier Function and Structure of Stratum Corneum Lipid Membranes: Insights from Molecular Dynamics Simulations" by Reuter, Joseph, Lian and Lunter, published in Molecular Pharmaceutics (2025) 22 (7): 4280–4292 [101]. The full article can be found in Annex 2 of this work.

This work describes the findings of an investigation into the effect of the presence of different ceramide species on model SC lipid bilayers using MD simulations, analyzing the structural properties of the membranes and their permeability for water molecules. The permeabilities of the systems were a focus of this study, as the calculated water permeation coefficients of the simulated, microscopic SC lipid bilayers correspond to the macroscopic skin property of TEWL and therefore the skin barrier function in general. Hence, it was of great interest to connect the experimental findings from *in vitro* as well as *in vivo* studies on the role of ceramides on the skin barrier function with more theoretical insights into the molecular mechanisms behind these phenomena, provided by the MD simulations. Thus, the main aim of this study was to replicate the findings of experimental as well as clinical studies such as described in the previous chapter: Namely, that a high abundance of ceramide NP in the skin lipid matrix is associated with a lower skin barrier permeability and, correspondingly, that a high abundance of ceramide NS in the same lipid matrix would be linked to a higher degree of permeability, as one would find in an impaired skin barrier. To investigate the influence of either ceramide NP or NS on the properties of a skin lipid mixture, two lipid bilayer systems were prepared: The center of the systems constituted the lipid membrane, which consisted of equal parts cholesterol, lignoceric acid and one of the two ceramide species,

either ceramide NP24 or ceramide NS24. These lipids were then arranged in a typical lipid bilayer structure and placed in a bulk water box surrounding the membrane. Following the assembly step, the systems underwent initial equilibration: Starting with an energy minimization, subsequent equilibration simulation runs were conducted, which initially kept the number of atoms, temperature and volume constant (NVT simulation) to stabilize the system, with the following runs only keeping the number of atoms, pressure and temperature constant (NPT simulation). These NPT conditions model the physical conditions in the real SC the closest and were also used during all production simulations. These simulation runs, spanning a time frame of 200 ns and using the equilibrated model systems as the starting point, were then used to derive and determine basic membrane properties of the systems in question, such as the membrane thickness, the area-per-lipid values and the density and hydrogen bonding of the lipid molecules in the membrane. Based on these results, the membranes containing either ceramide NP or ceramide NS were then compared in terms of their structural parameters. Beside the unmodified production simulations, a second set of systems was set up to compare the water permeability of the systems, which could not be derived from the native production simulations. To determine this measurement, simulations with constrained water molecules were employed: To this end, 60 subsystems for each model membrane containing either ceramide NS or NP were modeled, each based on the respective original system containing the lipid membrane as well as the water box surrounding it. Yet, in addition to the original systems, a water molecule was inserted at a fixed position every 1.5 nanometers along the transmembrane axis z, with a random displacement on the systems x,y plane parallel to the membrane at this position (See Figure 8).

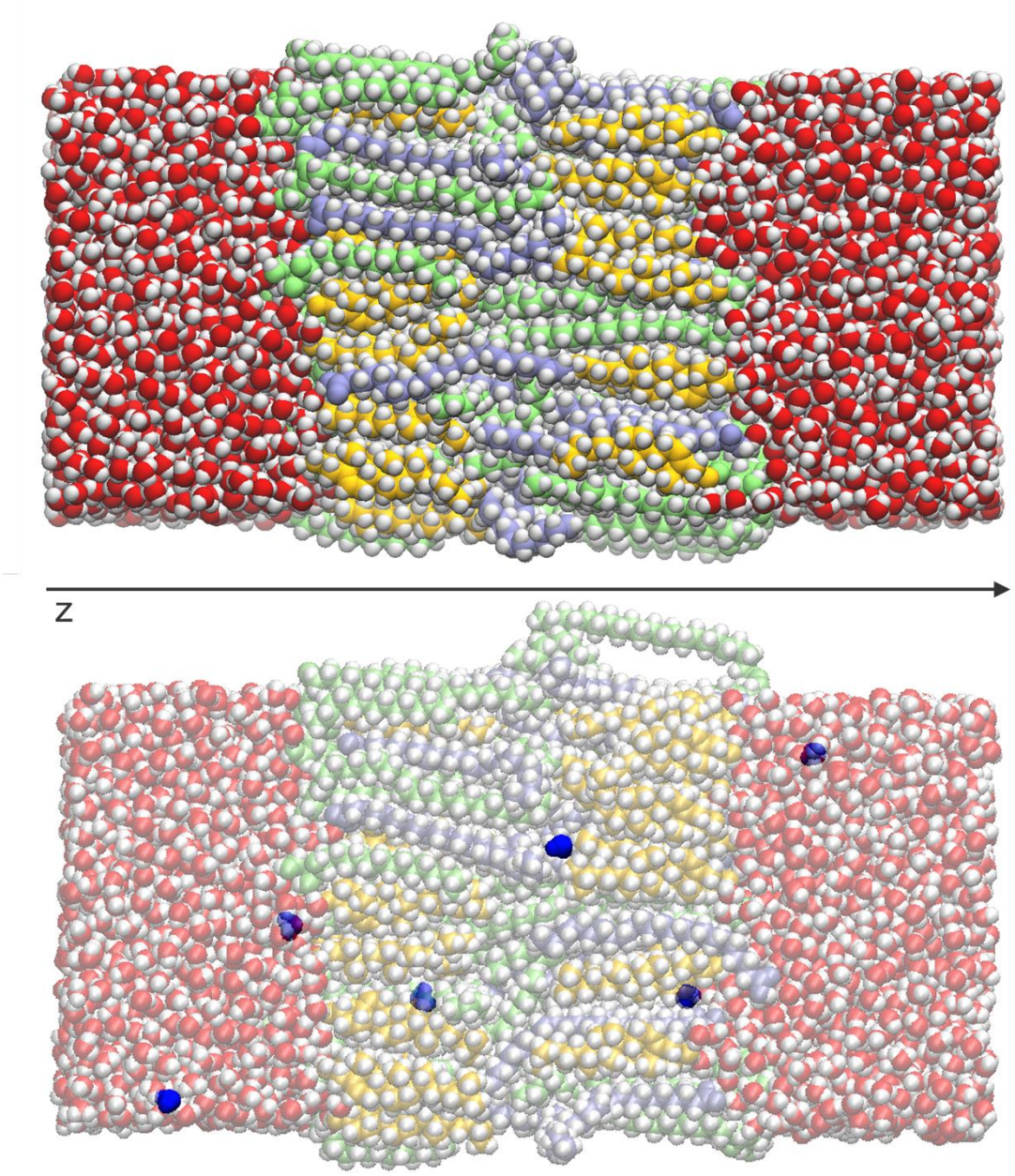

Figure 8: Visualization of a simulated skin lipid bilayer system surrounded by a water box (Top) with and without the inserted water molecules along the transmembrane z-axis used for the permeability measurements (Bottom). Color Legend: Cholesterol: Orange; Ceramide: Lime; Fatty acid: Ice blue, Bulk water: Red, Inserted water molecules: Blue, Hydrogen atoms in white.

The positions of the water molecules along the transmembrane axis were shifted by 0.1 nm between each of the 60 subsystems, which, combined with the total sampling length of the transmembrane axis being 9 nm, resulted in sampling the entire transmembrane axis four times. By applying fixed constraints to the water molecules, they then kept their position along the z-axis and, in the following simulation runs,

experienced forces acting on them depending on their position and local solubility in the membrane, which was in turn used to determine the membrane permeability: As the constraint force has to directly counteract these external forces from the system acting on the water molecules, it is possible to determine a force curve over the transmembrane axis by averaging the constraint force acting on each molecule over the time of the simulation, the integration of which yields the free energy curve of a water molecule in the membrane depending on its position on the transmembrane axis [102]. The permeability of the membrane was then calculated using the inhomogeneous solubility diffusion model, using the calculated free energy as well as the local diffusion coefficient of the molecules, which was also derived from the simulations [120-122]. Using this methodology, the water permeabilities of the membranes containing ceramide NP as well as ceramide NS were then calculated and compared (See Figure 9).

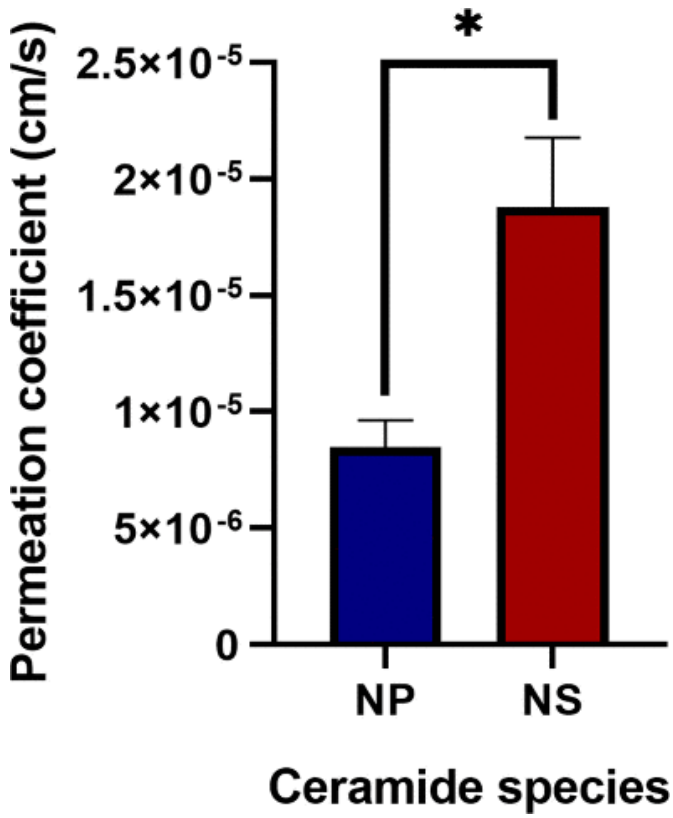

Figure 9: Permeation coefficients of the bilayers containing different ceramide species. Mean ± SEM, n=4. The asterisk denotes a significance level of $p < 0.05$.

The results revealed membranes containing ceramide NP to exhibit a significantly lower water permeability than the membranes containing ceramide NS, with the values for the systems containing ceramide NP measuring less than half of the permeabilities obtained for the systems containing ceramide NS. But while these results agreed well with the previous observations of the experimental and clinical studies [61, 62], the nature of the MD simulations also allowed for the investigation of structural changes to the bilayer membranes introduced by the different ceramide species: Hence, it was found that in systems containing ceramide NP, two notable structural parameters of the lipid membranes changed from the systems containing ceramide NS: Firstly, the positioning of the two other types of membrane lipids, cholesterol as well as lignoceric acid, tended towards an average position closer to the membrane center than found in the corresponding NS-based systems. Secondly, the degree of overall hydrogen bonding as well as the lipid-water and lipid-lipid hydrogen bonding was notably different between the membranes: The ceramide NS-containing system showed a higher degree of lipid-lipid hydrogen bonding, while on the other hand, the study found the ceramide NP-containing system to show a markedly higher degree of lipid-water hydrogen bonding. It was consequently found that these seemingly unrelated phenomena could be traced back towards a common cause: The headgroup conformation probability distribution of the different ceramide species. As the ceramides' headgroup linking the two hydrophobic lipid chains together can arrange in different conformations, these conformations also influence the geometry of the whole ceramide molecule. The effect of the different conformations, which are commonly denoted as either the "hunched" or "posturing" conformations [116], is especially noticeable in the rotation of the headgroup as well as the distance between the lipid chains (see figure 10). The relative propensity of the ceramide NP and NS to arrange in one of those conformations was determined by the probability distribution of the distance between the lipid chains, with a closer interchain distance hinting towards the hunched conformation, and a wider gap between the chains being characteristic of the posturing conformation. The ceramides showed different propensity to position themselves in one of the conformations, with ceramide NS in particular staying overwhelmingly in the hunched conformation, while ceramide NP exhibited a higher tendency to arrange in the posturing conformation.

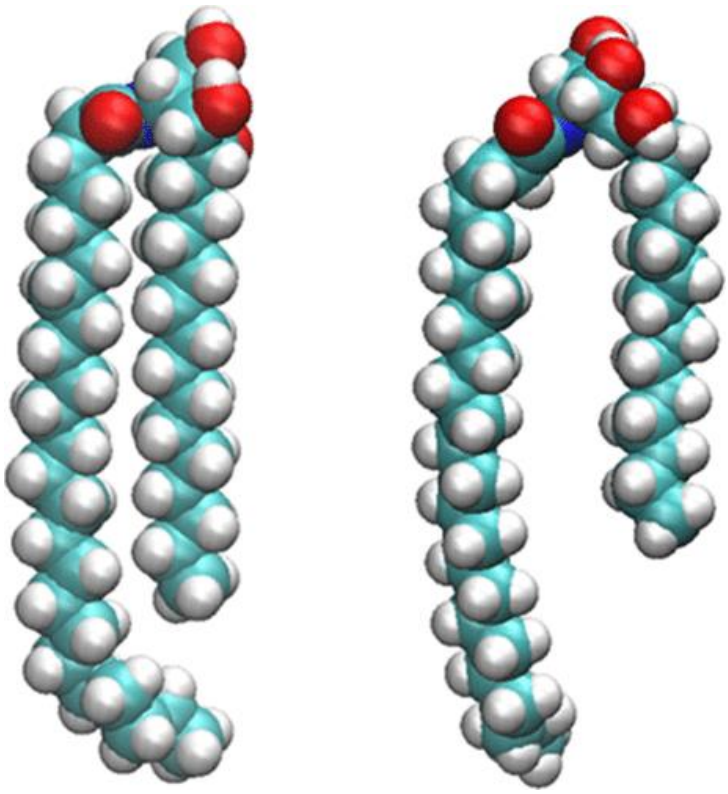

Figure 10: Comparison between the “hunched” conformation (left) and the “posturing” conformation (right) of a ceramide NP molecule. Note the wider gap between lipid tails as well as the different headgroup orientation in the posturing conformation.

Interestingly, this higher tendency of ceramide NP compared to ceramide NS to arrange in the posturing conformation could be linked back to the differences in lipid density as well as hydrogen bonding: In the posturing conformation, the carbon chains of the lipid tails open up, exposing the amide nitrogen of the headgroup from below, which can act as a hydrogen bonding site for other lipids in the membrane. This is the case for cholesterol in particular, which can then intercalate between the lipid tails and position itself slightly below the ceramide as opposed to taking position beside it, which would then result in the observed shift of the density curve to the membrane center. In addition, the headgroup of the ceramides in the lipid membrane orients itself towards the water phase when in the posturing conformation, facilitating hydrogen bonding between the functional groups of the polar ceramide head and the bulk water phase. On the other hand, the headgroup of the hunched conformation is turned more towards the other lipids in the membrane rather than the water phase, leading in turn to more lipid-lipid hydrogen bonds. This “re-orientation” from the hunched conformation facing

towards the other lipids of the membrane, to the posturing conformation facing towards the bulk water phase is depicted in Figure 11, which could be related to the findings of a previous study that similarly found a connection between lower membrane permeabilities and an increased lipid-water hydrogen bonding [110].

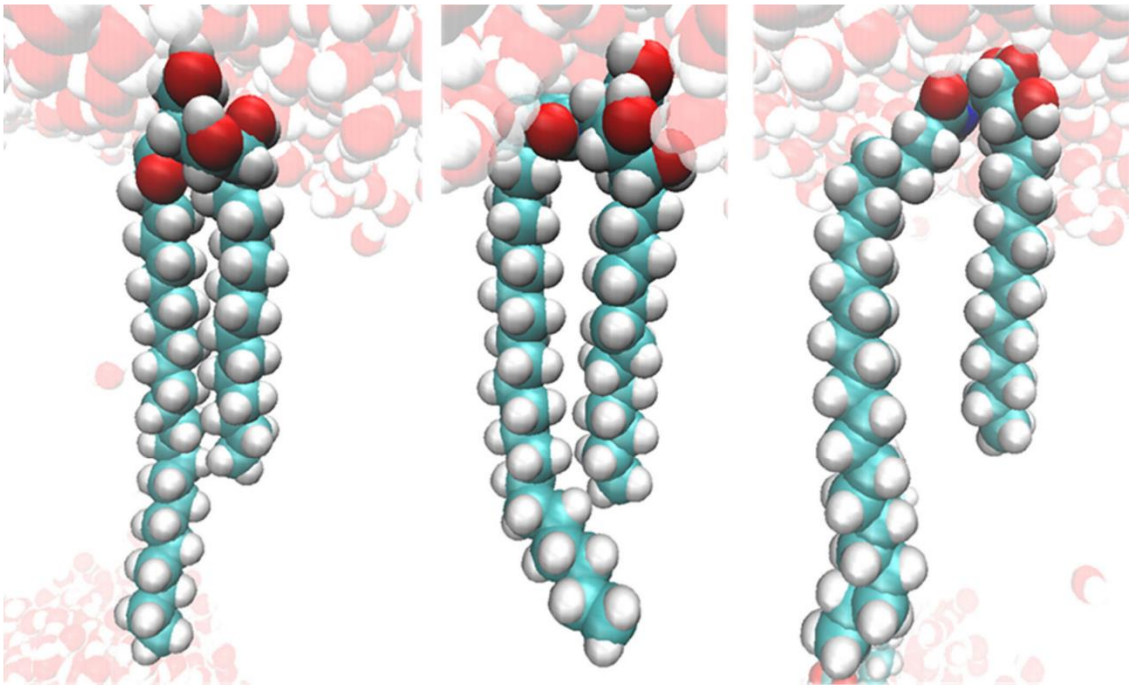

Figure 11: Visualizations of ceramide NP molecules in the lipid membrane arranging in different conformations, from the hunched conformation on the left to the posturing conformation on the right, with an additional intermediate conformation in the middle. The shift towards the posturing conformation is accompanied by an orientation of the headgroup towards the bulk water phase, facilitating lipid-water hydrogen bonding.

These insights into the changes in the membrane structure may offer a venue towards possible mechanistic explanations for the associated changes in the membrane barrier function caused by the presence of different ceramides in the bilayer. Elucidation of the microscopic interrelations between structure and permeability could then further help to explain the phenomena of the macroscopic scale in experimental and clinical studies on this topic, which will be discussed in depth in the next chapter.

3.4 Discussion

The role and importance of ceramides for the integrity of the skin barrier function as well as the skin health in general have gradually moved more and more in the focus of skin research: While early studies investigating a possible link between the general abundance of the ceramides in the SC and skin health were successful in generating fundamental insights into this topic [32, 52, 73, 74, 77], a wider picture of the relationships between the different ceramide classes and species with various skin conditions has emerged with the advent of more advanced analysis methods such as LC-MS, allowing for a much finer-grained analysis of the ceramidome [86]. With these methods being able to track the changes in concentration of individual ceramide species identified by ceramide class and chain length, studies using these high-resolution analysis methods were the first to be able to relate changes in the relative composition of the skins ceramidome to altered states of skin health [31, 34, 56]. In particular, clinical studies investigating the ceramidome of patients with atopic dermatitis or psoriasis found anomalies in the concentration of individual ceramide species, as opposed to just a shift in total ceramide abundance, which were found to be characteristic for the skin of patients suffering from these conditions [31, 34, 62, 64]. These anomalies generally translated into a higher abundance of ceramides with shorter chain lengths in their fatty acid moiety at the lesional skin sites as well as a higher prevalence of ceramides containing sphingosine as their LCB. While this characteristic pattern in the changes of the ceramide profile from healthy to impaired skin is now well known in the context of inflammatory skin diseases in particular, it was not clear if this pattern would also emerge from other causes of impaired skin health, such as surfactant-induced skin damage: This type of skin impairment is especially relevant in the context of developing new cosmetic as well as pharmaceutical dermal formulations, a large share of which contain emulsifiers to at least some degree, of which the overwhelming majority are considered surfactants. Hence, as to predict and evaluate the potential of topically applied emulsifiers to damage the skin or at least impair the skin barrier, a deeper understanding of their effects on the SC is needed. Consulting the literature detailing the impact of surfactants on the skin lipids, most investigations did not investigate the impact of surfactant treatment on the ceramide profile in detail, instead focusing only on the impact of the treatment on the total amount of ceramides in the

skin [74, 75]. In contrast, the investigations of Fulmer & Kramer and di Nardo et al. [39, 73] indeed differentiated the impact of the treatment by examining the changes of abundance of different ceramide classes, but had to rely on comparatively low-resolution analysis methods such as thin layer chromatography, which hindered further ceramide profiling. Thus, the lack of previous studies investigating the changes in the ceramide composition following surfactant treatment using high-resolution analysis methods formed the aim of the study summarized in chapter 3.2: Namely, to investigate the impact of a range of commonly used pharmaceutical emulsifiers on the skin health of human volunteers as well as to gain insight into the detailed influence of the surfactant treatment on the skin ceramides on a molecular level. The results of this investigation are worth a closer look: Assessing the skin tolerability of the emulsifiers, all investigated substances exhibited a surprisingly low impact on the total ceramide content of the skin, which, especially in the case of SLS, seemingly contrasts previous findings from the literature on the effects of surfactant treatment of skin. Many of these studies describe a significant lowering in the SC lipid concentration or even specifically the ceramide concentration in the skin after surfactant treatment, and in particular after treatment with a harsh surfactant such as SLS [75, 76, 87, 123]. One likely explanation for this seeming disagreement of results lies in the resistance to surfactant treatment of live human skin as used in the present study and animal, especially porcine cadaver skin as was often used in literature: Owing to the significantly stronger skin barrier of human *in vivo* skin compared to *ex vivo* skin of pigs [124], the surfactant treatment may have a weaker effect on the living tissue than expected. In addition, ceramides are significantly less prone to extraction from the skin than free fatty acids [74], which may have weakened the observed effect even more and highlights the importance of differentiating between measurements of the total skin lipid abundance and of the ceramide content in particular. These considerations are also supported by previous studies on human volunteers, which, at least in similar strengths of the surfactant solution as used here, also found no significant drop in total ceramide abundance after surfactant treatment [39, 74].

Nonetheless, the study found significant impairment of the skin barrier at the sites treated with SLS, which, importantly, could be linked to changes in the ceramide profile of the skin sites using regression modeling. The resulting patterns, describing how changes to the relative ratios of the ceramides to each other are linked to the measured

changes in the skin barrier, allowed a deeper insight into the nature of surfactant-induced damage to the skin on a molecular level: Notably, equivalent patterns to the ones found in disease-impaired skin such as in atopic dermatitis or psoriasis patients could also be found in the surfactant-treated skin of healthy volunteers, potentially suggesting a common, or at least similar, underlying mechanism associated with an impaired skin barrier function. Of particular relevance to this hypothesis is the fact that while the observed changes in the ceramide profile, in particular the shift of the NP/NS ratio towards NS as well as the higher prevalence of shorter-chain ceramides, have been previously found in the context of patients and untreated healthy volunteers with an impaired skin barrier [34, 62, 66, 70], this study was able to induce these changes with a one-time surfactant treatment. Yet, when hypothesizing about a link between the ceramides found in the SC and the skin barrier function, the question of the nature of this connection emerges: Specifically, one could ask if the observation of certain ceramide species found more prominently in skin with a lower barrier function signifies that the ceramides in question may cause the decrease in skin barrier function at least in part by themselves, or whether if the elevated levels of these ceramides are to be viewed rather as another symptom of the same underlying condition causing the skin barrier impairment. A promising path to resolve this question lies in the investigation of the effects of the presence of individual ceramide species on models simulating the skin lipid matrix of the SC. If it could be demonstrated that there is indeed a mechanistic explanation describing how certain ceramides could actually cause an impairment of the skin barrier, the hypothesis of the ceramidome as a controlling factor of the skin barrier would significantly gain in strength. Thus, a number of *in vitro* as well as *in silico* studies started to explore this topic: The *in vitro* investigation of Nădăban et al. [61] investigated synthetic skin lipid membranes containing, aside from the identical components of a long-chained FFA and cholesterol, either a higher abundance of ceramide NP or ceramide NS in the ceramide component of the lipids. They notably found a significantly lower TEWL in the model membrane containing more ceramide NP, in agreement with the clinical observations and strengthening the hypothesis of at least a partial dependence of the membrane permeabilities on the type of ceramide class present. These findings are also corroborated by the results from an investigation by Uche et al., which also found skin lipid membranes containing sphingosine-based ceramides to exhibit a higher permeability than those containing phytosphingosine-

based ceramides [63]. Another study by Školová et al. [125] similarly found differences in the permeabilities of skin lipid membranes containing different ceramide classes, yet with an important caveat: In their work, ceramide NP, containing phytosphingosine, actually showed the highest permeability of the investigated ceramide classes, exhibiting a greater flux of the permeants than those containing ceramides NS and NDS. Yet, to properly put these results into context, it is important to note that the permeability results of all mentioned investigations were obtained using different model permeants: Školová et al. investigated the permeability of indomethacin and theophylline through the membranes, Uche et al. studied the organic molecule ethyl-p-aminobenzoate, while Nădăban et al. explicitly studied the TEWL, describing the skin permeability for water, thereby significantly affecting the measured barrier function. The results of all studies strongly hint towards there being in fact a dependence of the skin barrier function on the presence of different ceramide species, yet, the studies are at least to some degree in disagreement about the nature of this dependence. Adding to the insights from the *in vitro* results, studies using *in silico* methodology, in particular MD simulations, also assessed the impact of different ceramide class on virtual SC lipid membranes: Nădăban et al., in another comparative study, examined the results of MD simulations of the SPP combined with neutron diffraction measurements and found only slight differences in the structure of the membranes, with the main difference being a higher degree of hydrogen bonding in the NP-abundant membranes due to the additional hydroxyl group of the lipids [115]. Yet, without the inclusion of permeability measurements from the simulations, the potential impact of these differences on the barrier function of the membranes could not be properly assessed. Permeability data for virtual skin lipid membranes in the literature in general is limited to a small number of ceramide classes, with ceramide NS-containing membranes being the most commonly described [99, 102, 112, 126]. In contrast, permeability data for skin lipid bilayers containing ceramide NP is rare [104]. Also, a direct comparison between the permeability values found by different studies for skin lipid membranes containing different ceramides turns out to be challenging, as the basic force field parameters as well as the methodologies for determining the permeability of a model membranes are not uniform across the literature, complicating comparisons. To mend the bridge between different force fields and methodologies between the various studies in the literature, the simulation study described in chapter 3.3 was devised, with the fundamental goal

of a thorough, systematic comparison between simulated membranes containing either ceramide NP or ceramide NS in terms of measured permeability as well as potential underlying changes in the membrane structure. The findings of this investigation are important in two different aspects: Firstly, comparison of the results concerning the permeability of the skin lipid bilayers from this study with the literature data strongly affirms the findings of the previous *in vitro* and *in silico* studies: Not only do the results in Figure 9 qualitatively agree with the experimental values found by Nădăban et al. for the synthetic lipid membranes [61], but the obtained permeability coefficients also agree very well with those described in the simulation studies from Piasentin et al. for ceramide NS [102] as well as Lundborg et al. for ceramide NP [104], which actually differed from this investigation in the combination of the force field parameters and permeability measurement methods. Yet, the purpose of the study was not limited to simply confirming previous findings, but also to offer new insights into changes of the membrane structure and its properties, potentially offering explanations for the permeability differences observed. The most prominent finding in this regard was the observed difference in propensity of ceramide NP and NS to arrange in the different headgroup conformations, which in turn lead to changes in the ability of other lipids to intercalate between the ceramide tails and the hydrogen bonding pattern of the ceramides. Both of these phenomena can be linked to the resulting permeability of the membranes: While the difference in “openings” between the ceramide tails for other lipids might influence the permeability due to a correspondingly higher lipid density at this space in the membrane, evidence for this intercalation is strongest for cholesterol molecules and relies on the higher degree of hydrogen bonding between its hydroxyl group and the amide of ceramide NP over ceramide NS. For lignoceric acid, the hydrogen bonding of the carboxyl headgroup is actually more pronounced with the amide of ceramide NS over ceramide NP, seemingly proving the opposite. Yet, this observation has to be put into the context of the lipid positioning in the membrane: Both the polar headgroups of ceramides as well as fatty acids localize at the membrane surface, with the amide group of the ceramide therefore being able to hydrogen bond with neighboring fatty acid molecules even without intercalation of the fatty acid between the ceramide tails. This is exacerbated by the higher tendency of ceramide NS to arrange into the hunched conformation, which then orients the functional groups of the

ceramide headgroup towards the membrane, increasing lipid-lipid hydrogen bonding as was observed in the study and can be seen in Table 3.

Table 3: Overview of the Lipid-Water and Lipid-Lipid as well as the ceramide hydrogen bonds found in the simulated systems.

Hydrogen Bond Type	**Average number of hydrogen bonds per time frame per lipid (NP | NS)**	
All Lipids – Water	2.637 ± 0.006	2.407 ± 0.005
All Lipids – All Lipids	0.478 ± 0.003	0.555 ± 0.002
CER – Water	4.322 ± 0.002	3.607 ± 0.002
CER – Other Lipids	1.393 ± 0.001	1.620 ± 0.001

Yet, this hydrogen bonding pattern seems to contrast with the findings of Nădăban et al. [115], who found a higher degree of lipid-lipid hydrogen bonding of skin lipid membranes containing a higher abundance of ceramide NP over NS, and hypothesized a connection to an increased barrier function. While this hypothesis is plausible, the findings of Mistry & Notman [110] also lend credence to another idea: In their study on the permeability enhancing effect of propylene glycol on skin lipid bilayers, they found higher concentrations of propylene glycol to not only proportionately increase the permeability of the membrane for water, but to also decrease the degree of lipid-water hydrogen bonding in the systems. Surprisingly, this effect only held for the lipid-water hydrogen bonds, with the degree of lipid-lipid hydrogen bonding of the systems being unaffected even at very high concentrations of propylene glycol and correspondingly low barrier function of the membrane. Their findings, in the light of the results from our study, may hint towards the lipid-water hydrogen bonding degree of the simulated systems having a higher relevance for the permeability of the membrane than previously thought, at least in bilayer systems surrounded by a bulk water phase. This may also be a suitable explanation for the discrepancy between the similar findings of Mistry & Notman and us as opposed to those of Nădăban et al: While in both the systems of Mistry & Notman as well as in our systems fully hydrated bilayers were simulated, Nădăban et al. studied membranes in a state of reduced hydration, which would consequently significantly affect the hydrogen bonding patterns of the systems in question

and again complicates a direct comparison, which in itself would be an interesting subject of future research.

To date, a conclusive mechanistic explanation for the influence of ceramides on the skin barrier function remains yet to be found and will continue to be subject and goal of future research. Nonetheless, the insights gained in the course of this research project, summarized and published in the presented articles, may offer new approaches and serve as stepping stones to future drives to reveal the true nature of the interplay between the lipids of the SC and its barrier function.

4 References

[1] P. M. Elias, “Stratum corneum defensive functions: an integrated view,” *J Invest Dermatol,* vol. 125, no. 2, pp. 183-200, Aug, 2005.

[2] R. R. Wickett, and M. O. Visscher, “Structure and function of the epidermal barrier,” *American Journal of Infection Control,* vol. 34, no. 10, Supplement, pp. S98-S110, 2006/12/01/, 2006.

[3] P. M. Elias, “Structure and Function of the Stratum Corneum Extracellular Matrix,” *Journal of Investigative Dermatology,* vol. 132, no. 9, pp. 2131-2133, 2012/09/01/, 2012.

[4] J. A. Bouwstra, A. Nădăban, W. Bras, C. McAbe, A. Bunge, and G. S. Gooris, “The skin barrier: An extraordinary interface with an exceptional lipid organization,” *Progress in Lipid Research,* vol. 92, pp. 101252, 2023/11/01/, 2023.

[5] E. Proksch, J. M. Brandner, and J.-M. Jensen, “The skin: an indispensable barrier,” *Experimental Dermatology,* vol. 17, no. 12, pp. 1063-1072, 2008.

[6] J. A. McGrath, and J. Uitto, "Structure and Function of the Skin," *Rook's Textbook of Dermatology*, pp. 1-50.

[7] J. Kanitakis, “Anatomy, histology and immunohistochemistry of normal human skin,” *Eur J Dermatol,* vol. 12, no. 4, pp. 390-9; quiz 400-1, Jul-Aug, 2002.

[8] L. Zahra, “The anatomy, physiology and function of all skin layers and the impact of ageing on the skin,” *Wound Practice and Research,* vol. 32, no. 1, March, 2024.

[9] K. C. Madison, “Barrier function of the skin: "la raison d'être" of the epidermis,” *J Invest Dermatol,* vol. 121, no. 2, pp. 231-41, Aug, 2003.

[10] P. M. Elias, “Epidermal Lipids, Barrier Function, and Desquamation,” *Journal of Investigative Dermatology,* vol. 80, no. 1, Supplement, pp. S44-S49, 1983/06/01/, 1983.

[11] S. Brito, M. Baek, and B.-H. Bin, “Skin Structure, Physiology, and Pathology in Topical and Transdermal Drug Delivery,” *Pharmaceutics,* vol. 16, no. 11, pp. 1403, 2024.

[12] J. A. Bouwstra, and M. Ponec, “The skin barrier in healthy and diseased state,” *Biochimica et Biophysica Acta (BBA) - Biomembranes,* vol. 1758, no. 12, pp. 2080-2095, 2006/12/01/, 2006.

[13] A. Tezel, and S. Mitragotri, “On the origin of size-dependent tortuosity for permeation of hydrophilic solutes across the stratum corneum,” *Journal of Controlled Release,* vol. 86, no. 1, pp. 183-186, 2003/01/09/, 2003.

[14] S. Mitragotri, “Modeling skin permeability to hydrophilic and hydrophobic solutes based on four permeation pathways,” *Journal of Controlled Release,* vol. 86, no. 1, pp. 69-92, 2003/01/09/, 2003.
[15] G. Lian, L. Chen, and L. Han, “An evaluation of mathematical models for predicting skin permeability,” *Journal of Pharmaceutical Sciences,* vol. 97, no. 1, pp. 584-598, 2008/01/01/, 2008.
[16] S. Mitragotri, “A theoretical analysis of permeation of small hydrophobic solutes across the stratum corneum based on Scaled Particle Theory,” *Journal of Pharmaceutical Sciences,* vol. 91, no. 3, pp. 744-752, 2002/03/01/, 2002.
[17] P. S. Talreja, G. B. Kasting, N. K. Kleene, W. L. Pickens, and T.-F. Wang, “Visualization of the lipid barrier and measurement of lipid pathlength in human stratum corneum,” *AAPS PharmSci,* vol. 3, no. 2, pp. 13, 2001/06/01, 2001.
[18] M. E. Johnson, D. Blankschtein, and R. Langer, “Evaluation of Solute Permeation through the Stratum Corneum: Lateral Bilayer Diffusion as the Primary Transport Mechanism,” *Journal of Pharmaceutical Sciences,* vol. 86, no. 10, pp. 1162-1172, 1997/10/01/, 1997.
[19] J. Kushner, D. Blankschtein, and R. Langer, “Evaluation of the porosity, the tortuosity, and the hindrance factor for the transdermal delivery of hydrophilic permeants in the context of the aqueous pore pathway hypothesis using dual-radiolabeled permeability experiments,” *Journal of Pharmaceutical Sciences,* vol. 96, no. 12, pp. 3263-3282, 2007/12/01/, 2007.
[20] J. A. Bouwstra, and P. L. Honeywell-Nguyen, “Skin structure and mode of action of vesicles,” *Advanced Drug Delivery Reviews,* vol. 54, pp. S41-S55, 2002/11/01/, 2002.
[21] J. A. Bouwstra, P. L. Honeywell-Nguyen, G. S. Gooris, and M. Ponec, “Structure of the skin barrier and its modulation by vesicular formulations,” *Prog Lipid Res,* vol. 42, no. 1, pp. 1-36, Jan, 2003.
[22] J. van Smeden, M. Janssens, G. S. Gooris, and J. A. Bouwstra, “The important role of stratum corneum lipids for the cutaneous barrier function,” *Biochim Biophys Acta,* vol. 1841, no. 3, pp. 295-313, Mar, 2014.
[23] I. Iwai, H. Han, L. d. Hollander, S. Svensson, L.-G. Öfverstedt, J. Anwar, J. Brewer, M. Bloksgaard, A. Laloeuf, D. Nosek, S. Masich, L. A. Bagatolli, U. Skoglund, and L. Norlén, “The Human Skin Barrier Is Organized as Stacked Bilayers of Fully Extended Ceramides with Cholesterol Molecules Associated with the Ceramide Sphingoid Moiety,” *Journal of Investigative Dermatology,* vol. 132, no. 9, pp. 2215-2225, 2012/09/01/, 2012.
[24] D. C. Swartzendruber, P. W. Wertz, D. J. Kitko, K. C. Madison, and D. T. Downing, “Molecular models of the intercellular lipid lamellae in mammalian stratum corneum,” *Journal of Investigative Dermatology,* vol. 92, no. 2, pp. 251-257, 1989.
[25] D. Groen, D. S. Poole, G. S. Gooris, and J. A. Bouwstra, “Is an orthorhombic lateral packing and a proper lamellar organization important for the skin barrier function?,” *Biochimica et Biophysica Acta (BBA) - Biomembranes,* vol. 1808, no. 6, pp. 1529-1537, 2011/06/01/, 2011.
[26] J. B. G. P. G. Gooris, and H. K. M. Ponec, “New aspects of the skin barrier organization,” *Skin Pharmacol Appl Skin Physiol,* vol. 14, no. 1, pp. 52-62, 2001.
[27] A. S. Michaels, S. K. Chandrasekaran, and J. E. Shaw, “Drug permeation through human skin: Theory and invitro experimental measurement,” *AIChE Journal,* vol. 21, no. 5, pp. 985-996, 1975/09/01, 1975.
[28] L. Chedik, S. Baybekov, F. Cosnier, G. Marcou, A. Varnek, and C. Champmartin, “An update of skin permeability data based on a systematic review of recent research,” *Scientific Data,* vol. 11, no. 1, pp. 224, 2024/02/21, 2024.
[29] B. N. Deacon, N. Piasentin, Q. Cai, T. Chen, and G. Lian, “An examination of published datasets of skin permeability and partition coefficients,” *Toxicology in Vitro,* vol. 93, pp. 105702, 2023/12/01/, 2023.

[30] J. W. Fluhr, K. R. Feingold, and P. M. Elias, “Transepidermal water loss reflects permeability barrier status: validation in human and rodent in vivo and ex vivo models,” *Exp Dermatol,* vol. 15, no. 7, pp. 483-92, Jul, 2006.
[31] M. Janssens, J. van Smeden, G. S. Gooris, W. Bras, G. Portale, P. J. Caspers, R. J. Vreeken, T. Hankemeier, S. Kezic, R. Wolterbeek, A. P. Lavrijsen, and J. A. Bouwstra, “Increase in short-chain ceramides correlates with an altered lipid organization and decreased barrier function in atopic eczema patients [S],” *Journal of Lipid Research,* vol. 53, no. 12, pp. 2755-2766, 2012.
[32] A. P. M. Lavrijsen, J. A. Bouwstra, G. S. Gooris, A. Weerheim, H. E. Boddé, and M. Ponec, “Reduced Skin Barrier Function Parallels Abnormal Stratum Corneum Lipid Organization in Patients with Lamellar Ichthyosis,” *Journal of Investigative Dermatology,* vol. 105, no. 4, pp. 619-624, 1995/10/01/, 1995.
[33] J. van Smeden, M. Janssens, E. C. J. Kaye, P. J. Caspers, A. P. Lavrijsen, R. J. Vreeken, and J. A. Bouwstra, “The importance of free fatty acid chain length for the skin barrier function in atopic eczema patients,” *Experimental Dermatology,* vol. 23, no. 1, pp. 45-52, 2014.
[34] J. Ishikawa, H. Narita, N. Kondo, M. Hotta, Y. Takagi, Y. Masukawa, T. Kitahara, Y. Takema, S. Koyano, and S. Yamazaki, “Changes in the ceramide profile of atopic dermatitis patients,” *Journal of Investigative Dermatology,* vol. 130, no. 10, pp. 2511, 2010.
[35] J. van Smeden, H. Al-Khakany, Y. Wang, D. Visscher, N. Stephens, S. Absalah, H. S. Overkleeft, J. M. F. G. Aerts, A. Hovnanian, and J. A. Bouwstra, “Skin barrier lipid enzyme activity in Netherton patients is associated with protease activity and ceramide abnormalities[S],” *Journal of Lipid Research,* vol. 61, no. 6, pp. 859-869, 2020/06/01/, 2020.
[36] Y. Uchida, and K. Park, “Ceramides in Skin Health and Disease: An Update,” *American Journal of Clinical Dermatology,* vol. 22, no. 6, pp. 853-866, 2021/11/01, 2021.
[37] F. F. Sahle, T. Gebre-Mariam, B. Dobner, J. Wohlrab, and R. H. Neubert, “Skin diseases associated with the depletion of stratum corneum lipids and stratum corneum lipid substitution therapy,” *Skin Pharmacol Physiol,* vol. 28, no. 1, pp. 42-55, 2015.
[38] A. Weerheim, and M. Ponec, “Determination of stratum corneum lipid profile by tape stripping in combination with high-performance thin-layer chromatography,” *Arch Dermatol Res,* vol. 293, no. 4, pp. 191-9, Apr, 2001.
[39] A. W. Fulmer, and G. J. Kramer, “Stratum corneum lipid abnormalities in surfactant-induced dry scaly skin,” *J Invest Dermatol,* vol. 86, no. 5, pp. 598-602, May, 1986.
[40] M. A. Lampe, A. L. Burlingame, J. Whitney, M. L. Williams, B. E. Brown, E. Roitman, and P. M. Elias, “Human stratum corneum lipids: characterization and regional variations,” *J Lipid Res,* vol. 24, no. 2, pp. 120-30, Feb, 1983.
[41] J. van Smeden, W. A. Boiten, T. Hankemeier, R. Rissmann, J. A. Bouwstra, and R. J. Vreeken, “Combined LC/MS-platform for analysis of all major stratum corneum lipids, and the profiling of skin substitutes,” *Biochim Biophys Acta,* vol. 1841, no. 1, pp. 70-9, Jan, 2014.
[42] M. Kawana, M. Miyamoto, Y. Ohno, and A. Kihara, “Comparative profiling and comprehensive quantification of stratum corneum ceramides in humans and mice by LC/MS/MS,” *J Lipid Res,* vol. 61, no. 6, pp. 884-895, Jun, 2020.
[43] M. Suzuki, Y. Ohno, and A. Kihara, “Whole picture of human stratum corneum ceramides, including the chain-length diversity of long-chain bases,” *J Lipid Res,* vol. 63, no. 7, pp. 100235, Jul, 2022.
[44] J. A. Bouwstra, G. S. Gooris, F. E. R. Dubbelaar, and M. Ponec, “Cholesterol sulfate and calcium affect stratum corneum lipid organization over a wide temperature range,” *Journal of Lipid Research,* vol. 40, no. 12, pp. 2303-2312, 1999/12/01/, 1999.

[45] P. Shamaprasad, A. Nădăban, C. R. Iacovella, G. S. Gooris, A. L. Bunge, J. A. Bouwstra, and C. McAbe, “The phase behavior of skin-barrier lipids: A combined approach of experiments and simulations,” *Biophysical Journal,* vol. 123, no. 18, pp. 3188-3204, 2024/09/17/, 2024.
[46] E. H. Mojumdar, D. Groen, G. S. Gooris, D. J. Barlow, M. J. Lawrence, B. Deme, and J. A. Bouwstra, “Localization of Cholesterol and Fatty Acid in a Model Lipid Membrane: A Neutron Diffraction Approach,” *Biophysical Journal,* vol. 105, no. 4, pp. 911-918, 2013/08/20/, 2013.
[47] E. H. Mojumdar, G. S. Gooris, and J. A. Bouwstra, “Phase behavior of skin lipid mixtures: the effect of cholesterol on lipid organization,” *Soft Matter,* vol. 11, no. 21, pp. 4326-4336, 2015.
[48] J. Zbytovská, M. A. Kiselev, S. S. Funari, V. M. Garamus, S. Wartewig, K. Palát, and R. Neubert, “Influence of cholesterol on the structure of stratum corneum lipid model membrane,” *Colloids and Surfaces A: Physicochemical and Engineering Aspects,* vol. 328, no. 1, pp. 90-99, 2008/10/01/, 2008.
[49] K. P. Ananthapadmanabhan, S. Mukherjee, and P. Chandar, “Stratum corneum fatty acids: their critical role in preserving barrier integrity during cleansing,” *Int J Cosmet Sci,* vol. 35, no. 4, pp. 337-45, Aug, 2013.
[50] M. Uchiyama, M. Oguri, E. H. Mojumdar, G. S. Gooris, and J. A. Bouwstra, “Free fatty acids chain length distribution affects the permeability of skin lipid model membranes,” *Biochimica et Biophysica Acta (BBA) - Biomembranes,* vol. 1858, no. 9, pp. 2050-2059, 2016/09/01/, 2016.
[51] R. Westerberg, P. Tvrdik, A.-B. Undén, J.-E. Månsson, L. Norlén, A. Jakobsson, W. H. Holleran, P. M. Elias, A. Asadi, and P. Flodby, “Role for ELOVL3 and fatty acid chain length in development of hair and skin function,” *Journal of Biological Chemistry,* vol. 279, no. 7, pp. 5621-5629, 2004.
[52] S. Motta, M. Monti, S. Sesana, R. Caputo, S. Carelli, and R. Ghidoni, “Ceramide composition of the psoriatic scale,” *Biochim Biophys Acta,* vol. 1182, no. 2, pp. 147-51, Sep 8, 1993.
[53] A. H. Futerman, and H. Riezman, “The ins and outs of sphingolipid synthesis,” *Trends in Cell Biology,* vol. 15, no. 6, pp. 312-318, 2005/06/01/, 2005.
[54] S. A. Summers, B. Chaurasia, and W. L. Holland, “Metabolic Messengers: ceramides,” *Nat Metab,* vol. 1, no. 11, pp. 1051-1058, Nov, 2019.
[55] M. Janssens, J. van Smeden, G. S. Gooris, W. Bras, G. Portale, P. J. Caspers, R. J. Vreeken, T. Hankemeier, S. Kezic, R. Wolterbeek, A. P. Lavrijsen, and J. A. Bouwstra, “Increase in short-chain ceramides correlates with an altered lipid organization and decreased barrier function in atopic eczema patients[S],” *Journal of Lipid Research,* vol. 53, no. 12, pp. 2755-2766, 2012/12/01/, 2012.
[56] K.-M. Eckl, R. Tidhar, H. Thiele, V. Oji, I. Hausser, S. Brodesser, M.-L. Preil, A. Önal-Akan, F. Stock, D. Müller, K. Becker, R. Casper, G. Nürnberg, J. Altmüller, P. Nürnberg, H. Traupe, A. H. Futerman, and H. C. Hennies, “Impaired Epidermal Ceramide Synthesis Causes Autosomal Recessive Congenital Ichthyosis and Reveals the Importance of Ceramide Acyl Chain Length,” *Journal of Investigative Dermatology,* vol. 133, no. 9, pp. 2202-2211, 2013/09/01/, 2013.
[57] E. H. Mojumdar, Z. Kariman, L. van Kerckhove, G. S. Gooris, and J. A. Bouwstra, “The role of ceramide chain length distribution on the barrier properties of the skin lipid membranes,” *Biochim Biophys Acta,* vol. 1838, no. 10, pp. 2473-83, Oct, 2014.
[58] R. Gupta, B. S. Dwadasi, and B. Rai, “Molecular Dynamics Simulation of Skin Lipids: Effect of Ceramide Chain Lengths on Bilayer Properties,” *The Journal of Physical Chemistry B,* vol. 120, no. 49, pp. 12536-12546, 2016/12/15, 2016.
[59] L. E. Uche, G. S. Gooris, J. A. Bouwstra, and C. M. Beddoes, “Increased Levels of Short-Chain Ceramides Modify the Lipid Organization and Reduce the Lipid Barrier of Skin Model Membranes,” *Langmuir,* vol. 37, no. 31, pp. 9478-9489, 2021/08/10, 2021.

[60] B. Školová, B. Janůšová, J. Zbytovská, G. Gooris, J. Bouwstra, P. Slepička, P. Berka, J. Roh, K. Palát, A. Hrabálek, and K. Vávrová, “Ceramides in the Skin Lipid Membranes: Length Matters,” *Langmuir,* vol. 29, no. 50, pp. 15624-15633, 2013/12/17, 2013.
[61] A. Nădăban, J. Rousel, D. El Yachioui, G. S. Gooris, C. M. Beddoes, R. M. Dalgliesh, M. Malfois, R. Rissmann, and J. A. Bouwstra, “Effect of sphingosine and phytosphingosine ceramide ratio on lipid arrangement and barrier function in skin lipid models,” *J Lipid Res,* vol. 64, no. 8, pp. 100400, Aug, 2023.
[62] U. Yokose, J. Ishikawa, Y. Morokuma, A. Naoe, Y. Inoue, Y. Yasuda, H. Tsujimura, T. Fujimura, T. Murase, and A. Hatamochi, “The ceramide [NP]/[NS] ratio in the stratum corneum is a potential marker for skin properties and epidermal differentiation,” *BMC Dermatology,* vol. 20, no. 1, pp. 6, 2020/08/31, 2020.
[63] L. E. Uche, G. S. Gooris, C. M. Beddoes, and J. A. Bouwstra, “New insight into phase behavior and permeability of skin lipid models based on sphingosine and phytosphingosine ceramides,” *Biochim Biophys Acta Biomembr,* vol. 1861, no. 7, pp. 1317-1328, Jul 1, 2019.
[64] W. Łuczaj, A. Wroński, P. Domingues, M. R. Domingues, and E. Skrzydlewska, “Lipidomic Analysis Reveals Specific Differences between Fibroblast and Keratinocyte Ceramide Profile of Patients with Psoriasis Vulgaris,” *Molecules,* vol. 25, no. 3, Jan 31, 2020.
[65] K.-M. Joo, J.-H. Hwang, S. Bae, D.-H. Nahm, H.-S. Park, Y.-M. Ye, and K.-M. Lim, “Relationship of ceramide–, and free fatty acid–cholesterol ratios in the stratum corneum with skin barrier function of normal, atopic dermatitis lesional and non-lesional skins,” *Journal of Dermatological Science,* vol. 77, no. 1, pp. 71-74, 2015.
[66] Y. Sho, T. Sakai, T. Sato, M. Sonezaki, H. Taima, H. Taguchi, K. Kaizu, T. Nishizaka, Y. Takagi, and Y. Hatano, “Stratum Corneum Ceramide Profiles Provide Reliable Indicators of Remission and Potential Flares in Atopic Dermatitis,” *Journal of Investigative Dermatology,* vol. 142, no. 12, pp. 3184-3191.e7, 2022/12/01/, 2022.
[67] H. Farwanah, K. Raith, R. H. H. Neubert, and J. Wohlrab, “Ceramide profiles of the uninvolved skin in atopic dermatitis and psoriasis are comparable to those of healthy skin,” *Archives of Dermatological Research,* vol. 296, no. 11, pp. 514-521, 2005/05/01, 2005.
[68] A. Kihara, “Synthesis and degradation pathways, functions, and pathology of ceramides and epidermal acylceramides,” *Progress in Lipid Research,* vol. 63, pp. 50-69, 2016/07/01/, 2016.
[69] E. Sawada, N. Yoshida, A. Sugiura, and G. Imokawa, “Th1 cytokines accentuate but Th2 cytokines attenuate ceramide production in the stratum corneum of human epidermal equivalents: An implication for the disrupted barrier mechanism in atopic dermatitis,” *Journal of Dermatological Science,* vol. 68, no. 1, pp. 25-35, 2012/10/01/, 2012.
[70] F. Akiyama, N. Takahashi, Y. Ueda, S. Tada, N. Takeuchi, Y. Ohno, and A. Kihara, “Correlations between Skin Condition Parameters and Ceramide Profiles in the Stratum Corneum of Healthy Individuals,” *International Journal of Molecular Sciences,* vol. 25, no. 15, pp. 8291, 2024.
[71] C. Barba, C. Alonso, M. Martí, A. Manich, and L. Coderch, “Skin barrier modification with organic solvents,” *Biochimica et Biophysica Acta (BBA) - Biomembranes,* vol. 1858, no. 8, pp. 1935-1943, 2016/08/01/, 2016.
[72] B. A. Čuříková-Kindlová, A. Vovesná, A. Nováčková, and J. Zbytovská, “In Vitro Modeling of Skin Barrier Disruption and its Recovery by Ceramide-Based Formulations,” *AAPS PharmSciTech,* vol. 23, no. 1, pp. 21, 2021/12/14, 2021.
[73] A. di Nardo, K. Sugino, P. Wertz, J. Ademola, and H. I. Maibach, “Sodium lauryl sulfate (SLS) induced irritant contact dermatitis: a correlation study between

ceramides and in vivo parameters of irritation," *Contact Dermatitis,* vol. 35, no. 2, pp. 86-91, Aug, 1996.
[74] C. L. Froebe, F. A. Simion, L. D. Rhein, R. H. Cagan, and A. Kligman, "Stratum corneum lipid removal by surfactants: relation to in vivo irritation," *Dermatologica,* vol. 181, no. 4, pp. 277-83, 1990.
[75] G. Imokawa, "Surfactant-Induced Depletion of Ceramides and Other Intercellular Lipids: Implication for the Mechanism Leading to Dehydration of the Stratum corneum," *Exogenous Dermatology,* vol. 3, no. 2, pp. 81-98, 2005.
[76] Y. Takagi, H. Nakagawa, K. Higuchi, and G. Imokawa, "Characterization of Surfactant-Induced Skin Damage through Barrier Recovery Induced by Pseudoacylceramides," *Dermatology,* vol. 211, no. 2, pp. 128-134, 2005.
[77] G. Imokawa, S. Akasaki, Y. Minematsu, and M. Kawai, "Importance of intercellular lipids in water-retention properties of the stratum corneum: induction and recovery study of surfactant dry skin," *Archives of Dermatological Research,* vol. 281, no. 1, pp. 45-51, 1989/02/01, 1989.
[78] D. Bommannan, R. O. Potts, and R. H. Guy, "Examination of Stratum Corneum Barrier Function In Vivo by Infrared Spectroscopy," *Journal of Investigative Dermatology,* vol. 95, no. 4, pp. 403-408, 1990/10/01/, 1990.
[79] G. M. Golden, D. B. Guzek, A. E. Kennedy, J. E. McKie, and R. O. Potts, "Stratum corneum lipid phase transitions and water barrier properties," *Biochemistry,* vol. 26, no. 8, pp. 2382-2388, 1987.
[80] E. Berdyshev, I. Bronova, D. Y. M. Leung, and E. Goleva, "Methodological Considerations for Lipid and Polar Component Analyses in Human Skin Stratum Corneum," *Cell Biochemistry and Biophysics,* vol. 79, no. 3, pp. 659-668, 2021/09/01, 2021.
[81] J. J. Pitt, "Principles and applications of liquid chromatography-mass spectrometry in clinical biochemistry," *Clin Biochem Rev,* vol. 30, no. 1, pp. 19-34, Feb, 2009.
[82] F.-F. Hsu, "Electrospray ionization with higher-energy collision dissociation tandem mass spectrometry toward characterization of ceramides as [M + Li]+ ions: Mechanisms of fragmentation and structural identification," *Analytica Chimica Acta,* vol. 1142, pp. 221-234, 2021/01/15/, 2021.
[83] F.-F. Hsu, "Complete structural characterization of ceramides as [M−H]− ions by multiple-stage linear ion trap mass spectrometry," *Biochimie,* vol. 130, pp. 63-75, 2016/11/01/, 2016.
[84] F.-F. Hsu, J. Turk, M. E. Stewart, and D. T. Downing, "Structural studies on ceramides as lithiated adducts by low energy collisional-activated dissociation tandem mass spectrometry with electrospray ionization," *Journal of the American Society for Mass Spectrometry,* vol. 13, no. 6, pp. 680-695, 2002/06/01, 2002.
[85] W. Boiten, S. Absalah, R. Vreeken, J. Bouwstra, and J. van Smeden, "Quantitative analysis of ceramides using a novel lipidomics approach with three dimensional response modelling," *Biochim Biophys Acta,* vol. 1861, no. 11, pp. 1652-1661, Nov, 2016.
[86] Y. Masukawa, H. Narita, E. Shimizu, N. Kondo, Y. Sugai, T. Oba, R. Homma, J. Ishikawa, Y. Takagi, T. Kitahara, Y. Takema, and K. Kita, "Characterization of overall ceramide species in human stratum corneum," *Journal of Lipid Research,* vol. 49, no. 7, pp. 1466-1476, 2008/07/01/, 2008.
[87] Y. Liu, and D. J. Lunter, "Systematic Investigation of the Effect of Non-Ionic Emulsifiers on Skin by Confocal Raman Spectroscopy—A Comprehensive Lipid Analysis," *Pharmaceutics,* vol. 12, no. 3, pp. 223, 2020.
[88] D. Lunter, V. Klang, D. Kocsis, Z. Varga-Medveczky, S. Berkó, and F. Erdő, "Novel aspects of Raman spectroscopy in skin research," *Exp Dermatol,* vol. 31, no. 9, pp. 1311-1329, Sep, 2022.
[89] G. Brezesinski, L. Opálka, C. Shen, C. Groetzsch, E. Schneck, and A. Eichner, "Structure–Function Relationship of the Most Abundant Ceramide Subspecies

Studied on Monolayer Models Using GIXD and Langmuir Isotherms," *Langmuir,* vol. 41, no. 22, pp. 14255-14264, 2025/06/10, 2025.
[90] Y. Badhe, T. Schmitt, R. Gupta, B. Rai, and R. H. H. Neubert, "Investigating the nanostructure of a CER[NP]/CER[AP]-based stratum corneum lipid matrix model: A combined neutron diffraction & molecular dynamics simulations approach," *Biochimica et Biophysica Acta (BBA) - Biomembranes,* vol. 1864, no. 10, pp. 184007, 2022/10/01/, 2022.
[91] Y. Chen, M. Liao, K. Ma, Z. Wang, B. Demé, J. Penfold, J. R. Lu, J. R. P. Webster, and P. Li, "Implications of surfactant hydrophobic chain architecture on the Surfactant-Skin lipid model interaction," *Journal of Colloid and Interface Science,* vol. 608, pp. 405-415, 2022/02/15/, 2022.
[92] M. P. Allen, "Introduction to molecular dynamics simulation," *Computational soft matter: from synthetic polymers to proteins,* vol. 23, no. 1, pp. 1-28, 2004.
[93] W. F. van Gunsteren, and H. J. C. Berendsen, "Computer Simulation of Molecular Dynamics: Methodology, Applications, and Perspectives in Chemistry," *Angewandte Chemie International Edition in English,* vol. 29, no. 9, pp. 992-1023, 1990.
[94] S. Pronk, S. Páll, R. Schulz, P. Larsson, P. Bjelkmar, R. Apostolov, M. R. Shirts, J. C. Smith, P. M. Kasson, D. van der Spoel, B. Hess, and E. Lindahl, "GROMACS 4.5: a high-throughput and highly parallel open source molecular simulation toolkit," *Bioinformatics,* vol. 29, no. 7, pp. 845-54, Apr 1, 2013.
[95] D. Van Der Spoel, E. Lindahl, B. Hess, G. Groenhof, A. E. Mark, and H. J. C. Berendsen, "GROMACS: Fast, flexible, and free," *Journal of Computational Chemistry,* vol. 26, no. 16, pp. 1701-1718, 2005.
[96] L. Wang, "The universe as balls and springs: molecular dynamics in Python."
[97] M. Karplus, and J. A. McCammon, "Molecular dynamics simulations of biomolecules," *Nature Structural Biology,* vol. 9, no. 9, pp. 646-652, 2002/09/01, 2002.
[98] P. Shamaprasad, C. O. Frame, T. C. Moore, A. Yang, C. R. Iacovella, J. A. Bouwstra, A. L. Bunge, and C. McAbe, "Using molecular simulation to understand the skin barrier," *Progress in Lipid Research,* vol. 88, pp. 101184, 2022/11/01/, 2022.
[99] C. Das, P. D. Olmsted, and M. G. Noro, "Water permeation through stratum corneum lipid bilayers from atomistic simulations," *Soft Matter,* vol. 5, no. 22, pp. 4549-4555, 2009.
[100] A. Del Regno, and R. Notman, "Permeation pathways through lateral domains in model membranes of skin lipids," *Physical Chemistry Chemical Physics,* vol. 20, no. 4, pp. 2162-2174, 2018.
[101] M. Reuter, E. Joseph, G. Lian, and D. J. Lunter, "Presence of Different Ceramide Species Modulates Barrier Function and Structure of Stratum Corneum Lipid Membranes: Insights from Molecular Dynamics Simulations," *Molecular Pharmaceutics*, 2025/06/25, 2025.
[102] N. Piasentin, G. Lian, and Q. Cai, "Evaluation of Constrained and Restrained Molecular Dynamics Simulation Methods for Predicting Skin Lipid Permeability," *ACS Omega,* vol. 6, no. 51, pp. 35363-35374, Dec 28, 2021.
[103] N. Piasentin, G. Lian, and Q. Cai, "In Silico Prediction of Stratum Corneum Partition Coefficients via COSMOmic and Molecular Dynamics Simulations," *The Journal of Physical Chemistry B,* vol. 127, no. 12, pp. 2719-2728, 2023/03/30, 2023.
[104] M. Lundborg, A. Narangifard, C. L. Wennberg, E. Lindahl, B. Daneholt, and L. Norlén, "Human skin barrier structure and function analyzed by cryo-EM and molecular dynamics simulation," *Journal of Structural Biology,* vol. 203, no. 2, pp. 149-161, 2018/08/01/, 2018.
[105] R. Thomas, P. R. Prabhakar, D. J. Tobias, and M. von Domaros, "Insights into Dermal Permeation of Skin Oil Oxidation Products from Enhanced Sampling Molecular Dynamics Simulation," *The Journal of Physical Chemistry B,* vol. 129, no. 6, pp. 1784-1794, 2025/02/13, 2025.

[106] M. Lundborg, C. L. Wennberg, A. Narangifard, E. Lindahl, and L. Norlén, “Predicting drug permeability through skin using molecular dynamics simulation,” *J Control Release,* vol. 283, pp. 269-279, Aug 10, 2018.
[107] E. Wang, and J. B. Klauda, “Structure and Permeability of Ceramide Bilayers and Multilayers,” *The Journal of Physical Chemistry B,* vol. 123, no. 11, pp. 2525-2535, 2019/03/21, 2019.
[108] R. Notman, and J. Anwar, “Breaching the skin barrier — Insights from molecular simulation of model membranes,” *Advanced Drug Delivery Reviews,* vol. 65, no. 2, pp. 237-250, 2013/02/01/, 2013.
[109] C. Wennberg, M. Lundborg, E. Lindahl, and L. Norlén, “Understanding Drug Skin Permeation Enhancers Using Molecular Dynamics Simulations,” *J Chem Inf Model,* vol. 63, no. 15, pp. 4900-4911, Aug 14, 2023.
[110] J. Mistry, and R. Notman, “Mechanisms of the Drug Penetration Enhancer Propylene Glycol Interacting with Skin Lipid Membranes,” *The Journal of Physical Chemistry B,* vol. 128, no. 16, pp. 3885-3897, 2024/04/25, 2024.
[111] D. Altun, P. Larsson, C. A. S. Bergström, and S. Hossain, “Molecular dynamics simulations of lipid composition and its impact on structural and dynamic properties of skin membrane,” *Chemistry and Physics of Lipids,* vol. 265, pp. 105448, 2024/11/01/, 2024.
[112] Y. Badhe, R. Gupta, and B. Rai, “Structural and barrier properties of the skin ceramide lipid bilayer: a molecular dynamics simulation study,” *Journal of Molecular Modeling,* vol. 25, no. 5, pp. 140, 2019/04/30, 2019.
[113] E. Wang, and J. B. Klauda, “Molecular Structure of the Long Periodicity Phase in the Stratum Corneum,” *Journal of the American Chemical Society,* vol. 141, no. 42, pp. 16930-16943, 2019/10/23, 2019.
[114] N. Rivero, M. C. Daza, and M. Doerr, “Effect of the CER[NP]:CER[AP] a ratio on the structure of a stratum corneum model lipid matrix - a molecular dynamics study,” *Chemistry and Physics of Lipids,* vol. 250, pp. 105259, 2023/01/01/, 2023.
[115] A. Nădăban, C. O. Frame, D. El Yachioui, G. S. Gooris, R. M. Dalgliesh, M. Malfois, C. R. Iacovella, A. L. Bunge, C. McCabe, and J. A. Bouwstra, “The Sphingosine and Phytosphingosine Ceramide Ratio in Lipid Models Forming the Short Periodicity Phase: An Experimental and Molecular Simulation Study,” *Langmuir*, 2024/06/25, 2024.
[116] E. Wang, and J. B. Klauda, “Models for the Stratum Corneum Lipid Matrix: Effects of Ceramide Concentration, Ceramide Hydroxylation, and Free Fatty Acid Protonation,” *The Journal of Physical Chemistry B,* vol. 122, no. 50, pp. 11996-12008, 2018/12/20, 2018.
[117] M. Reuter, H. Schoenfelder, A. Gaiser, S. Volc, and D. Lunter, “Emulsifier-induced changes to the human skin barrier – Connection to ceramide profiles and assessment as a skin lesion model,” *Skin Pharmacology and Physiology*, 2025.
[118] A. L. Boulesteix, and K. Strimmer, “Partial least squares: a versatile tool for the analysis of high-dimensional genomic data,” *Brief Bioinform,* vol. 8, no. 1, pp. 32-44, Jan, 2007.
[119] B.-H. Mevik, and R. Wehrens, “Introduction to the pls Package,” *Help section of the “Pls” package of R studio software*, pp. 1-23, 2015.
[120] S. J. Marrink, and H. J. C. Berendsen, “Permeation Process of Small Molecules across Lipid Membranes Studied by Molecular Dynamics Simulations,” *The Journal of Physical Chemistry,* vol. 100, no. 41, pp. 16729-16738, 1996/01/01, 1996.
[121] H. J. C. Berendsen, and S.-J. Marrink, “Molecular dynamics of water transport through membranes: Water from solvent to solute,” *Pure and Applied Chemistry,* vol. 65, no. 12, pp. 2513-2520, 1993.
[122] J. M. Diamond, and Y. Katz, “Interpretation of nonelectrolyte partition coefficients between dimyristoyl lecithin and water,” *J Membr Biol,* vol. 17, no. 2, pp. 121-54, 1974.

[123] Z. Zhang, and D. J. Lunter, “Confocal Raman microspectroscopy as an alternative method to investigate the extraction of lipids from stratum corneum by emulsifiers and formulations,” *European Journal of Pharmaceutics and Biopharmaceutics,* vol. 127, pp. 61-71, 2018/06/01/, 2018.
[124] C. Choe, J. Schleusener, J. Lademann, and M. E. Darvin, “Human skin in vivo has a higher skin barrier function than porcine skin ex vivo-comprehensive Raman microscopic study of the stratum corneum,” *J Biophotonics,* vol. 11, no. 6, pp. e201700355, Jun, 2018.
[125] B. Školová, A. Kováčik, O. Tesař, L. Opálka, and K. Vávrová, “Phytosphingosine, sphingosine and dihydrosphingosine ceramides in model skin lipid membranes: permeability and biophysics,” *Biochimica et Biophysica Acta (BBA) - Biomembranes,* vol. 1859, no. 5, pp. 824-834, 2017/05/01/, 2017.
[126] H. Wang, and F. Meng, “The permeability enhancing mechanism of menthol on skin lipids: a molecular dynamics simulation study,” *J Mol Model,* vol. 23, no. 10, pp. 279, Sep 15, 2017.

Annex 1: Emulsifier-Induced Changes to the Human Skin Barrier: Connection to Ceramide Profiles and Assessment as a Skin Lesion Model

Moritz Reuter[a], Hans Schoenfelder[a], Annette Gaiser[a], Sebastian Volc[b], Dominique Jasmin Lunter[a]

[a] Department of Pharmaceutical Technology, Faculty of Science, Eberhard Karls Universität Tübingen, Auf der Morgenstelle 8, 72076 Tuebingen, Germany

[b] Department of Dermatology, University of Tuebingen, Liebermeisterstraße 25, 72076 Tuebingen, Germany

Skin Pharmacology and Physiology

Year 2025, Volume 38, Issue 3, Pages 79–91
DOI: 10.1159/000545234

Skin Pharmacology and Physiology

Research Article

Skin Pharmacol Physiol 2025;38:79–91
DOI: 10.1159/000545234

Received: December 10, 2024
Accepted: March 5, 2025
Published online: March 28, 2025

Emulsifier-Induced Changes to the Human Skin Barrier: Connection to Ceramide Profiles and Assessment as a Skin Lesion Model

Moritz Reuter[a] Hans Schoenfelder[a] Annette Gaiser[a] Sebastian Volc[b] Dominique Lunter[a]

[a]Department of Pharmaceutical Technology, Institute of Pharmacy and Biochemistry, Faculty of Science, Eberhard Karls University Tübingen, Tübingen, Germany; [b]Department of Dermatology, University Clinics Tübingen, Tübingen, Germany

Keywords
Skin analytics · Emulsifiers · Stratum corneum · Ceramides · Skin lipids · Lipidomics · Skin barrier

Abstract
Introduction: Emulsifiers are common excipients in dermal products stabilizing formulations such as creams and emulsions. But due to their potential for skin irritation, emulsifiers for pharmaceutical use should be tested regarding their tolerability before introducing them to the skin of patients. In this study, a systematic investigation with six oil in water-emulsifiers was performed on the forearms of 12 healthy human volunteers, six female, and six male. ***Methods:*** We analyzed the effects of pharmaceutical emulsifiers on the macroscopic skin health parameters measured as transepidermal water loss (TEWL) and skin hydration and measured the ceramide profile of the treated skin sites using liquid chromatography coupled to mass spectrometry in order to assess the skin tolerability of the investigated emulsifiers. In a second step, a Partial Least Squares Regression was employed to investigate relationships between changes in the ceramide profile to changes in the TEWL of skin treated with a nonionic as well as an anionic emulsifier. ***Results:*** Skin health measurements showed that the applied emulsifiers inflicted no significant changes compared to the water-treated sample, demonstrating a remarkable skin tolerability. The employed regression model showed a good fit as well as adequate prediction and identified ceramide species associated with impaired skin barrier function. Furthermore, it was found that the relationship between the ceramide profile and the skin barrier function in emulsifier-induced skin damage shows distinct similarities to the interplay of ceramides and skin barrier function in lesional skin linked to atopic dermatitis, hinting toward a common underlying mechanism and opening up possibilities to simulate disease-related changes to the skin for the development of skin damage models. ***Conclusion:*** In conclusion, these detailed investigations yield insight into possible mechanisms of emulsifier-induced skin damage and show its versatility in the investigation of pharmaceutical emulsifiers for formulation development as well as basic research.

Introduction

The stratum corneum (SC), being the uppermost layer of the epidermis, plays a crucial role in the integrity and upkeep of the physiological skin barrier [1]. Essential to the barrier function of the SC is its typical brick-and-mortar structure, describing the typical arrangement of the corneocytes (bricks) being embedded in a lamellar

karger@karger.com
www.karger.com/spp

Correspondence to:
Dominique Lunter, dominique.lunter@uni-tuebingen.de

Karger

Table 1. Nomenclature for ceramides used

Long chained base/fatty acid moiety	Non-hydroxylated FA	Hydroxylated FA	ω-esterified FA
Sphingosine	NS	AS	EOS
Phytosphingosine	NP	AP	EOP
Hydroxysphingosine	NH	AH	EOH
Dihydrosphingosine	DS	(ADS)	(EODS)

Chain lengths are given by number after the letters. Abbreviations in brackets indicate ceramides not investigated in this study. Nomenclature according to Motta et al. [21].

lipid matrix (mortar) [2]. This structure ensures protection against mechanical force and UV radiation provided by the corneocytes, while the continuous lipid matrix serves as a diffusion barrier for exogenous permeants as well as water from within the body. Impairment of this barrier results in increased permeability of the skin for environmental chemical substances as well as an increased trans-epidermal water loss (TEWL) of the body, which is a typical result of a disrupted intercellular SC lipid matrix [3–5]. The lipid matrix itself is comprised of cholesterol, free fatty acids and ceramides, of which ceramides are the largest component by weight and are increasingly becoming a focus of skin research [4]. Investigations have been published investigating their structural variety, abundance in the SC and their implication in various skin conditions, such as inflammatory skin diseases or impaired skin barrier in general [3, 6–17] as well as their potential in formulations aiming to alleviate these conditions [18–20]. The main goal of these studies was to investigate characteristic patterns of changes in the ceramide abundance or profile, which then can be linked to skin conditions. Characteristic changes in the ceramide profile of psoriatic skin [12, 21–23], ichthyosis-affected skin [24, 25] as well as skin affected with atopic dermatitis (AD) [22, 23, 26–30] have been documented in detail. These studies yield valuable insight into the mechanisms and implications of disease-related shifts in the ceramide profile, with some of them also investigating links and correlations between ceramide profile fluctuations and skin barrier function [22, 28, 30]. In particular, ceramide profile changes in clinical manifestations of AD and its accompanying effects on the skin barrier show quite distinct patterns. Lesional as well as non-lesional skin of patients with AD shows a significantly lower total ceramide content than the skin of healthy control subjects, while also exhibiting significant changes in the ceramide profile. [22, 27, 28, 31, 32]. Interestingly, lesional and non-lesional skin of the same AD patient cannot be differentiated by the total ceramide content of the skin, but only by the changes in the ceramide profile. Thus, the ratios of the different ceramide species and chain lengths found in the SC are the most significant ceramidomic discriminator between lesional and non-lesional AD skin. Typical for the changes observed in impaired, lesional skin is a shift toward shorter chain length ceramides, an increased ratio of ceramide NS to ceramide NP as well as a reduction in the ultra-long chain ceramide classes such as EOS, EOH, and EOP (see Table 1 for an overview of the ceramides investigated in this work) [22, 26, 28, 30]. The importance of seemingly tiny changes in the ceramide profile is demonstrated by the stark differences in the skin barrier properties of non-lesional and lesional skin, such as the TEWL and the skin hydration level. Interestingly, while AD patients' skin total ceramide content is lower than that of healthy control subjects, differences in skin properties are not observable in non-lesional skin [28, 32]. This implies that the relative composition of the ceramide species, and not the total ceramide content in the SC, plays a crucial role in skin health and properties of AD skin. This may be an important consideration in the development of novel model systems of AD improving on previous models [33] as well as in the pharmaceutical design of formulations for the treatment of lesional skin in AD [20, 31, 34, 35].

Yet, it is important to note that skin barrier impairment is not limited to diseased skin. Damage to the skin barrier can also be induced by contact with surfactants such as pharmaceutically or cosmetically used emulsifiers, especially with repeated exposure [36–40]. The mechanisms of the effect on the skin barrier are still not completely understood. Studies focusing on the SC lipid matrix found a disordering of the lipids following surfactant treatment [41], with multiple studies finding evidence for SC lipid extraction by surfactants and hence a disruption of the lipids of the skin barrier [41–44]. Other investigations postulated mechanisms based on

increased hydration of the space between the SC lipid leaflets [45] or denaturation of the keratin found in the corneocytes [46, 47], which may go hand in hand with changes in the composition of the lipid matrix, like the ceramide profile, in altering the skin barrier. While some basic research on the role of ceramides in emulsifier-induced skin damage has been performed [36, 38, 40, 43, 44], with some studies decades old, the effects of the various ceramide species and their influence on skin barrier function as well as skin health in general in this context still are not fully understood. Today, highly sophisticated methods like liquid chromatography coupled to mass spectrometry (LC-MS) have become widely available and offer the opportunity to investigate ceramide profiles in much more detail and may thus contribute to leveraging the knowledge on emulsifiers impact on SC ceramides to the next level.

The aim of this study was to gain deeper insight into the impact of emulsifiers on the SC via multiple analytical approaches. The first part comprises a general investigation and comparison of the effects of pharmaceutically and cosmetically utilized emulsifiers using a multimodal approach. This includes the biophysical skin health parameters such as TEWL to determine skin barrier integrity as well as capacitance measurements for skin hydration levels of 12 healthy volunteers. Afterward, the ceramide content and profile of the emulsifier treated sites were taken and the emulsifiers' impact on the ceramides analyzed to gain a better understanding on the impact of emulsifiers on the ceramides. To further investigate the mechanisms and possible links behind changes in the ceramide profile and impairment of skin barrier function caused by emulsifier treatment, a partial least squares (PLSs) regression analysis of changes in the ceramide profiles and skin health parameters was carried out in the second part of the study. The analysis compared the effects of an anionic surfactant to a nonionic emulsifier, with the goal to better understand their respective impact on the SC as well as to assess their respective suitability for the development of a skin damage model of lesional skin as found in AD, potentially eliminating the need for patient screening in development of new formulations for treatments of AD.

Materials and Methods

Materials

An overview of the investigated emulsifiers and information regarding their classification, suppliers, and hydrophilic-lipophilic balance (HLB) values can be found in Table 2. An overview of the ceramide standards used for this study can be found in Table 3. LC-MS grade 2-Propanol, methanol, acetonitrile, formic acid, and ethyl acetate were obtained from Carl Roth GmbH & Co. KG (Karlsruhe, Germany). LC-MS-Grade ammonium formate was obtained by Sigma-Aldrich Co. (St. Louis, MO, USA). All aqueous solutions were prepared using ultra-pure water from Elga Maxima (High Wycombe, Great Britain). Nitrogen was obtained from an in-house tank and argon 5.0 was obtained from Westfalen AG (Muenster, Germany). Here, 2 mL reaction vessels were obtained from Greiner Bio-One GmbH (Frickenhausen, Germany). Needles from Sterican 20 G × 1 $\frac{1}{2}$″, and 2 mL syringes were obtained from B. Braun Melsungen AG (Melsungen, Germany). Chromafil® Filters Xtra H-PTFE-20/25 and HPLC vials N8 flat, screw neck 8-425, screw caps N8, center hole, red rubber, FEP 1.3 mm were obtained from Macherey Nagel GmbH & Co. KG (Dueren, Germany).

Preparation of Emulsifier Solutions

Testing solutions of C20, S2, S20, S100, HPMC, and SLS were prepared as a 1% solution by stirring the substances in ultra-pure water, sonicating the resulting solutions (Bandelin Sonorex; Bandelin electronic GmbH & Co. KG, D-Berlin, Germany) for 15 min and then vortexing them for 1 min (IKA Vortex 2; IKA-Werke GmbH & Co. KG, Staufen, Germany) as described previously [39]. The plain ultra-pure water was used as a control.

Study Design

The study was carried out in accordance with the Declaration of Helsinki and the study protocol approved by the Ethics Committee at the Medical Faculty of the University of Tübingen (Approval No.: 221/2022BO2). All participants gave their informed written consent to their inclusion in the study. The participating 12 volunteers were of Caucasian ethnicity and in the age range of 25–52, with 6 male volunteers and 6 female. A questionnaire was given to every person asking about chronic skin diseases like eczema, AD, etc., even in childhood, as well as skin lesions, wounds, tattoos, scars, or excessive hair growth on the forearms. The volunteers were asked to refrain from showering or using any dermal skin products 12 h before the study and were requested not to conduct excessive exercise activities during the study.

The nondominant forearms were used for the investigation. The test areas were marked by a template to ensure appropriate space between the wrist, elbow, and the different samples. The test areas were randomized for every volunteer to avoid bias. Volunteers had to acclimate

Table 2. Overview of the investigated emulsifiers

Emulsifier used	Abbreviation	HLB value	Commercial name	Classification	Supplier
Sodium lauryl sulfate	SLS	40	–	Anionic	Caelo[a]
PEG-20 cetyl ether	C20	15.7	Brij™ C20	Nonionic	Croda[b]
PEG-2 stearyl ether	S2	4.9	Brij™ S2	Nonionic	Croda[b]
PEG-20 stearyl ether	S20	15.3	Brij™ S20	Nonionic	Croda[b]
PEG-100 stearyl ether	S100	18.8	Brij™ S100	Nonionic	Croda[b]
Hydroxypropyl methylcellulose	HPMC	*	Methocel E4M®	Nonionic (Polymer)	Caelo[a]

*No HLB value given by the supplier, apparent viscosity 4,000. [a]Caesar & Loretz GmbH (Hilden, Germany). [b]Croda GmbH (Nettetal, Germany).

Table 3. Overview of the ceramide standards used

Systematic name	Abbreviation	Commercial name
N-[26-oleoyloxy(d9) hexacosanoyl]-D-erythro-sphingosine	EOS26d9	CER1 (d18:1/26:0/18:1(d9))
N-palmitoyl(d9) D-ribo-phytosphingosine	NP16d9	CER3(d9)
N-(2′-(R)-hydroxypalmitoyl(d9)) D-erythro-sphingosine	AS16d9	CER5-2′R(d9)
N-(2′-(R)-hydroxypalmitoyl(d9)) D-ribo-phytosphingosine	AP16d9	CER6-2′R(d9)
N-(2′-(R)-hydroxypalmitoyl(d9)) 6R-hydroxysphingosine	AH16d9	CER7-2′R, 6R(d9)
N-palmitoyl(d9) 6R-hydroxysphingosine	NH16d9	CER8(d9)
N-[26-oleoyloxy(d9) hexacosanoyl]-D-ribo-phytosphingosine	EOP26d9	CER9(d9) (t18:0/26:0/18:1(d9))
N-palmitoyl(d9) dihydrosphingosine	DS16d9	CER10(d9)
N-palmitoyl(d7)-D-erythro-sphingosine	NS16d7	Deuterated Ceramide Lipidomix®
N-lignoceroyl(d7)-D-erythro-sphingosine	NS24d7	Deuterated Ceramide Lipidomix®

All ceramide standard substances were obtained from Avanti Polar Lipids Incorporation (Birmingham, AL, USA).

before the measurements for 30 min in the testing room at 25 ± 1°C and 32 ± 2% relative humidity. Temperature and relative humidity were recorded by a Klima logg pro TFA 30.3039 IT (Dostmann GmbH & Co. KG, Wertheim, Germany). After the acclimatization, 50 µL of the aqueous solutions were pipetted on filter paper discs (12 mm in diameter; SmartPractice®, Phoenix, AZ, USA). The filters were put onto the skin and then occluded with Finn Chambers® on Scanpor® (SmartPractice®). The volunteers were allowed to resume normal activities, and instructed to be careful with the Finn Chambers® on their forearms. After 4 h of incubation, the Finn Chambers® were peeled off and aqueous residues were dabbed off with tissues. The volunteers had to wait 15 min for equilibration in the testing room before proceeding. Then, second measurements were performed and the tape stripping procedure was initiated as specified in 2.8.

Measurement of TEWL

The TEWL was measured by the basic device Multi Probe Adapter MPA 6 and probe Tewameter® TM Hex (Courage & Khazaka electronic GmbH, Köln, Germany) and calculated by the software MPA CTplus (Courage & Khazaka electronic GmbH). Measurements were performed before and after treatment on all eight test areas. Every measurement lasted 90 s, with 30 s as equilibration and 60 s of measurement to collect stable values.

Measurement of Skin Hydration

The skin hydration was measured by the basic device Multi Probe Adapter MPA 6 and probe Corneometer® CM 825 (Courage & Khazaka electronic GmbH) and calculated by the proprietary software. Measurements were performed in triplicate.

Measurement of Skin Erythema

The erythema was measured by basic device Multi Probe Adapter MPA 6 and probe Mexameter® MX 18 (Courage & Khazaka electronic GmbH) and final values calculated by the proprietary software. Measurements were performed in triplicate with respect to changing the position as recommended by the manufacturer.

Measurement of Skin-pH

The skin-pH was measured by the basic device Multi Probe Adapter MPA 6 and probe Skin-pH-Meter® PH 905 (Courage & Khazaka electronic GmbH) and final values calculated by the proprietary software.

Tape Stripping

Tape stripping was used to obtain in vivo SC samples for the analysis of the ceramide profiles. After the incubation time of 4 h and the afore-described measurements, six consecutive strips (12 mm diameter; D-Squame® Stripping Discs Clinical and Derm, Dallas, TX, USA) were taken from every test area. A pressure control stick (D-Squame® Pressure Instrument Clinical and Derm, Dallas, TX, USA) was used to ensure constant pressure and the tape stripping direction was rotated by 90° for every tape to ensure uniform sampling. The tapes were weighed (AX26 DeltaRange® Mettler Toledo, Greifensee, Switzerland) before and after stripping to calculate the removed SC mass. Afterward, the tapes were extracted for LC-MS analysis, which is described in 2.9.

LC-MS Sample Preparation

The tapes from Tape Stripping were extracted with 2 mL methanol/ethyl acetate (80/20, V/V) in reaction vessels. The internal standards of Ceramide NS16d7, NS24d7, and EOS26d9 were added and the samples shaken (by IKA Vibrax VXR basic; IKA-Werke GmbH & Co. KG, Staufen, Germany) for 3 h. After shaking, the samples were sonicated for 15 min (Bandelin Sonorex; Bandelin electronic GmbH & Co. KG, Berlin, Germany) and vortexed for 1 min (IKA-Werke GmbH & Co. KG). In the next step, the samples were centrifuged for 10 min at 13,400 rpm (MiniSpin® Eppendorf SE, Hamburg, Germany). The supernatant was removed with a 20 G × $1\frac{1}{2}''$ needle and 2 mL syringe and filtered (Chromafil® Xtra H-PTFE-20/25; Macherey Nagel GmbH & Co. KG, Dueren, Germany) into HPLC vials (Vial N8 flat, screw neck 8-425, screw caps N8, center hole, red rubber, FEP 1.3 mm; Macherey-Nagel GmbH & Co. KG, Dueren, Germany).

LC-MS Analysis

All samples were analyzed using reverse-phase ultra-high-performance liquid chromatography (UHPLC) (Nexera LC-40; Shimadzu Corporation, Kyoto, Japan) with mass spectrometry (LCMS-8045; Shimadzu Corporation, Kyoto, Japan). The UHPLC separation step was performed with a RP C8 column (HPLC Nucleodur C8 Gravity 3 μm Macherey-Nagel GmbH & Co. KG with Column-Protection-System Guard Column Holder Macherey-Nagel GmbH & Co. KG, Dueren, Germany) using a binary gradient, with the total method duration being 20 min. The UHPLC used a flow rate of 0.4 mL/min and the following gradient: Eluent A: 10 μM ammonium formate in water; Eluent B: 0.1% (v/v) formic acid in isopropanol/acetonitrile 50/50. Concentration of eluent B over time: 0 min: 10%; 0.5 min: 20%; 1 min: 40%; 12.5 min: 92.5% (nonlinear curve); 12.6 min: 100%; 17 min: 100%; 18 min: 20%; 20 min: 20%. After chromatographic separation, the ceramide content was determined in the MS using the following settings: electrospray ionization (ESI) positive ionization mode; interface voltage: 3 kV; interface temperature: 220°C; desolvation temperature: 355°C. Ceramides were quantified using a multiple reaction monitoring (MRM) method. Precursor ions in the Quadrupole 1 were either the $[M + H]^+$ ion for the ceramide groups NP, AP, DS, EOS, EOP, and EOH, or $[M - H_2O + H]^+$ for ceramide groups NS, AS, NH, and AH. After fragmentation, the fragments specific for the different long-chained base (LCB) segments of the ceramides [11] were used for product ion quantification of the ceramides. A full table of the precursor ions, collision energies as well as the corresponding product ions can be found in the online supplementary material (for all online suppl. material, see https://doi.org/10.1159/000545234). Ceramide species included in the method were chosen for their high abundance in human skin. They comprise the ten most abundant ceramide species in the human SC [48, 49] with a chain length range of C20 to C28 for non-EO ceramides (with AS16 added due to its unusually high abundance) as well as C28 to C35 for EO ceramides. The obtained intensities were then normalized to the internal standards of ceramide NS16d7, NS24d7 as well as ceramide EOS26d9, matching closest to the retention time as well as the ceramide species. Concentrations were then calculated from the normalized intensities using calibration curves of AH16d9, NH16d9, AP16d9, NP16d9, AS16d9, NS16d9, DS16d9 as well as EOS26d9 and EOP26d9. For the EOH ceramides, the AH16d9 calibration curve was used for the calculation, due to the nonavailability of deuterated EOH standard substances. The calculated concentrations were then normalized

using the mass of the extracted SC to obtain the final ceramide content. The value of all tapes for a specific test area and volunteer was then averaged. Data processing was performed using Shimadzu LabSolutions (Shimadzu Deutschland GmbH, Duisburg, Germany), Microsoft Excel (Microsoft, Redmond, WA, USA) as well as R (R Foundation for Statistical Computing, Vienna, Austria).

Statistical Analysis

The data originated from 12 subjects ($n = 12$). Fisher's Least Significant Difference test was used in GraphPad Prism 8.0 to detect statistical differences (GraphPad Software Inc., La Jolla, CA, USA). To build a statistical model linking changes in the ceramide content to changes in the TEWL, PLSs regression analysis was applied to the results. As SLS and C20 were determined in a previous study [41] to have a particularly high potential for damaging the skin, they were chosen to analyze the suitability for building a regression model using either an anionic surfactant (SLS) or a nonionic surfactant (C20). For each volunteer, the differences in the content of each ceramide species between the water-treated skin site as well as the either the SLS- or the C20-treated skin site were calculated and used as the predictor matrix. Columns containing missing values were excluded. For the response matrix, the differences in the TEWL values after treatment of the respective skin sites were calculated, and the obtained differences were used. Predictors and response were standardized, and PLS models were built [50]. The obtained models were validated using leave-one-out cross-validation. Selection of the number of PLS components was done by selecting the model with the fewest components as well as within a minimum of the root mean square error of prediction obtained from cross-validation and a maximum number of components of 5. R^2 as the goodness-of-fit parameter as well as Q^2 as the predictive property parameter were calculated. All regression-related computations were performed in R.

Results

Skin Health Parameters

For in vivo human skin studies the TEWL is a value for the determination of skin health or disease, and, in particular, a parameter of the intactness of the skin barrier function [39]. Therefore, this measurement was taken to assess the potential for skin barrier damage by treatment with the different emulsifier solutions, while capacitance measurements were used to investigate changes in the skin hydration, indicating the skin tolerability of the emulsifiers in question. The S2/C20/S20/S100 line was chosen to represent nonionic emulsifiers with varying hydrophilicity, but the same underlying molecular structure of pegylated fatty alcohol-ethers. SLS was chosen to be representative of common anionic emulsifiers, while HPMC was chosen as a nonionic polymeric emulsifier. All volunteers showed TEWL values below 20 $g \cdot m^{-2} \cdot h^{-1}$, suggesting their skin was healthy and intact prior to the study. Figure 1a shows the TEWL changes after emulsifier treatment. SLS-treated skin areas showed the highest TEWL change value of the investigated emulsifiers, with a significant increase when compared with water-treated skin used as control ($p = 0.0189$). The other emulsifiers behaved like the control treatment and showed no significant increase in TEWL change.

Capacitance results in Figure 1b show that the skin treated with SLS significantly ($p = 0.0015$) lost hydration. The other emulsifiers behaved like the control and were not significantly different. As increased TEWL and decreased hydration are often linked, the observed trends correlate well. The results of the skin pH measurements as well as the erythema index showed no difference between the treatment sites.

Total Ceramide Content

A comparison of the total ceramide content of the skin sites treated with the individual emulsifiers can be seen in Figure 2a. There is no significant difference in total ceramide content between the different treatments. This was somewhat surprising as TEWL and hydration measurements suggested changes of the skin barrier properties for the SLS-treated sites, while there was no difference in total ceramide content either. We thus chose to more closely evaluate the different ceramide species.

Regression Analysis

A PLS regression linking the changes in the ceramide profile to changes in the TEWL value between water and SLS-treated skin as well as between water and C20-treated skin was performed. The PLS regression methodology was chosen as it is most appropriate in case of low sample size compared to the number of predictor variables in the model as well as the multicollinearity present in the data set [51]. The SLS-based model yielded a 2-component PLS model with an R^2 value of 0.67 and a Q^2 value of 0.44, indicating good prediction properties with slight overfitting. The C20-based model yielded a 2-component PLS model with an R^2 value of 0.27 and a Q^2 value of <0, indicating no predictive value. The prediction plot of the SLS-based regression model can be seen in Figure 2b. Following these results, the model based on the SLS-

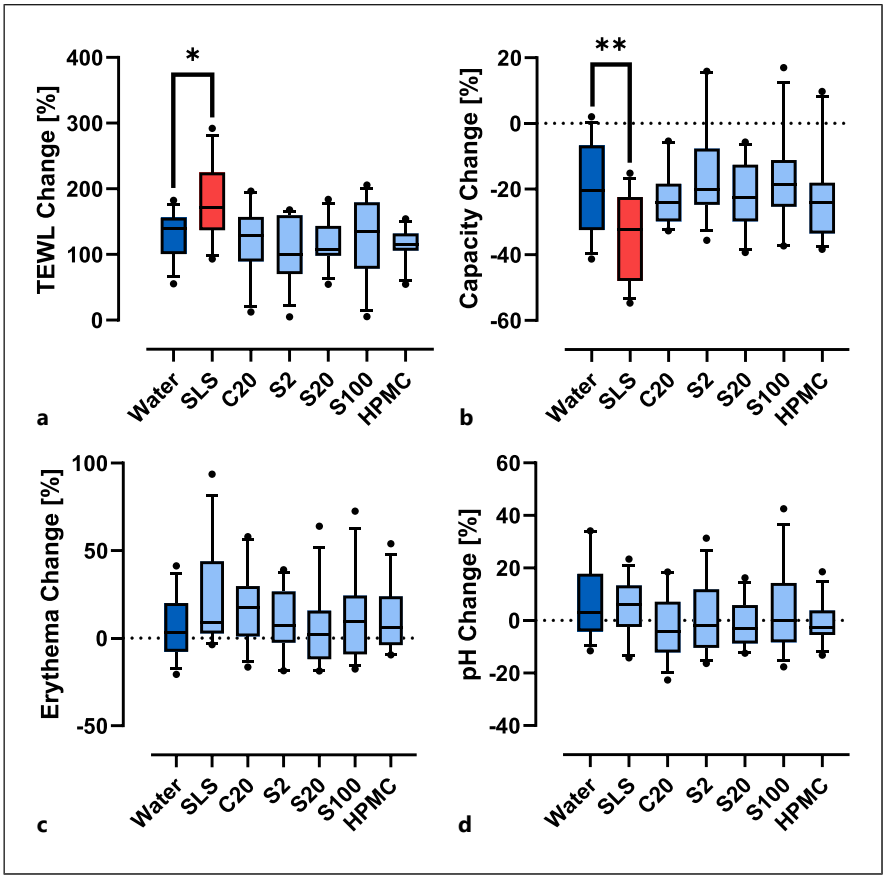

Fig. 1. Skin health parameter measurement results. **a** TEWL. **b** Skin capacitance (skin hydration). **c** Skin pH. **d** Erythema measurement. Each box encloses the values' interquartile range, the boxed line represents the median. Whiskers from 10th to 90th percentile. $n = 12$. Color index – deep blue: water, control treatment; light blue: no significant difference from control treatment; red: significant difference from control treatment. Significant differences are further indicated by the number of asterisks as follows: $*p < 0.05$; $**p < 0.01$.

treated skin was chosen for further investigation into model properties. The regression coefficients for each ceramide, obtained from the model, are shown in a heat map format in Figure 3. A table containing the numerical values can be found in the online supplementary material. A high correlation coefficient (red color) implies a correlation with positive changes in TEWL value, which is associated with an impaired skin barrier or damaged skin in general. Studying the coefficients in relation to chain length, one can see that for most non-EO subgroups, the correlation coefficients of longer chain lengths tend toward lower values, implying an association with a well-functioning skin barrier. The results also show a high dependency of the regression coefficients on the subgroup type. While ceramides of the subgroups NP and AP (especially with an emphasis on longer chain lengths) show generally lower regression coefficients (associated with intact barrier properties), sphingosine-based ceramides such as NS and AS show higher regression coefficients (associated with barrier impairment). AH, NH, and DS show a more balanced effect on the skin barrier function, with the shorter chain lengths generally having positive coefficients and the longer chain lengths having negative coefficients. EO-type ceramides cannot be classified the same way. While all the EO-type ceramide classes show generally low regression coefficients, indicating a beneficial effect on the skin barrier integrity, this effect is more pronounced in classes EOH and EOP. Furthermore, as seen in Figure 2d, there exists a positive correlation between longer chain lengths and a higher regression coefficient, reversing the trend seen in the non-EO ceramide classes (Fig. 2c). This effect is mostly driven by the ultra-long chained EOS ceramides and is quite noteworthy, yet none of the EO-type ceramides show a strong association with skin barrier impairment.

Discussion

In vivo studies investigating the impact of emulsifiers on human skin are a valuable resource to examine the suitability of emulsifiers as excipients in dermal formulations as well as to gain insight into the possible effects on the SC and mechanisms thereof. As these phenomena can

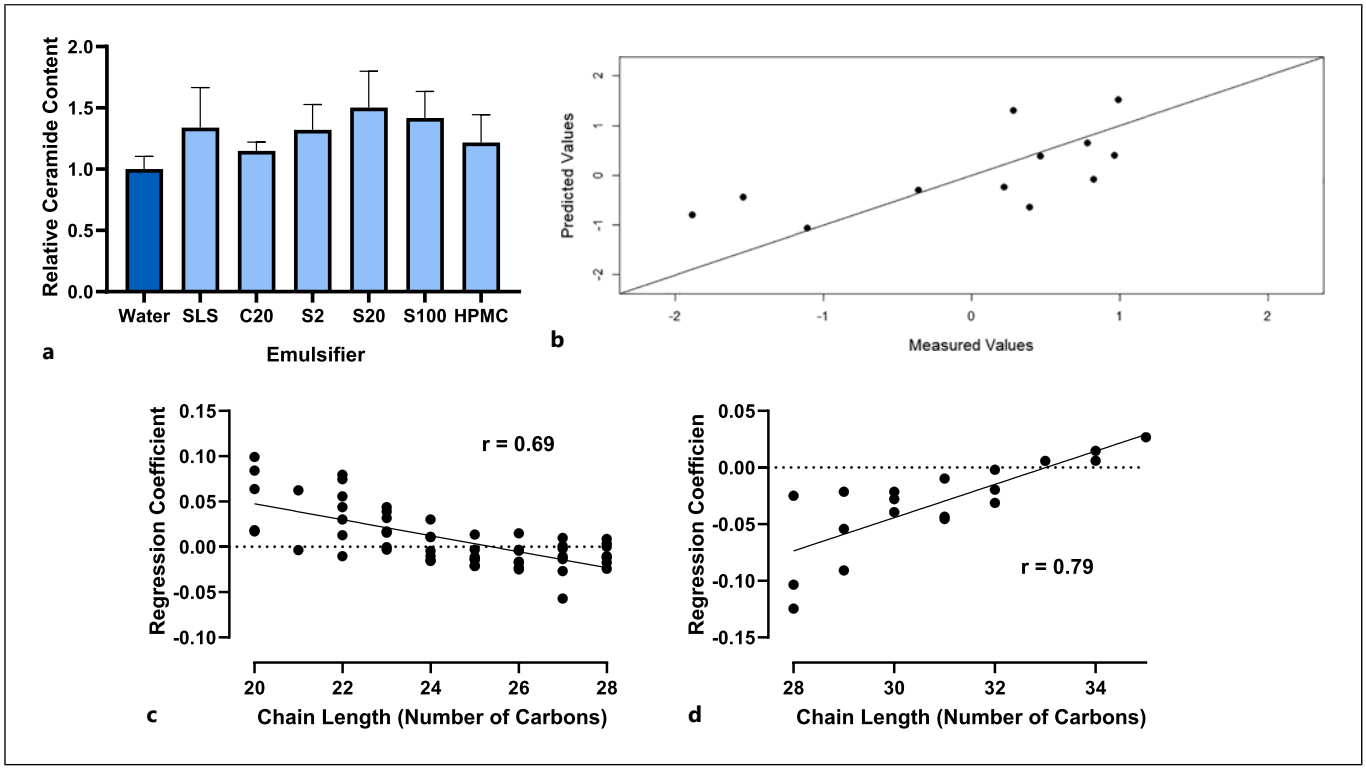

Fig. 2. a Total ceramide content relative to the control. Control (water) has a relative content of 1. Mean ± standard error of the mean (SEM), $n = 12$. **b** Prediction plot of the cross-validated PLS model based on the SLS-treated skin sites. Predicted values from the model are graphed on the *x*-axis, measured values are graphed on the *y*-axis. The dashed line represents perfect prediction. Regression scatterplots graphing the ceramide fatty acid chain length against the regression coefficients obtained from the model based on the SLS-treated skin sites. **c** Non-EO-type ceramides. **d** EO-type ceramides.

be investigated directly in living, human skin, there are no uncertainties as to the transferability of results, be it from one species to another as when utilizing animal models or from cadaver skin to living tissue, as in in vitro models utilizing excised skin samples. Previous studies investigating effects of emulsifier treatment on skin health found different degrees of skin tolerability of the emulsifiers studied To mention examples, Vater et al. [52] found phospholipid-based emulsifiers to have a very high skin tolerability, while our group previously investigated pegylated nonionic emulsifiers and found there was a wide spread in skin tolerability as well as influence on the SC lipids [41, 53]. The current study employs similar methods to determine the skin health parameters, i.e., TEWL and hydration measurements to determine the skin barrier function. Utilizing these parameters to determine the skin tolerability, all investigated nonionic emulsifiers showed neither a significant impairment of the skin barrier nor a decreased hydration of the treated sites, exhibiting an exceptionally high-skin tolerability. Only the treatment sites where anionic SLS was applied showed a significant drop in skin hydration as well as a notable impairment of the skin barrier function (increase in TEWL). While this was expected and SLS was used as a positive control for the general skin tolerability assessment in previous studies [41, 53], the results on nonionic emulsifiers contrasts quite clearly with our previous results as even C20, which was previously characterized to have the highest skin-damaging potential [41] did not show any adverse effects in this current in vivo study. The measurements and comparison of the treatment sites' total ceramide content continues the same trend. The comparison showed no significant differences of the effects of the investigated emulsifiers to the water control, with none of the studied nonionic emulsifiers altering the total ceramide content of the SC to a significant degree. Interestingly, SLS, despite its detrimental effects on the skin health parameters, also showed no significant decrease in total ceramide content. These results are seemingly in contrast to previous studies [37, 38, 41, 42, 54], which showed a significant effect of emulsifier treatment as well as marked differences in the effect of

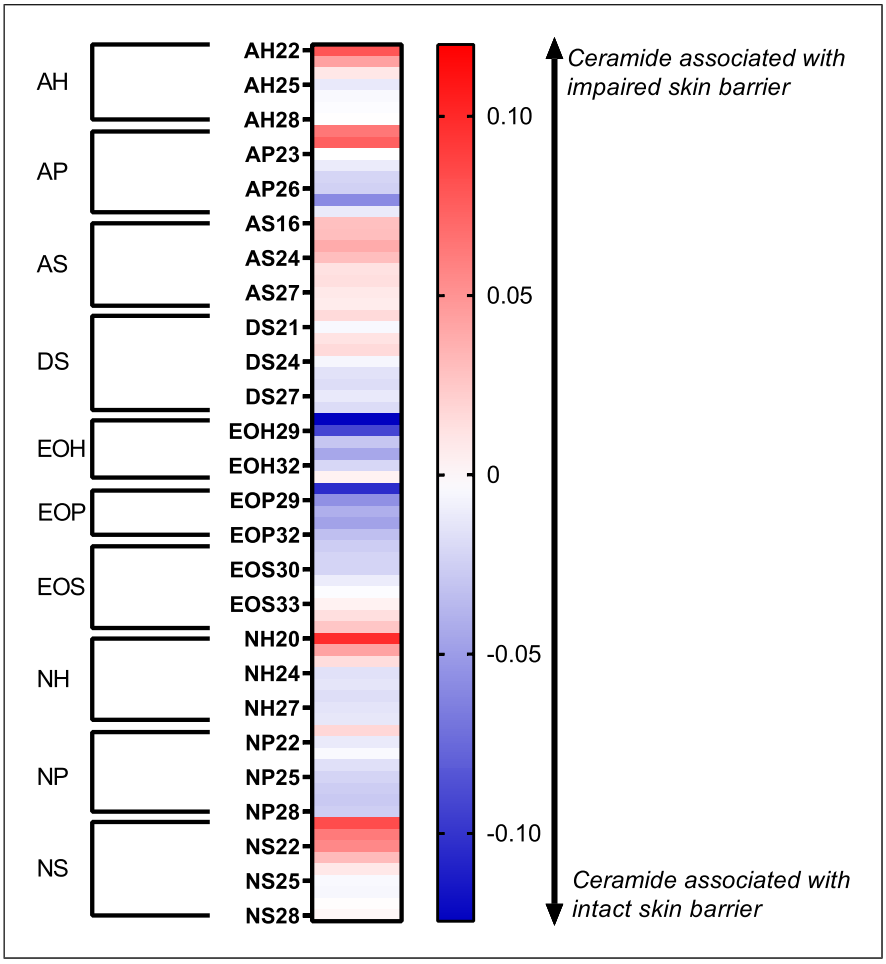

Fig. 3. Heatmap of the coefficient values of the PLS model based on the SLS-treated skin sites. Ceramides are grouped by family and organized by chain length, with the color of the field indicating the degree of association with an impaired or intact skin barrier. A positive regression coefficient implies a positive correlation between the ceramide in question and measured skin impairment, implying a higher abundance of this ceramide in damaged skin. Positive coefficient values are colored red, negative coefficient values (being associated with an intact skin barrier) are colored blue.

different emulsifiers, but a few important points have to be noted to contextualize these results. First, while the mentioned studies showed a significant lipid removal from the skin due to the emulsifiers, they did not discriminate the lipid species, but investigated ceramides, free fatty acids, and cholesterol as a whole. The reason for this being the fact that the method used (confocal Raman spectroscopy) cannot differentiate between the different lipid species. Free fatty acids in particular are being known to be easily removed from the SC with emulsifiers, which might explain the discrepancy [55]. Second, many of the studies investigated the emulsifier effects in ex vivo skin, which is understood to have a lower barrier function than living skin, which may make it more susceptible to emulsifier effects in general. The notable exception to both of these points is the study of Imokawa [42], which showed ceramide removal from human in vivo skin, but using a five-fold higher SLS concentration than used in our current study. On the other hand, Froebe et al. [43] and Fulmer et al. [44] showed in their respective studies that total ceramide content following emulsifier treatment undergoes only slight changes. Yet, this does not mean that emulsifier treatment has no effect at all on the ceramides in the SC. Changes in the ceramide profile following emulsifier treatment are documented to occur and relate to changes in skin health parameters [36, 40, 44]. This is being advanced and detailed in the ceramide profiling and regression analysis done in our current investigation. Correlations between emulsifier-induced changes in the ceramide profile and the skin barrier impairment, measured as TEWL, were established using a PLS regression model linking the two measurements to characterize the impact of nonionic emulsifiers such as C20 as well as the harsh anionic surfactant SLS. In vivo investigations into correlations between skin barrier function and ceramide profile exist, yet focus mainly on healthy skin or disease-related skin barrier impairment, such as lesional AD skin [22, 27, 28, 30]. On the other hand, correlation studies of emulsifier-induced skin damage are scarce [36]. For the present work,

comparisons to the known effects and changes on the ceramide profile in AD are essential, as we aim to not only gain insight into the changes in the ceramide profile linked to the SC impact of emulsifier treatment, but to also assess the feasibility of using surfactant damage to healthy skin as a possible model of AD lesional skin by analysis of the correlations drawn between skin health and ceramides by our regression models. Looking at the models built using the available data, only the SLS-based analysis produced meaningful values regarding correlation between ceramides and the skin barrier function, eclipsing the model based on C20-treated skin sites in goodness-of-fit as well as the closely associated prediction potential. Furthermore, the ceramide-skin barrier correlations as found in the studied SLS-based model are in good agreement with the findings of studies on those of lesional skin in AD The results from the SLS-based model associate a high abundance of ceramide NP and low abundance of ceramide NS with an intact skin barrier, exhibiting the same effects as described in the literature regarding AD [22, 28], with the ceramide species with an alpha-hydroxylated fatty acid moiety, AP and AS, showing similar behavior to NP and NS, respectively. In the present model, the effects of EO ceramides present a strong association between ceramides of the classes EOH as well as EOP and an intact skin barrier, as was observed in atopic lesions by Janssens et al. [30] as well as to a slightly lesser extent by Ishikawa et al. [28], with class EOS having a more attenuated effect in our study, matching closer with Janssens' et al. [30] model than Ishikawa's et al. [28], and inviting further investigation into the effects of the ultra-long chain ceramide classes. Regarding the effect of ceramide chain length, studies by Janssens et al. [30] as well as Ishikawa et al. [28] linked a higher abundance of shorter chain length-ceramides to an impaired barrier function, which is the same correlation that our current study found in SLS-induced skin damage, at least regarding the non-EO ceramides. For the EO ceramides, this study found the trend to reverse, although this effect should be seen as having limited significance, with the EO ceramides especially with a chain length above 32 carbons occurring only as traces and therefore having a higher chance of falling below the limit of quantification, which results in incomplete data for this range. Nonetheless, especially as the existing studies analyzing the effects of ceramide chain length tend to focus on non-EO ceramides [17, 28], this finding warrants further investigation in future studies. Overall, we have found clear analogies in the results regarding the connection between skin barrier properties and changes in the ceramide profile for damage caused by surfactant treatment of the skin and lesional AD skin. This is of particular relevancy, as the total ceramide content does not undergo significant changes. Adding to that, we found the reduction of the hydration and impairment of the barrier function of the SLS-treated skin to mirror the one found in lesional AD skin as reported in previous studies [36, 43]. Furthermore, SLS has long been used as an irritant marker in patch testing for type IV hypersensitization. Combined, these findings paint a convincing picture of the suitability of healthy, SLS-treated skin to be the basis for the development of future skin damage models emulating AD lesions as found in patients, enhancing the possibilities for evaluation of topical treatments for skin diseases to be tested in volunteers, thereby reducing the need for patient screening in a clinical setting.

Conclusion

This study investigated the impact of pharmaceutically used emulsifiers on the SC, taking into account biophysical skin barrier parameters as well as changes in the ceramide profile to assess skin tolerability of these emulsifiers as well as to further elucidate the interplay between ceramides and skin barrier function when exposed to emulsifiers. All of the investigated nonionic emulsifiers showed no significant effect on the skin barrier parameters as well as the total ceramide content. This makes these emulsifiers particularly suitable for use in pharmaceutical as well as cosmetic applications. To further investigate how surfactant-mediated impairment of skin barrier function relates to changes in the ceramide profile, data from SLS-treated skin were used to build a regression model, from which the regression coefficients, and therefore the effects of individual ceramide species on the skin barrier functionality could be obtained. The analysis showed characteristic relationships between shorter ceramide-linked fatty acid chain lengths and an impaired skin barrier as well as typical links between a higher abundance of ceramide classes NP and AP and a lower abundance of ceramide classes NS and AS with an intact skin barrier. This is in close agreement with the results from literature studies examining skin barrier impairment as is found in AD lesions. The main finding of this study is therefore the close similarity in the skin damage caused by SLS treatment to the typical skin impairments of lesional AD skin. This finding therefore enables and strengthens the validity of SLS-induced skin barrier disruption models to simulate disease-related skin barrier impairments as found in AD and hint toward a common underlying mechanism linking the ceramide profile to the skin barrier properties. This indicates a promising direction of future basic research as

well as its use in clinical research for development of formulations for treatment of inflammatory skin diseases and AD in particular.

Acknowledgments

The volunteers are acknowledged for their patience with the time-consuming measurements.

Statement of Ethics

Studies were carried out in accordance with the Declaration of Helsinki and the study in accordance with the ethics protocol approved by the Ethics Committee of the Medical Faculty of the University of Tübingen (Approval No.: 221/2022BO2). All participants gave their informed written consent to their inclusion in the study.

Conflict of Interest Statement

The authors have no conflicts of interest to declare.

Funding Sources

This research did not receive any specific grant from funding agencies in the public, commercial, or not-for-profit sectors.

Author Contributions

M.R.: LC-MS method development and validation, LC-MS sample preparation and measurements, statistical analysis, data curation, and writing – original draft. H.S.: study organization, sample administration, skin health measurements, data curation, and writing – review and editing. A.G.: tape stripping and data curation, and writing – review and editing. S.V.: study supervision and writing – review and editing. D.L.: conceptualization, methodology, study organization and supervision, resources, and writing – review and editing.

Data Availability Statement

The data that support the findings of this study are not publicly available for the privacy of the volunteers but are available from the corresponding author D.L. upon reasonable request.

References

1 Elias PM. Stratum corneum defensive functions: an integrated view. J Invest Dermatol. 2005;125(2):183–200. https://doi.org/10.1111/j.0022-202X.2005.23668.x
2 Menon GK, Cleary GW, Lane ME. The structure and function of the stratum corneum. Int J Pharm. 2012;435(1):3–9. https://doi.org/10.1016/j.ijpharm.2012.06.005
3 van Smeden J, Janssens M, Gooris GS, Bouwstra JA. The important role of stratum corneum lipids for the cutaneous barrier function. Biochim Biophys Acta. 2014;1841(3):295–313. https://doi.org/10.1016/j.bbalip.2013.11.006
4 Wertz PW, van den Bergh B. The physical, chemical and functional properties of lipids in the skin and other biological barriers. Chem Phys Lipids. 1998;91(2):85–96. https://doi.org/10.1016/s0009-3084(97)00108-4
5 Feingold KR, Elias PM. Role of lipids in the formation and maintenance of the cutaneous permeability barrier. Biochim Biophys Acta. 2014;1841(3):280–94. https://doi.org/10.1016/j.bbalip.2013.11.007
6 Beddoes CM, Gooris GS, Barlow DJ, Lawrence MJ, Dalgliesh RM, Malfois M, et al. The importance of ceramide headgroup for lipid localisation in skin lipid models. Biochim Biophys Acta Biomembr. 2022;1864(6):183886. https://doi.org/10.1016/j.bbamem.2022.183886
7 Berkers T, Visscher D, Gooris GS, Bouwstra JA. Topically applied ceramides interact with the stratum corneum lipid matrix in compromised ex vivo skin. Pharm Res. 2018;35(3):48. https://doi.org/10.1007/s11095-017-2288-y
8 Ge F, Sun K, Hu Z, Dong X. Role of omega-hydroxy ceramides in epidermis: biosynthesis, barrier integrity and analyzing method. Int J Mol Sci. 2023;24(5):5035. https://doi.org/10.3390/ijms24055035
9 Groen D, Poole DS, Gooris GS, Bouwstra JA. Investigating the barrier function of skin lipid models with varying compositions. Eur J Pharm Biopharm. 2011;79(2):334–42. https://doi.org/10.1016/j.ejpb.2011.05.007
10 Lee J-Y, Jeon S, Han S, Liu K-H, Cho Y, Kim K-P. Positive correlation of triacylglycerols with increased chain length and unsaturation with ω-O-acylceramide and ceramide-NP as well as acidic pH in the skin surface of healthy Korean adults. Metabolites. 2022;13(1):31. https://doi.org/10.3390/metabo13010031
11 Kawana M, Miyamoto M, Ohno Y, Kihara A. Comparative profiling and comprehensive quantification of stratum corneum ceramides in humans and mice by LC/MS/MS. J Lipid Res. 2020;61(6):884–95. https://doi.org/10.1194/jlr.RA120000671
12 Łuczaj W, Wroński A, Domingues P, Domingues MR, Skrzydlewska E. Lipidomic analysis reveals specific differences between fibroblast and keratinocyte ceramide profile of patients with psoriasis vulgaris. Molecules. 2020;25(3):630. https://doi.org/10.3390/molecules25030630
13 Łuczaj W, Jastrząb A, do Rosário Domingues M, Domingues P, Skrzydlewska E. Changes in phospholipid/ceramide profiles and eicosanoid levels in the plasma of rats irradiated with UV rays and treated topically with cannabidiol. Int J Mol Sci. 2021;22(16):8700. https://doi.org/10.3390/ijms22168700
14 Vávrová K, Kováčik A, Opálka L. Ceramides in the skin barrier. Eur Pharmaceut J. 2017;64(2):28–35. https://doi.org/10.1515/afpuc-2017-0004
15 Wertz PW. Linoleate-containing acylglucosylceramide, acylceramide, and events associated with formation of the epidermal permeability barrier. Skin Pharmacol Physiol. 2023;36(5):225–34. https://doi.org/10.1159/000535049
16 Kessner D, Ruettinger A, Kiselev MA, Wartewig S, Neubert RHH. Properties of ceramides and their impact on the stratum corneum structure: part 2 – stratum corneum lipid model systems. Skin Pharmacol Physiol. 2008;21(2):58–74. https://doi.org/10.1159/000112956
17 Novotný J, Janůsová B, Novotný M, Hrabálek A, Vávrová K. Short-chain ceramides decrease skin barrier properties. Skin Pharmacol Physiol. 2009;22(1):22–30. https://doi.org/10.1159/000183923
18 Shin K-O, Ishida K, Mihara H, Choi Y, Park J-H, Park S-H, et al. Diesel particulate matter permeation into normal human skin and intervention using a topical ceramide formulation. Skin Pharmacol Physiol. 2024;37(1–3):32–9. https://doi.org/10.1159/000539291

19 Altgilbers S, Rippke F, Filbry A, Conzelmann S, Vietzke JP, Burkhardt T, et al. A biomimetic combination of actives enhances skin hydration and barrier function via modulation of gene expression: results of two double-blind, vehicle-controlled clinical studies. Skin Pharmacol Physiol. 2022;35(2):102–11. https://doi.org/10.1159/000520009
20 Lim SH, Kim EJ, Lee CH, Park GH, Yoo KM, Nam SJ, et al. A lipid mixture enriched by ceramide NP with fatty acids of diverse chain lengths contributes to restore the skin barrier function impaired by topical corticosteroid. Skin Pharmacol Physiol. 2022;35(2):112–23. https://doi.org/10.1159/000518517
21 Motta S, Monti M, Sesana S, Caputo R, Carelli S, Ghidoni R. Ceramide composition of the psoriatic scale. Biochim Biophys Acta. 1993;1182(2):147–51. https://doi.org/10.1016/0925-4439(93)90135-n
22 Yokose U, Ishikawa J, Morokuma Y, Naoe A, Inoue Y, Yasuda Y, et al. The ceramide [NP]/[NS] ratio in the stratum corneum is a potential marker for skin properties and epidermal differentiation. BMC Dermatol. 2020;20(1):6. https://doi.org/10.1186/s12895-020-00102-1
23 Merleev AA, Le ST, Alexanian C, Toussi A, Xie Y, Marusina AI, et al. Biogeographic and disease-specific alterations in epidermal lipid composition and single-cell analysis of acral keratinocytes. JCI Insight. 2022;7(16):e159762. https://doi.org/10.1172/jci.insight.159762
24 Lavrijsen APM, Bouwstra JA, Gooris GS, Weerheim A, Boddé HE, Ponec M. Reduced skin barrier function parallels abnormal stratum corneum lipid organization in patients with lamellar ichthyosis. J Invest Dermatol. 1995;105(4):619–24. https://doi.org/10.1111/1523-1747.ep12323752
25 Eckl K-M, Tidhar R, Thiele H, Oji V, Hausser I, Brodesser S, et al. Impaired epidermal ceramide synthesis causes autosomal recessive congenital ichthyosis and reveals the importance of ceramide acyl chain length. J Invest Dermatol. 2013;133(9):2202–11. https://doi.org/10.1038/jid.2013.153
26 Di Nardo A, Wertz P, Giannetti A, Seidenari S. Ceramide and cholesterol composition of the skin of patients with atopic dermatitis. Acta Derm Venereol. 1998;78(1):27–30. https://doi.org/10.1080/00015559850135788
27 Joo K-M, Hwang J-H, Bae S, Nahm D-H, Park H-S, Ye Y-M, et al. Relationship of ceramide–, and free fatty acid–cholesterol ratios in the stratum corneum with skin barrier function of normal, atopic dermatitis lesional and non-lesional skins. J Dermatol Sci. 2015;77(1):71–4. https://doi.org/10.1016/j.jdermsci.2014.10.001
28 Ishikawa J, Narita H, Kondo N, Hotta M, Takagi Y, Masukawa Y, et al. Changes in the ceramide profile of atopic dermatitis patients. J Invest Dermatol. 2010;130(10):2511–4. https://doi.org/10.1038/jid.2010.161
29 Sho Y, Sakai T, Sato T, Sonezaki M, Taima H, Taguchi H, et al. Stratum corneum ceramide profiles provide reliable indicators of remission and potential flares in atopic dermatitis. J Invest Dermatol. 2022;142(12):3184–91.e7. https://doi.org/10.1016/j.jid.2022.06.012
30 Janssens M, van Smeden J, Gooris GS, Bras W, Portale G, Caspers PJ, et al. Increase in short-chain ceramides correlates with an altered lipid organization and decreased barrier function in atopic eczema patients. J Lipid Res. 2012;53(12):2755–66. https://doi.org/10.1194/jlr.P030338
31 Sahle FF, Gebre-Mariam T, Dobner B, Wohlrab J, Neubert RH. Skin diseases associated with the depletion of stratum corneum lipids and stratum corneum lipid substitution therapy. Skin Pharmacol Physiol. 2015;28(1):42–55. https://doi.org/10.1159/000360009
32 Imokawa G, Abe A, Jin K, Higaki Y, Kawashima M, Hidano A. Decreased level of ceramides in stratum corneum of atopic dermatitis: an etiologic factor in atopic dry skin? J Invest Dermatol. 1991;96(4):523–6. https://doi.org/10.1111/1523-1747.ep12470233
33 Simonsen L, Fullerton A. Development of an in vitro skin permeation model simulating atopic dermatitis skin for the evaluation of dermatological products. Skin Pharmacol Physiol. 2007;20(5):230–6. https://doi.org/10.1159/000104421
34 Elias PM, Wakefield JS, Man MQ. Moisturizers versus current and next-generation barrier repair therapy for the management of atopic dermatitis. Skin Pharmacol Physiol. 2019;32(1):1–7. https://doi.org/10.1159/000493641
35 Tessema EN, Gebre-Mariam T, Neubert RHH, Wohlrab J. Potential applications of phyto-derived ceramides in improving epidermal barrier function. Skin Pharmacol Physiol. 2017;30(3):115–38. https://doi.org/10.1159/000464337
36 di Nardo A, Sugino K, Wertz P, Ademola J, Maibach HI. Sodium Lauryl Sulfate (SLS) induced irritant contact dermatitis: a correlation study between ceramides and in vivo parameters of irritation. Contact Dermat. 1996;35(2):86–91. https://doi.org/10.1111/j.1600-0536.1996.tb02296.x
37 Imokawa G, Akasaki S, Minematsu Y, Kawai M. Importance of intercellular lipids in water-retention properties of the stratum corneum: induction and recovery study of surfactant dry skin. Arch Dermatol Res. 1989;281(1):45–51. https://doi.org/10.1007/BF00424272
38 Takagi Y, Nakagawa H, Higuchi K, Imokawa G. Characterization of surfactant-induced skin damage through barrier recovery induced by pseudoacylceramides. Dermatology. 2005;211(2):128–34. https://doi.org/10.1159/000086442
39 Schoenfelder H, Liu Y, Lunter DJ. Systematic investigation of factors, such as the impact of emulsifiers, which influence the measurement of skin barrier integrity by in-vitro Trans-Epidermal Water Loss (TEWL). Int J Pharm. 2023;638:122930. https://doi.org/10.1016/j.ijpharm.2023.122930
40 Park S, Kim J, Cho SI, Kim K, Cho H, Park C, et al. Induction of a hardening phenomenon and quantitative changes of ceramides in stratum corneum. Ann Dermatol. 2014;26(1):35–42. https://doi.org/10.5021/ad.2014.26.1.35
41 Liu Y, Lunter DJ. Systematic investigation of the effect of non-ionic emulsifiers on skin by confocal Raman spectroscopy: a comprehensive lipid analysis. Pharmaceutics. 2020;12(3):223. https://doi.org/10.3390/pharmaceutics12030223
42 Imokawa G. Surfactant-induced depletion of ceramides and other intercellular lipids: implication for the mechanism leading to dehydration of the stratum corneum. Exog Dermatol. 2005;3(2):81–98. https://doi.org/10.1159/000086158
43 Froebe CL, Simion FA, Rhein LD, Cagan RH, Kligman A. Stratum corneum lipid removal by surfactants: relation to in vivo irritation. Dermatologica. 1990;181(4):277–83. https://doi.org/10.1159/000247822
44 Fulmer AW, Kramer GJ. Stratum corneum lipid abnormalities in surfactant-induced dry scaly skin. J Invest Dermatol. 1986;86(5):598–602. https://doi.org/10.1111/1523-1747.ep12355351
45 Chen Y, Liao M, Ma K, Wang Z, Demé B, Penfold J, et al. Implications of surfactant hydrophobic chain architecture on the Surfactant-Skin lipid model interaction. J Colloid Interface Sci. 2022;608(Pt 1):405–15. https://doi.org/10.1016/j.jcis.2021.09.098
46 Seweryn A. Interactions between surfactants and the skin: theory and practice. Adv Colloid Interface Sci. 2018;256:242–55. https://doi.org/10.1016/j.cis.2018.04.002
47 Imokawa G, Sumura K, Katsumi M. Study on skin roughness caused by surfactants: II. Correlation between protein denaturation and skin roughness. J Am Oil Chem Soc. 1975;52(12):484–9. https://doi.org/10.1007/BF02640737
48 van Smeden J, Boiten WA, Hankemeier T, Rissmann R, Bouwstra JA, Vreeken RJ. Combined LC/MS-platform for analysis of all major stratum corneum lipids, and the profiling of skin substitutes. Biochim Biophys Acta. 2014;1841(1):70–9. https://doi.org/10.1016/j.bbalip.2013.10.002
49 Suzuki M, Ohno Y, Kihara A. Whole picture of human stratum corneum ceramides, including the chain-length diversity of long-chain bases. J Lipid Res. 2022;63(7):100235. https://doi.org/10.1016/j.jlr.2022.100235
50 Mevik B-H, Wehrens R. Introduction to the pls package. Help section of the "Pls" package of R studio software; 2015. p. 1–23.

51 Boulesteix A-L, Strimmer K. Partial least squares: a versatile tool for the analysis of high-dimensional genomic data. Brief Bioinform. 2007;8(1):32–44.
52 Vater C, Apanovic A, Riethmüller C, Litschauer B, Wolzt M, Valenta C, et al. Changes in skin barrier function after repeated exposition to phospholipid-based surfactants and sodium dodecyl sulfate in vivo and corneocyte surface analysis by atomic force microscopy. Pharmaceutics. 2021;13(4):436. https://doi.org/10.3390/pharmaceutics13040436
53 Liu Y, Ilić T, Pantelic I, Savić S, Lunter DJ. Topically applied lipid-containing emulsions based on PEGylated emulsifiers: formulation, characterization, and evaluation of their impact on skin properties ex vivo and in vivo. Int J Pharm. 2022;626:122202. https://doi.org/10.1016/j.ijpharm.2022.122202
54 Zhang Z, Lunter DJ. Confocal Raman microspectroscopy as an alternative method to investigate the extraction of lipids from stratum corneum by emulsifiers and formulations. Eur J Pharmaceutics Biopharmaceutics. 2018;127:61–71. https://doi.org/10.1016/j.ejpb.2018.02.006
55 Ananthapadmanabhan KP, Mukherjee S, Chandar P. Stratum corneum fatty acids: their critical role in preserving barrier integrity during cleansing. Int J Cosmet Sci. 2013;35(4):337–45. https://doi.org/10.1111/ics.12042

Annex 2: Presence of Different Ceramide Species Modulates Barrier Function and Structure of Stratum Corneum Lipid Membranes: Insights from Molecular Dynamics Simulations

Moritz Reuter[a], Edwin Joseph[b], Guoping Lian[b,c], Dominique Jasmin Lunter[a]

[a] Department of Pharmaceutical Technology, Faculty of Science, Eberhard Karls Universität Tübingen, Auf der Morgenstelle 8, 72076 Tuebingen, Germany

[b] Department of Chemical and Process Engineering, University of Surrey, Guildford GU27XH, U.K.

[c] Unilever R&D Colworth, Unilever, Sharnbrook MK441LQ, U.K.

Molecular Pharmaceutics

Year 2025, Volume 22, Issue 7, Pages 4280–4292
DOI: 10.1021/acs.molpharmaceut.5c00580

molecular pharmaceutics

pubs.acs.org/molecularpharmaceutics

Article

Presence of Different Ceramide Species Modulates Barrier Function and Structure of Stratum Corneum Lipid Membranes: Insights from Molecular Dynamics Simulations

Moritz Reuter, Edwin Joseph, Guoping Lian, and Dominique J. Lunter*

Cite This: *Mol. Pharmaceutics* 2025, 22, 4280−4292

Read Online

ACCESS | Metrics & More | Article Recommendations | Supporting Information

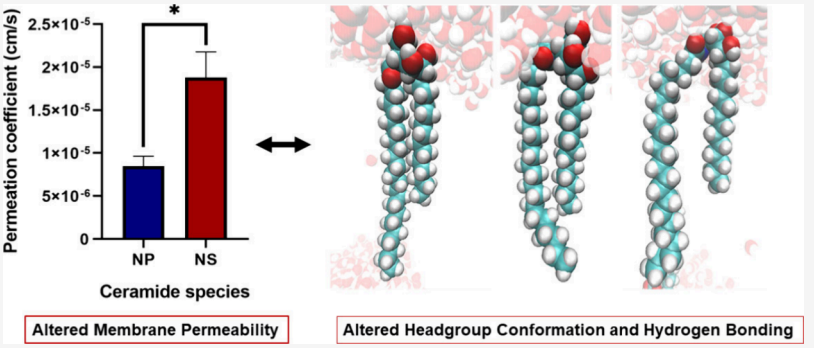

ABSTRACT: Ceramides, as major components of the human stratum corneum's (SC) lipid matrix, are considered crucial for regulating the skin's barrier function against the ingress of exogenous substances as well as to prevent water loss through the skin. Multiple clinical and experimental studies found different classes of ceramide species to affect the skin barrier nonuniformly, with some ceramides being associated with an impaired skin barrier, such as ceramide NS, while others are associated with a healthy, unimpaired skin, e.g., ceramide NP. This study investigates how the presence of these two ceramide classes in an SC lipid bilayer membrane influences the water permeability as well as the structure of the bilayer using molecular dynamics (MD) simulations. To this end, simulated membranes comprising free fatty acids, cholesterol, as well as either ceramide NS or ceramide NP were systematically compared in regard to differences in the membrane structure and water permeability, as well as to results found in the literature. The simulation found ceramide NP-containing membranes to have a significantly lower water permeability than ceramide NS-containing systems, with the permeability values of NP-based systems being almost half of those of the NS-based systems. Furthermore, the simulation also showed significant structural differences between the two systems in terms of headgroup conformation and lipid positioning in the membrane, hinting toward the molecular mechanisms underpinning the differences in permeability of the two systems. In conclusion, the MD simulation was able to reproduce effects of the presence of different ceramide species in the membrane that are consistent with experimental as well as clinical studies on skin barrier function and drug delivery and validate previous simulation-based investigations into SC lipid bilayer permeability.

KEYWORDS: *Stratum Corneum, Molecular Dynamics Simulations, Ceramides, Skin Barrier Function, Skin Permeability, Transepidermal Water Loss*

INTRODUCTION

Understanding the barrier function of the stratum corneum (SC), the uppermost layer of the skin, carries high relevance for a variety of biomedical and skin care applications, from the pathology of inflammatory skin diseases to the drug delivery of dermally applied active pharmaceutical ingredients as well as cosmetic care products.[1−4] As such, there have been an increasing number of investigations aiming to describe, model, and predict the behavior, structure, and underlying mechanisms of the skin's most vital barrier as well as its interactions with a wide range of topically applied compounds.[4−11] Integral to this barrier function of the SC is the brick-and-mortar structure, with the keratin-rich corneocytes (bricks) being embedded in a lamellar, continuous lipid matrix (mortar).[12] While the corneocytes provide a vital role in the protection against UV damage and mechanical stress, the lipid matrix guards against the ingress of xenobiotics as well as water loss

Received: April 22, 2025
Revised: June 17, 2025
Accepted: June 17, 2025
Published: June 25, 2025

from within, acting as the primary diffusion barrier of the skin.[13] The SC lipid matrix is comprised of equimolar parts of ceramides, free fatty acids (FFAs), and cholesterol,[12] forming characteristic periodic, lamellar structures, known as the short periodicity phase (SPP), which closely resembles a traditional bilayer structure, and the long periodicity phase (LPP), whose structure, depending on the exact structural model proposed, resembles a sandwiched multilayer structure.[14,15] The formation and structural characteristics of these lamellar structures have been shown to be highly dependent on the exact composition of the ceramide/FFA/cholesterol ratio, wherein a change in the ratio of the lipid components as well as the subtype of the lipid in question affect the properties of the entire system.[16−22] Higher ratios of cholesterol in the lipid composition have been associated with an increased fluidization of the bilayer system,[16] while for FFA and ceramides, pure or near-pure systems show high crystallinity and very low permeabilities in simulated systems.[23,24] Ceramides, in particular, can be further classified into families, depending on the headgroup type of the long chain base (LCB) moiety as well as the hydroxylation pattern of the fatty acid linked to the LCB.[25−27] Based on the current state of skin research, more than 16 different ceramide families have been found in human SC, with more than 1300 individual ceramide species when taking fatty acid as well as LCB chain length distribution into account.[27] Changes in the prevalence of certain lipid subtypes, especially chain lengths, have been associated with changes in the permeability in *in silico* studies investigating the effect of varying chain lengths on the fatty acid moiety of ceramides. The works by Gupta et al.[23] as well as Wang and Klauda[28] found a decrease in permeability of ceramide-containing bilayers with longer chain lengths, explained partly due to a higher membrane thickness. Critically, chain length distribution of FFA and ceramides also affects the skin barrier permeability *in vitro* and *in vivo*. Skolova et al.[29] found the permeability of SC lipid membranes to be decreasing with increasing ceramide acyl chain length, while Janssens et al.[30] as well as Ishikawa[31] and others associated shifts toward shorter ceramide acyl chain lengths as well as shorter FFA lengths in live human SC with higher skin barrier permeability, completing the picture of the permeability-decreasing effect of skin lipid chain lengths from *in silico* to *in vivo* studies. Regarding the effects of the relative prevalence of different ceramide families, this picture looks different. While in the human SC there is a wide range of ceramide families being found, with the 10 most abundant families representing over 99% of all detectable ceramides,[26] this diversity is often not reflected in MD studies. The majority of publications use the sphingosine-derived ceramide NS species in their simulated skin lipid membranes,[5,23,28,32−34] despite its actual abundance in the extracellular matrix of the human SC being quite limited, at around 5% of all ceramides in the SC lipid matrix.[25−27] On the other hand, the phytosphingosine-derived ceramide NP (depicted with ceramide NS in Figure 1) is the most abundant ceramide subgroup in the human SC lipid matrix, being more than five times as abundant as ceramide NS.[25−27] Nonetheless, studies investigating NP-containing systems are scarce in comparison to the ones involving NS-containing systems.[6,35]

From a clinical perspective, these ceramide subgroups are of special interest, as the ratio of ceramide NS to NP seems to play a vital role in the development of many skin conditions involving skin barrier impairment.[3,31,36,37] In particular, the ratio of NS to NP is shifted toward NS in inflamed or damaged skin with an impaired skin barrier, as one would find in atopic dermatitis or psoriasis patients as well as in surfactant-treated skin. Conversely, the ratio is shifted toward NP in intact and healthy skin.[2,31,36,38] Thus, this begs the question of whether there exists a mechanistic explanation for the different permeabilities of the skin barrier containing different ratios of ceramide species: Nădăban et al. published an in-depth comparison of SPP models of skin lipid mixture with ceramide ratios of 2:1 and 1:2 of NS:NP in which they found pronounced differences in the hydrogen bonding network of the two systems, while the models proved to be quite similar otherwise.[39] The group did not publish permeability data for the models, but there do exist permeability studies for SC lipid membrane models of the SPP using ceramide NP as well as NS. While most works investigated the permeability of SPP models comprising ceramide NS,[23,28,32,33,40] Lundborg et al. reported a study on the permeability of water in an SPP model comprising ceramide NP.[6] Regarding SPP models comprising ceramide NS, Piasentin et al. assembled and compared the assorted literature data regarding permeabilities of NS-containing SPP models.[33] Taking the data from Lundborg et al. as well as from Piasentin et al., one finds a permeability coefficient of 1.1×10^{-5} cm/s for NP-containing and 2.10×10^{-5} cm/s for NS-containing fully hydrated bilayers.[6,33] These data show a lower permeability of NP-containing membranes, as one would expect when hypothesizing a possible mechanistic background for the macroscopic effect of a lower skin barrier function and a higher permeability of ceramide NS-rich skin found in the clinical studies. However, a direct comparison is difficult, as the reported simulations were conducted using different methods (steered vs restrained water) as well as different force fields. While both studies based their simulations on the CHARMM36 force field, Lundborg et al.[6] modified the force field to more closely match the crystalline structure of ceramide NP, making the comparison to the values reported for NS-containing membranes reported by Piasentin et al.[33] more difficult.

Therefore, this study aims to systematically compare the two SC lipid bilayer systems containing either ceramide NS or ceramide NP as the ceramide component of the lipid mixture, using the same force field as well as the same method for determining the permeability for both systems. As such, the barrier properties are characterized as the permeability of water through the membrane using the constrained water permeation

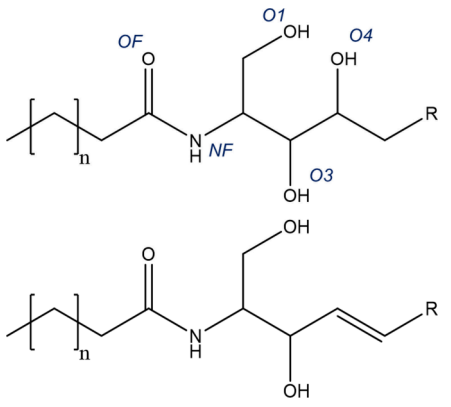

Figure 1. Comparison of the ceramide headgroup structure between ceramide NP (top) and ceramide NS (bottom). The heteroatoms of the ceramide NP structure are designated with their abbreviations used throughout the text.

https://doi.org/10.1021/acs.molpharmaceut.5c00580
Mol. Pharmaceutics 2025, 22, 4280−4292

method as published by Piasentin et al.,[33] while using the modified force field by Lundborg et al.[6] for all simulations.

Furthermore, we aim to investigate the structural and mechanistic differences between the two membrane models to gain greater insight into the effects of the presence of different ceramide species in the SC as well as to compare our findings to the literature results for *in silico* as well as experimental studies in order to further close the gap between clinical data and theoretical calculation.

MATERIALS AND METHODS

Generation of the Hydrated Bilayer Systems. To model the SC lipid matrix, hydrated bilayers of the SC lipids were constructed using a lipid ratio of FFA: Cholesterol: Ceramide at 1:1:1, wherein the FFA component is represented by lignoceric acid (C24) and the ceramide component either by ceramide NS 24:0/18:1 or by ceramide NP 24:0/18:0. The lipid bilayer membrane is surrounded on both sides with water molecules, representing a hydration level of 30 water molecules per lipid. Both constructed systems are similar to those established and studied in the literature for investigations of SC lipid membranes.[6,33] The system configurations were generated using the membrane builder[41] included in CHARMM-GUI,[42,43] comprising 75 lipids randomly distributed in each bilayer leaflet in a rectangular geometry, resulting in a system of 50 cholesterol, 50 FFA, and 50 ceramide molecules in the lipid bilayer and 4500 water molecules surrounding it.

All simulations were run in GROMACS 2023.4.[44,45] The CHARMM36 force field was modified as described by Lundborg et al.[6,46,47] and used for the main simulations. The reason for the choice of this force field over the unmodified CHARMM36[46,48] force field lies in the inclusion of ceramide NP into the simulated bilayer systems: As shown by Lundborg et al., ceramide NP is not correctly described by the unmodified CHARMM36 force field, requiring modifications to model the headgroup more accurately.[6] As such, we used the modified CHARMM36 force field, which uses the corrected headgroup geometry for ceramide NP and also adopts the applicable changes to the headgroup geometry for ceramide NS for the simulations of both systems containing the different ceramide species.[6] Nonetheless, the results of the permeability measurements using the unmodified CHARMM36 force field can be found in Supplementary Figure S2 in the Supporting Information. The water model used was CHARMM36 TIP3P.[49]

For each bilayer system containing a different ceramide species, the starting configuration underwent energy minimization and was equilibrated in two 2.5 ns simulation runs under NVT conditions, followed by a 2.5 ns and three 5 ns equilibration runs under NPT conditions, each with continuously weakening position restraints of the lipids, with the last NPT equilibration run being unconstrained, all according to the standard CHARMM-GUI protocol.[41−43] Afterward, an unconstrained simulation run under NPT conditions with a duration of 300 ns was carried out for the lipids to assume a stable configuration, and the final configuration of this run was used as a base for the permeability measurement simulations as well as the production runs for the structure analysis.

All simulations use a time step of 2 fs and three-dimensional periodic boundary conditions. Electrostatic interactions are calculated using PME,[50] while for the van der Waals interactions a cutoff at 1.2 nm with a smooth force-switch from 1 to 1.2 nm was used for calculation. H-bonds are constrained using the LINCS algorithm.[51] For equilibration as well as production simulations, temperature is set to 303.15 K using a V-rescale thermostat[52] with a time constant of 1 ps, coupled separately to lipids and water. Pressure in the systems is set to 1 bar with a semi-isotropic C-rescale barostat[53] with a time constant of 5 ps. A compressibility of $4.5 \times 1 \times 10^{-5}$ bar^{-1} is used.

Production Runs of the Equilibrated Systems. To obtain structural information about the unmodified systems without inserted water molecules, one 200 ns production run was executed for each equilibrated bilayer system using the same run parameters as the previous 300 ns NPT equilibration run. The trajectories of the production runs form the base for the calculation of the bilayer properties, hydrogen bonding values, and lipid order parameters.

Permeability Calculations Using Constrained Water Molecules. The simulations, measurement, and calculation methods using constrained molecular dynamics simulations for the permeability of the SC lipid systems are carried out according to the method described by Piasentin et al.[33] The aim of this method is to sample local ΔG as well as the diffusion coefficient D along the entire length of the transbilayer axis (z-axis), using constrained water molecules inserted into the system to obtain a profile of individual $\Delta G(z)$ and $D(z)$ values, describing the entire membrane and calculating its permeability using the inhomogeneous solubility diffusion model.

Starting from the final configuration of the unconstrained 300 ns simulation runs of the SC lipid systems, water molecules were inserted into the systems: The length of the reaction coordinate (RC), defined as the part of the z-axis to be sampled, was 9 nm. This length allows for sampling of the entire membrane as well as part of the water box surrounding it. Along the reaction coordinate, water molecules were inserted at regularly spaced intervals, "windows", of 0.1 nm, resulting in 90 equally spaced windows to sample the entire reaction coordinate. While their positions along the z-axis of the system were fixed, the positions of the inserted water molecules on the x-,y-plane were random. As to not distort the measurements by having the constrained water molecules potentially interacting with each other while also saving simulation time by not building a new configuration for every position window, the sampling was done using a total of 60 configurations each containing 6 water molecules spaced at regular intervals of 1.5 nm, ensuring no interaction of the constrained water molecules with each other as well as sampling the entire bilayer four times.[54]

Water molecules were inserted using the GROMACS tool "gmx insert-molecules" with a scaling of 0.25, meaning that the van-der-Waals radius of the inserted molecule was reduced to 25% of its original radius to insert the molecule in question for easier insertion into the system as well as a broader insertion range. To not disrupt the systems by abruptly inserting molecules into the configuration, the inserted water molecules were faded in by carrying out four sets of energy minimization/NVT/NPT simulations with a duration of 50 ps each with the electrostatics and van-der-Waals interactions gradually turning on using the coupling constant $\lambda = 0.25/0.5/075/1$, wherein $\lambda = 1$ represents regular interactions. Decoupling of the molecular interactions was accomplished by using the GROMACS functionalities for free energy calculations. The equilibration simulation runs with partially decoupled inter-

https://doi.org/10.1021/acs.molpharmaceut.5c00580
Mol. Pharmaceutics 2025, 22, 4280−4292

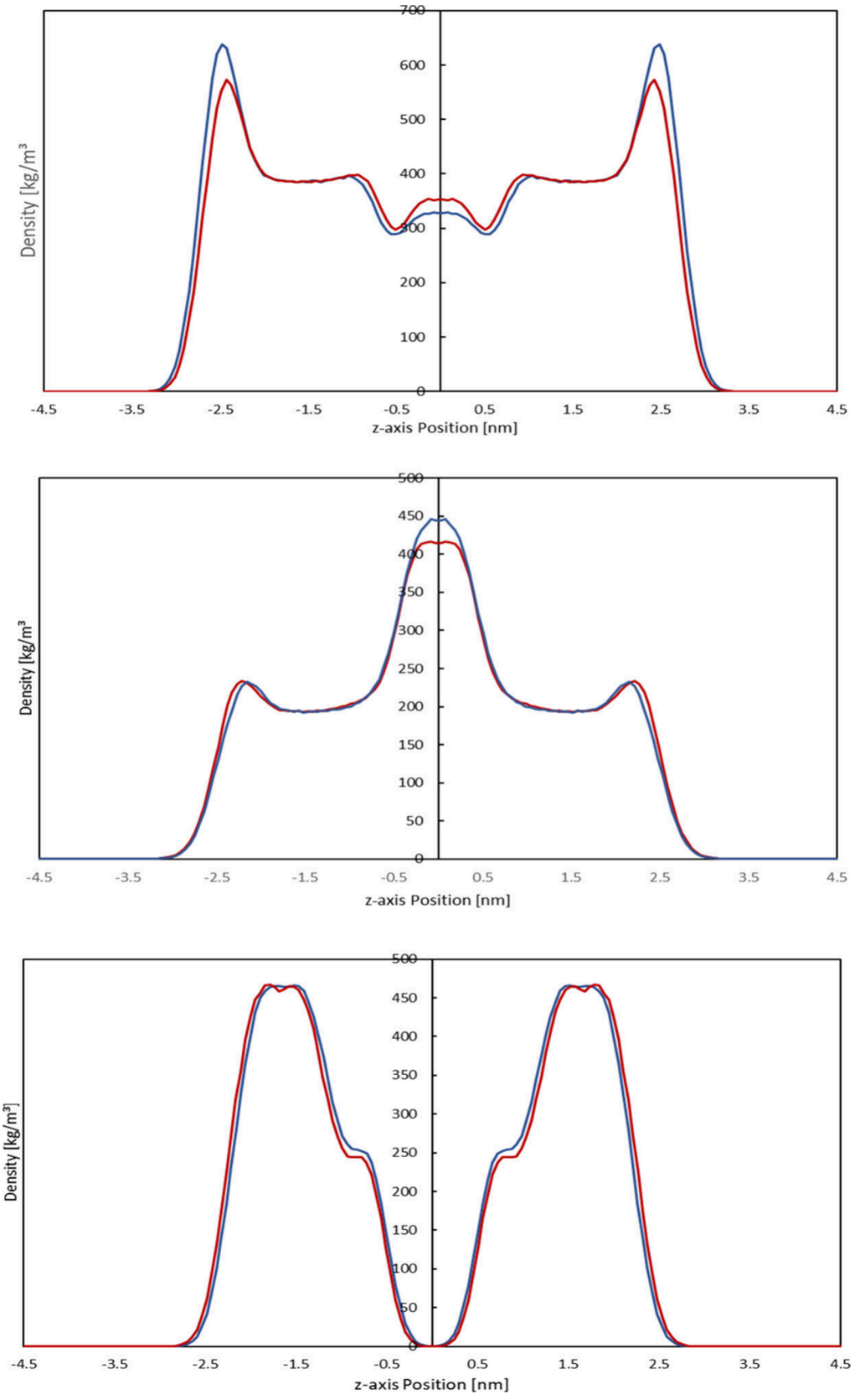

Figure 2. Comparison of the lipid density profiles for ceramides, free fatty acids, and cholesterol (from top to bottom) of SC lipid bilayers containing either ceramide NP (blue) or ceramide NS (red). In systems containing ceramide NP, cholesterol as well as free fatty acids show density peaks closer to the membrane center than in ceramide NS-containing systems, while the density peaks of ceramide NP itself are actually located more distant from the center than those of ceramide NS.

https://doi.org/10.1021/acs.molpharmaceut.5c00580
Mol. Pharmaceutics 2025, 22, 4280−4292

actions utilized a stochastic dynamics integrator and with a reduced time step of 1 fs as well as time constant for thermostat coupling of 2 ps, as recommended by the GROMACS manual. From the equilibration simulations with $\lambda = 1$ onward, the regular leapfrog integrator was used again. All inserted water molecules were constrained to a fixed z-position relative to the bilayer center, realized using the GROMACS "pull" command with the "pull-coord-type" set to "constraint". After the last 50 ps of equilibration with full interactions restored, the resulting systems then underwent a longer equilibration run of 100 ns. Following these equilibration runs, production runs started.

The production run of every 60 configurations lasted for 40 ns, during which the z-component of the force acting on the center of mass of the inserted water molecules as well as the z-position of the inserted water molecules were collected at every time step of the simulation (0.002 ps) while the coordinates of the entire system were stored in every 10 000 timesteps (20 ps).

To determine the permeability P for water across the investigated skin lipid membranes, the inhomogeneous solubility diffusion model was employed:[55−57]

$$\frac{1}{P} = \int_{-L/2}^{L/2} \frac{\exp\left[\frac{1}{RT}\Delta G(z)\right]}{D_z(z)} dz$$

In which L is the thickness of the bilayer, R is the universal gas constant, and wherein the free enthalpy of diffusion $\Delta G(z)$ as well as the diffusion coefficient in the z-direction $D_z(z)$ were calculated as follows:

ΔG was calculated using the Potential of mean constraint force (PMcF) method according to the equation

$$\Delta G(z_0) = -\int_{z_{out}}^{z_0} F(z)_t dz$$

wherein $\langle F(z)\rangle_t$ is the average of the force acting on the COM of the inserted water molecule averaged over the time of the simulation.[55,56] The force average was taken from every constrained water molecule in the set of simulations, yielding force averages along the entire RC, starting from bulk water and along the entire transmembrane axis. These values were then binned according to their 0.1 nm window along the RC, and averages as well as standard deviations and errors were calculated. ΔG was then determined via eq 1 by integration of the resulting curve using the trapezoidal rule. The error on the ΔG was derived by error propagation from the variance in the binned force average. To reduce the noise in the PMcF measurements associated with the first few nanoseconds of the run as well as to ensure robust sampling, only data from the last 20 ns of the production run was used for the permeability calculation.[10,33] To obtain the final ΔG profiles for the permeability calculation, the average force profiles over the reaction coordinate were symmetrized and then integrated to average the bilayer leaflet properties and to address membrane inhomogeneities in the sampling process.[10,33] Unsymmetrized average force profiles as well as unsymmetrized ΔG profiles can be found in the Supporting Information in Supplementary Figures S8 and S4, respectively.

D_z was calculated from the Kubo relation, using the equation

$$D_z(z_0) = \frac{(RT)^2}{\int_0^\infty \partial F(z_0.\ t) \times \partial F(z_0.0) dt}$$

in which $\delta F(z_0, t) = F(z_0, t) - \langle F(z_0)\rangle_t$ is the autocorrelation function (ACF) of the force acting on the molecule.[56,58,59]

The force ACF was obtained from the GROMACS tool "gmx analyze", from which the ACF of the first 50 ps of the simulation was determined and integrated using the trapezoidal rule. The time length of 50 ps was determined following the findings of Piasentin et al., according to whom 50 ps sufficed for a full convergence of the force ACF, especially with a force constant $k \to \infty$ with constrained simulations. All force ACFs decreased to less than 5% of their starting values and were, thus, considered converged.

The entire permeability calculation was carried out according to the PMcF/Kubo method described by Piasentin et al.[33]

Bilayer Properties Analysis. The properties of the bilayers were investigated for the validation of the method and the systems containing different ceramide species were compared. Density calculations for the investigated bilayers were performed using GROMACS' "gmx density" tool. Membrane thickness was determined from the density peak of the ceramides' amide nitrogen, and associated errors were obtained by block averaging over 6 Blocks of 50 ns of the production runs. Area per lipid (APL) measurements were calculated from the box vectors of each frame of the production runs as well as the number of lipids in each membrane fold and averaged over time, with the associated errors obtained from the oscillations around the average. Lipid order parameter S_z was determined using the GROMACS tool "gmx order" and lateral distance between ceramide chains using "gmx distance". Hydrogen bonding was analyzed using the GROMACS tool "gmx hbond".

Statistical Analysis and Visualization Tools. Statistical analysis was carried out using Graphpad Prism 8, and values were, when applicable, tested for significant differences using Student's two-sided t test. Visualizations of the simulations were prepared using VMD,[60] while graphs are prepared using Microsoft Excel and Graphpad Prism 8 as well as R Statistical Software using the package ggplot2.[61,62]

RESULTS

Bilayer Properties. Graphs comparing the lipid density profiles of the modeled systems can be found in Figure 2. The two types of bilayers show very little difference in their structural properties: The thickness of both bilayers, determined as the distance between the nitrogen atoms of the ceramide headgroups of opposing membrane leaflets, was found to be 4.96 ± 0.02 nm for NP-based bilayers as well as 4.96 ± 0.03 nm for NS-based bilayers. These results agree reasonably well with the findings of previous studies of Piasentin et al.[33] and Mistry & Notman[5] for hydrated equimolar skin lipid bilayers, who reported a membrane thickness of 4.90 ± 0.04 nm and 4.89 ± 0.04 nm, respectively. The small discrepancy between the previously published results and the slightly larger bilayer thickness found in this study can be explained by the choice of force field: While Piasentin et al. and Mistry & Notman both used the unmodified CHARMM36 force field, this study used the modified CHARMM36 force field as described by Lundborg et al., providing a modified headgroup geometry, which could

https://doi.org/10.1021/acs.molpharmaceut.5c00580
Mol. Pharmaceutics 2025, 22, 4280−4292

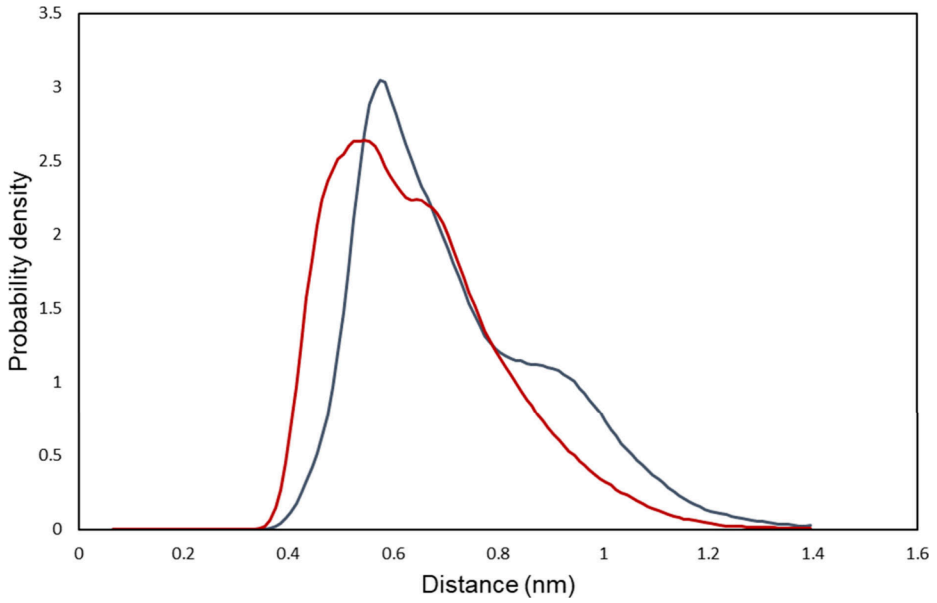

Figure 3. Probability distribution curves (smoothed) of the distance between the C16 atoms of the fatty acid and long chain base moieties of ceramide NP (blue) and NS (red). The probability distributions for the different ceramide types are distinctly different, with NP showing a higher propensity toward the posturing conformation (seen in the shoulder around 1 nm) when compared to NS, whose graph shows a shoulder much closer to the main peak of the hunched conformation, indicating a probable intermediate conformation.

affect the thickness of the systems. This was further confirmed by our finding that the unmodified CHARMM36 force field produced thinner bilayers (Supplementary Figure S6 in the Supporting Information). Nonetheless, the results obtained for the membranes in this study using the modified force field still much more closely match the other simulated results than the thickness obtained from experiments such as those reported by Školová et al.[63] and Schmitt et al.,[21] which was 5.39 nm (No error given) for an equimolar SC lipid membrane containing ceramide NS[63] and 5.41 ± 0.01 nm for an SC lipid membrane containing ceramide NP and AP,[21] differing significantly from the simulation's results, which is unfortunately characteristic for the type of lipid models investigated in this study. Similar to the membrane thickness, the area per lipid (APL) as a membrane density is very similar for both the NS- and NP-containing systems, both having an APL of 0.322 nm^2 ± 0.002 nm^2. This value corresponds well to the values found in the literature, wherein both Piasentin et al. and Mistry & Notman found an APL value of 0.325 nm^2, again using the unmodified CHARMM36 force field. Similar membrane density of the equimolar SC lipid systems was also reported by Wang and Klauda[64] for equimolar SC lipid systems containing the structurally even more different ceramide NS and ceramide AP. While the increased hydroxylation of phytosphingosine-based ceramides may pose a bigger steric hindrance to tight lipid packing in systems containing an unphysiologically high ceramide content, this effect is seemingly mitigated by an equimolar amount of lignoceric acid and cholesterol, resulting in similar APL values for both systems.

Comparing the density profiles of the systems, one notices slight differences in the locations of the density peaks: In the NP-containing bilayer system, the density curves of cholesterol as well as lignoceric acid are shifted slightly toward the membrane center, resulting in a higher density of lignoceric acid in the membrane center as the interdigitation of the lignoceric acid tails increases. Possible mechanistic explanations for this shift are derived from the hydrogen bonding pattern as well as the headgroup and tail conformations, as described in the following sections.

Lipid Order Parameters. The probability distribution of the lateral distance of the ceramide species' lipid chains grants insight into the distribution of possible headgroups as well as chain conformations of ceramides in the hairpin conformer. Wang and Klauda term the possible conformations the "hunched" and "posturing" conformation, with the hunched conformation having a characteristic peak in chain distance at around 0.5 nm, while the posturing ceramide chains are characterized by their peak at a wider distance of more than 0.8 nm.[64] The probability distributions of the C16 carbon atom's distances can be found in Figure 3. One peak with a very distinct shoulder at a higher chain separation distance is visible for the systems containing ceramide NP, indicating the presence of both a hunched as well as a posturing conformation. This contrasts to the NS-based systems, which only show a clear peak at around 0.5 nm, with a much closer shoulder at around 0.7 nm, very much favoring the hunched conformer, with the shoulder potentially constituting an intermediate conformation. Interestingly, the probability density distribution of both systems differs from the one found by Wang and Klauda, who did not find a "shoulder" in their distribution but a clear separation of the conformations' peaks in the distribution curves. We actually found the particular conformation distribution reported by Wang & Klauda[64] in the system containing ceramide NS simulated using the unmodified force field (Supplementary Figure S10), indicating that the modified force field, which, in particular, modifies the ceramide headgroup geometry, has a profound impact on the conformations adapted by the ceramides in the lipid membranes (For an illustration of the different conformations found in this study, see Figure 4).

The lipid order parameter S_z serves as an indicator for the alignment of a given carbon chain with the z-axis of the simulation box normal to the membrane. A higher S_z value indicates closer alignment with the membrane normal

https://doi.org/10.1021/acs.molpharmaceut.5c00580
Mol. Pharmaceutics 2025, 22, 4280−4292

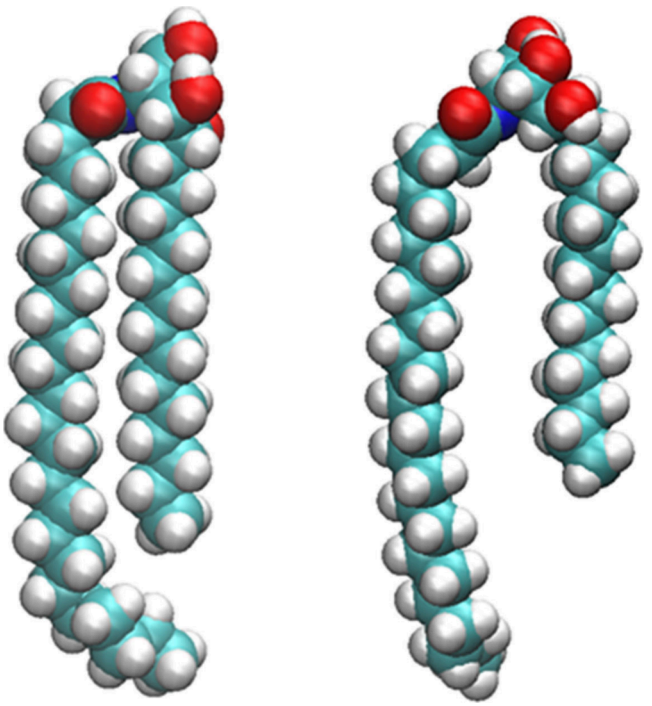

Figure 4. Isolated structures of ceramide NP molecules in either the "hunched" (left) conformation or the "posturing" conformation (right). The posturing conformation is characterized by the higher distance between the two carbon chains of the ceramide as well as the hydroxyl functional groups being rotated toward the membrane normal, therefore being able to interact to a higher degree with the molecules of the bulk water phase. (See Figure 8 and Table 1.) Additionally, due to the higher distance between the carbon chains, cholesterol molecules are able to intercalate between them and potentially hydrogen bond with the amide nitrogen, which can be seen in an increased number of hydrogen bonds between the amide of ceramide NP and cholesterol (Supplementary Table S1).

direction, implying a higher degree of lipid order. The S_z graphs for the lipid tails of the LCB and fatty acid moiety of the ceramides as well as the tail of lignoceric acid are depicted in Figure 5. For both lipid chains of the ceramides, a similar trend can be seen. While the differences are only slight in either case, the S_z values of ceramide NS show a higher degree of order closer to the headgroup-water interface with ceramide NP showing a higher degree of order toward the center of the bilayer membrane. This observation is consistent with a more prevalent posturing conformation of ceramide NP molecules. In this conformation, the carbon atoms in the lipid tails closer to the headgroup are less parallel to the membrane normal (Figure 4). Furthermore, the order parameter curve for lignoceric acid does not show the same pattern, with only a slight increase in the S_z value in the NP-containing systems toward the center of the membrane, further hinting toward a conformational difference of the simulated lipid membranes containing different ceramide species.

Hydrogen Bonding. The type and number of hydrogen bonds found in the simulated systems are provided in Table 1 and Supplementary Table S1.

The types of hydrogen bonds found in this system can roughly be classified into lipid−lipid hydrogen bonds as well as lipid−water hydrogen bonds, both of which differ between the studied membranes depending on the ceramide class occurring in the bilayer. We found that the NP-based systems show a

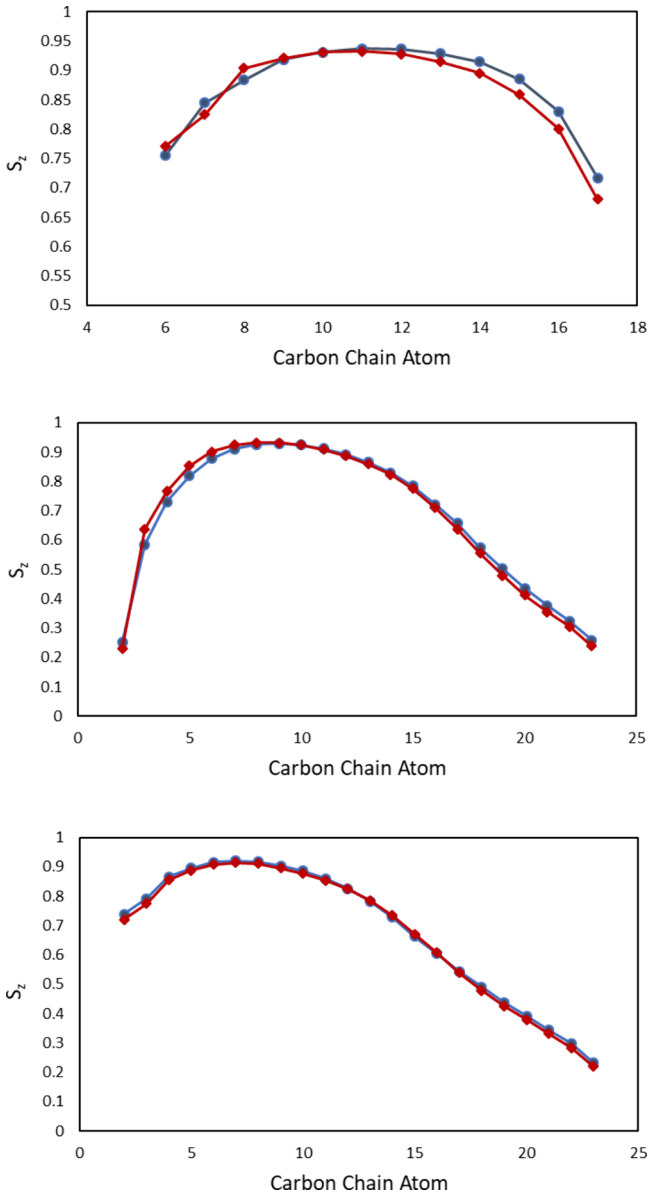

Figure 5. S_z lipid order parameter curves for carbon chains of the ceramide long chain bases, the fatty acids of the ceramides, and the free fatty acids (from top to bottom, Ceramide NP − blue, Ceramide NS − red). For the carbon chains pertaining to the ceramides, the lipid order is slightly lower for ceramide NP closer to the headgroup, while being higher closer to the membrane center. For the free fatty acids, the curves are essentially the same. Note the different scaling of the uppermost curve.

Table 1. Overview of the Hydrogen Bonds for All Lipids in the System, as well as the Ceramides, in Particular[a]

Hydrogen Bond Type	Average number of hydrogen bonds per time frame per lipid (NP/NS)
All Lipids − Water	2.637 ± 0.006/2.407 ± 0.005
All Lipids − All Lipids	0.478 ± 0.003/0.555 ± 0.002
CER − Water	4.322 ± 0.002/3.607 ± 0.002
CER − Other Lipids	1.393 ± 0.001/1.620 ± 0.001

[a]A more extensive overview of the hydrogen bonding can be found in the Supplementary Material.

https://doi.org/10.1021/acs.molpharmaceut.5c00580
Mol. Pharmaceutics 2025, 22, 4280−4292

higher degree of lipid−water hydrogen bonding and a lower degree of lipid−lipid hydrogen bonding. This is a curious result, as one would expect a higher degree of hydrogen bonding in general from the ceramide NP-based systems, given the additional hydroxyl group that it possesses over ceramide NS. A more in-depth analysis of the individual bonding molecules shows actually less hydrogen bonding of the ceramide molecules, in particular, to lipid molecules such as other ceramide as well as lignoceric acid or cholesterol molecules. In terms of lipid−lipid hydrogen bonding in general, only the hydrogen bonding of lignoceric acid with itself is slightly elevated in NP-containing systems. On the other hand, the difference in hydrogen bonding between ceramide NP and bulk water accounts roughly for the entire difference in lipid−water hydrogen bonds of the systems, with ceramide NP exhibiting a distinctively higher degree of hydrogen bonding with the water molecules outside the bilayer than ceramide NS. These results can be understood in the context of a propensity to different conformations by different ceramide species (see lipid order parameters and Figure 3): The posturing conformation is more frequently adopted by ceramide NP molecules, orienting the hydroxyl groups toward the bulk water phase (Figure 9) and facilitating lipid−water hydrogen bonding. On the other hand, the hydroxyl functions in the hunched conformation are turned toward the membrane, facilitating lipid−lipid hydrogen bonding.

Permeability, PMcF, and Diffusion Coefficient Calculations. The measured water permeability of the ceramide NP-containing bilayer is found to be significantly lower from that of the NS-containing bilayer, with the calculations for the permeation of a water molecule through the membrane returning a permeability of approximately $(0.85 \pm 0.12) \times 10^{5}$ cm/s for the NP-based SC lipid membrane and a permeability of approximately $(1.88 \pm 0.30) \times 10^{5}$ cm/s for the NS-based SC lipid membrane, as can be seen graphically in Figure 6.

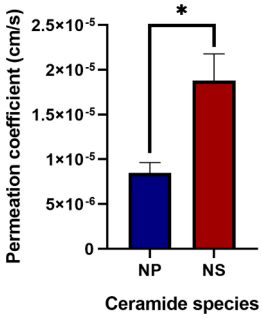

Figure 6. Bar graph of the measured permeation coefficients of the model systems. Ceramide NP-containing systems show a significantly lower permeability than ceramide NS-containing systems. Error bars indicate the standard error; an asterisk denotes a statistically significant difference with $p < 0.05$.

For further comparison, the PMcF profile is shown in Figure 7. The NP-containing bilayer's PMcF curve shows higher maxima at around 1.5 nm from the bilayer center, as well as tapering off to a higher level toward the membrane center. From this, it becomes clear that the difference in the permeability of the membranes is rooted mainly in the PMcF profile. The maxima of the PMcF most likely correspond to the ordered region of the membrane where not only the long chains of the lignoceric acid and the fatty acid moiety of the ceramides can be found but also the shorter chain of the LCBs. Interestingly, the maxima of the PMcF are shifted around 1 Å toward the membrane center in NP-containing membranes. This could be caused by the sterically more demanding additional hydroxyl group of ceramide NP shifting the region of the densest chain packing toward the membrane center, whereas the *trans*-configured double bond of ceramide NS in this place may be less obstructive to an ordered lipid packing, together with the inward shift of the lignoceric acid as well as the cholesterol density curve as seen in Figure 2.

The diffusion profiles D_z along the bilayer can be found in Figure 8 for both investigated membrane types. The diffusion coefficient profile along the membrane is very similar for both investigated systems, showing almost no significant difference between the two, which contrasts with the measured PMcF profile, which shows quite clear differences between the $\Delta G(z)$ derived from the two model systems. This indicates that the main difference in the resulting permeability values of the two systems stems from the differences in the PMcF profiles, as opposed to the D_z measurements.

DISCUSSION

The SC lipid matrix, and in particular its role as a permeation barrier for pharmaceutical ingredients, exogeneous chemicals, and endogeneous water, has been the subject of more and more theoretical investigations in terms of the underlying mechanisms and the critical molecular parameters influencing them.[5,7,10,11,23,32,65,66] While these studies yielded valuable insights into the mechanisms and effects of chemical penetration enhancers as well as the effect of varying the concentration, hydroxylation, and chain length of the SC lipids on the membrane,[11,23,32,64] studies investigating the effect of ceramide species on the permeability of SC lipid membranes are limited. We therefore investigated the effects of varying the ceramide species in SC lipid bilayers on their permeabilities by comparing SC lipid membranes comprising either ceramide NS or ceramide NP as the ceramide component of the system. We found a significantly lower water permeability of the studied ceramide NP-based membrane when compared to that of the ceramide NS-membrane, with the calculated permeability values of NS-containing membranes being almost double the permeability of NP-containing membranes. Although a direct comparison between the clinical and experimental findings and the results we obtained from the simulations is difficult, our simulation results are in qualitative agreement with previous studies investigating the effects of the ceramide NS:NP ratio on the skin barrier function in human skin as well as in experimental models:[31,36,39,67] Clinically, skin barrier impairments in inflammatory skin diseases are associated with higher levels of ceramide NS and lower levels of NP in the SC lipids and an increased transepidermal water loss (TEWL).[31,36,38] Similarly, Nădăban et al. experimentally found a significantly higher TEWL value for skin lipid models *in vitro* containing mainly ceramide NS over those models containing mainly ceramide NP. With regard to other investigations utilizing MD simulation methodology, the higher permeability of ceramide NS containing membranes is also in good agreement with previous findings: Lundborg et al.[6] reported a permeability of $(1.1 \pm 0.23) \times 10^{-5}$ cm/s for NP-containing membranes, while for NS-containing membranes, Piasentin et al.[33] reported a permeability of (2.10 ±

https://doi.org/10.1021/acs.molpharmaceut.5c00580
Mol. Pharmaceutics 2025, 22, 4280−4292

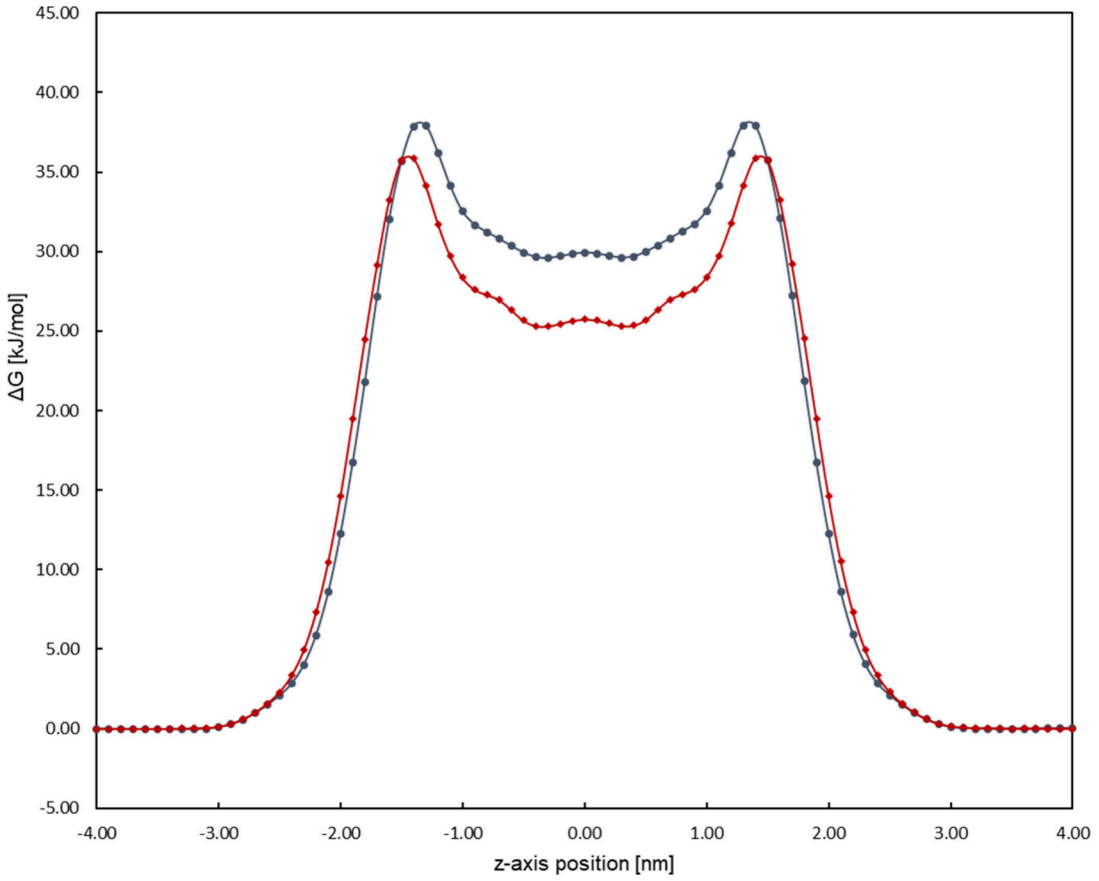

Figure 7. Symmetrized PMcF profile of the measured systems, as used for the permeability calculation. Ceramide NP (blue) shows higher values for the maximum PMcF in the area of ordered lipid tails as well as in the membrane center than ceramide NS (red). Error bars are omitted for clarity (The individual force profiles of the systems with associated error bars can be found in the Supporting Information).

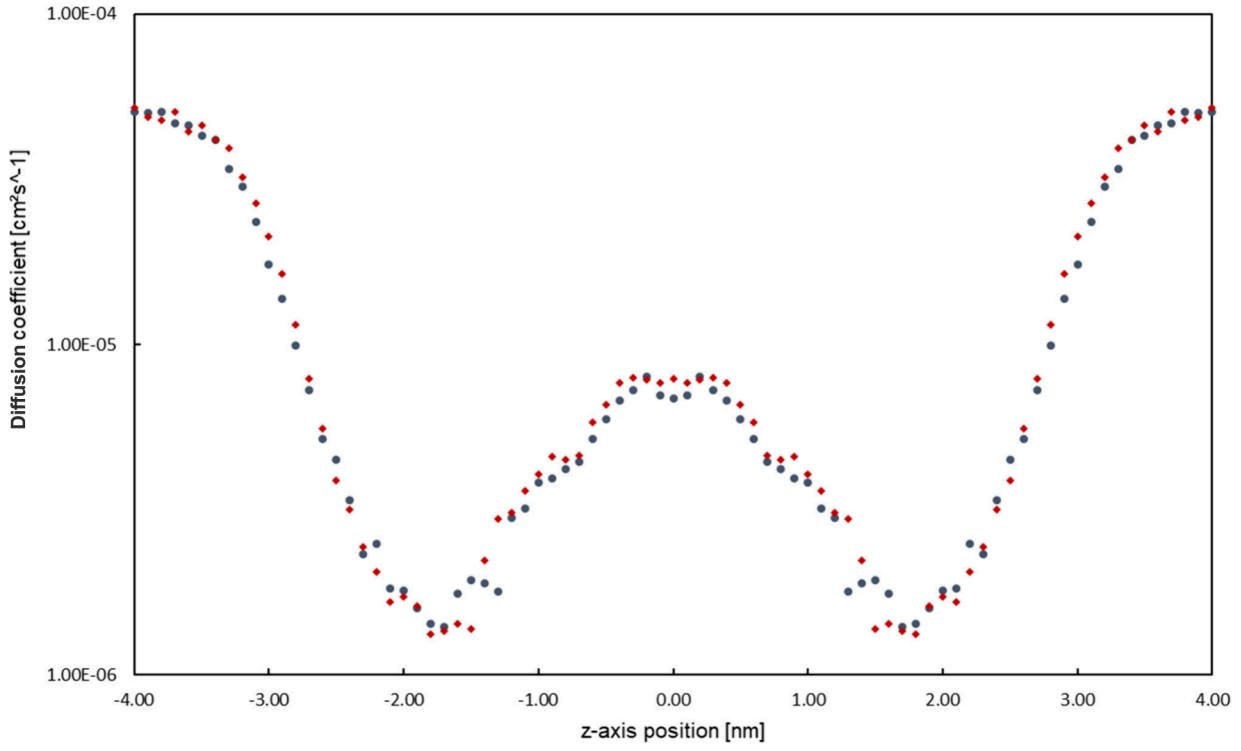

Figure 8. Symmetrized D_z profile of the measured systems (Ceramide NP − Blue and Ceramide NS − Red). Note the logarithmic scaling of the *y*-axis (Unsymmetrized profiles as well as the individual profiles with associated error bars can be found in the Supporting Information).

https://doi.org/10.1021/acs.molpharmaceut.5c00580
Mol. Pharmaceutics 2025, 22, 4280−4292

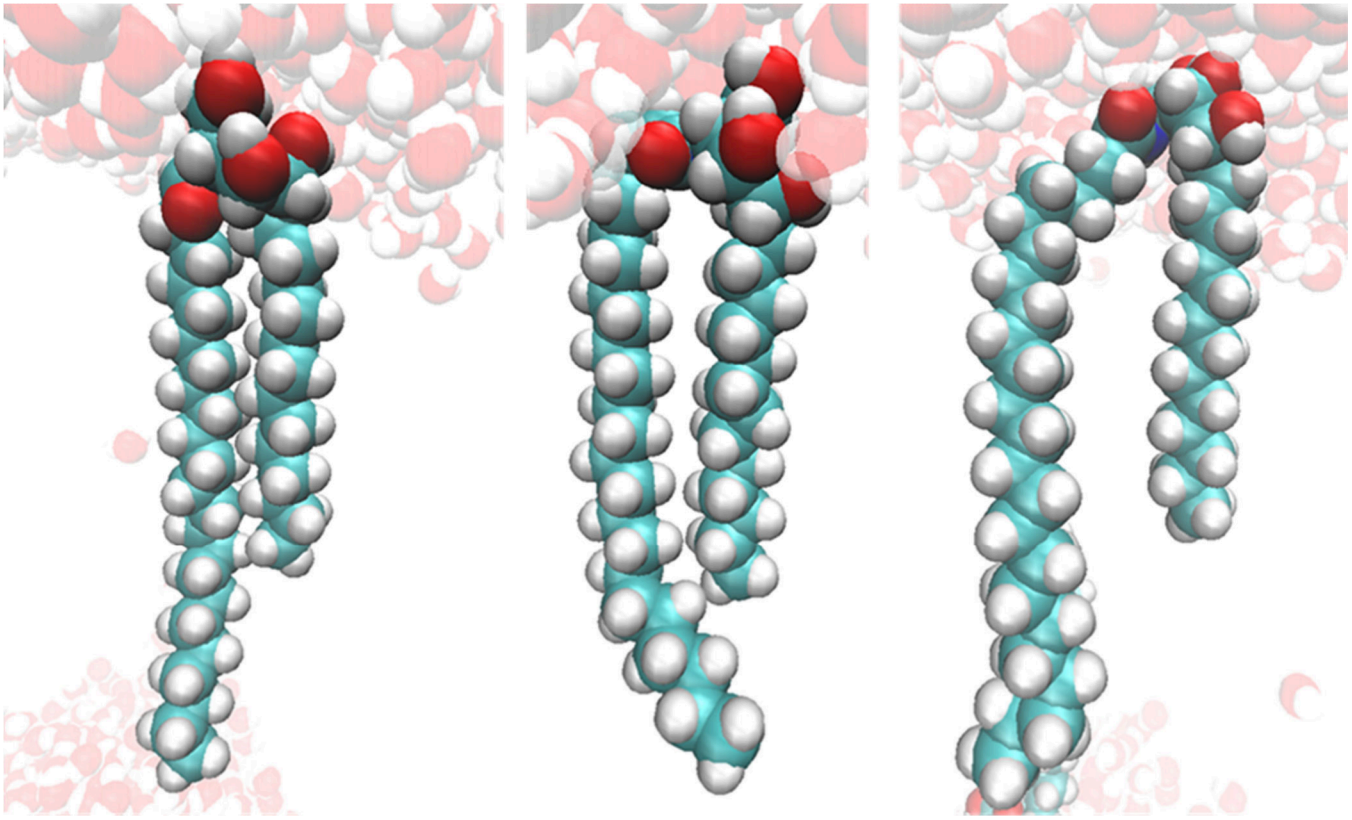

Figure 9. Snapshots of ceramide NP molecules in different conformations interacting with the bulk water phase, from the hunched conformation (left) to the posturing conformation (right), with an intermediate conformation in between. The orientation of the hydroxyl groups toward the water phases is much more pronounced in the posturing conformation, while the hunched conformation's hydroxyl groups are more oriented toward the lipid membrane.

0.39) × 10^{-5}, almost twice as high as the one found by Lundborg et al.[6]

Yet, it is important to note how this investigation differs from the mentioned works. The investigation by Lundborg et al.[6] used steered MD simulations, while in this work, we used the constrained MD simulation method described by Piasentin et al.[33] On the other hand, Piasentin et al. used the unmodified CHARMM36 force field,[46,48] whereas we used the CHARMM36 force field modified by Lundborg et al.[6] due to its more accurate representation of ceramide NP in the membrane (See the Supporting Information for a comparison using the unmodified force fields). Taking this into account, our work validates these previous findings by conducting simulations that directly compare SC lipid membranes containing ceramide NS or ceramide NP using the same force field as well as the same method of permeability measurement for both systems. As such, our results show that the difference in permeability found between these systems can indeed be explained by the choice of ceramide present in the system and not simply due to different force fields or permeability measurement methods.

Thus, the simulations reveal a structural molecular basis underpinning the experimental findings of an increase in the TEWL for ceramide NS-containing systems over ceramide NP-containing systems. The detected differences in permeability may originate from their structures. Despite both systems showing similarities in the overall membrane properties such as the lipid bilayer thickness and lipid order parameters, there still exist differences such as in the density distribution of lignoceric acid and cholesterol. In NP-containing systems, these lipids are shifted slightly toward the center by 0.5 to 1 Å, with this change in localization of lignoceric acid in particular resulting in a shift of the peak of the PMcF curves of the system. The maximum PMcF values can be found in the area of ordered lipid tails, which would be shifted together with the lipids. Note that this effect is exclusive to cholesterol and lignoceric acid: The relative positions of the ceramide headgroups actually show a slight shift away from the center. A possible explanation for the shift of the cholesterol could be the higher inclination of the NP-containing systems toward the posturing conformation as described by Wang and Klauda,[64] in which the ceramide is able to stabilize the cholesterol molecule below the headgroup in between the spaced lipid tails. This agrees with the observation of a higher degree of hydrogen bonding between the amide group and cholesterol found in NP-containing systems (Supplementary Table S1). Regarding the lignoceric acid, the additional hydroxyl group O4 of ceramide NP provides a hydrogen bonding site deeper in the membrane than the carbonyl oxygen OF and O3 of ceramide NS, therefore being able to stabilize the fatty acid closer to the membrane center (Figure 2 and Supplementary Table S1). The different conformational propensities of the systems may also explain the differences in the lipid−water hydrogen bonding: When comparing the ceramide NP molecule in the posturing and the ceramide NS molecule in the hunched conformation (Figure 5), the headgroup of the posturing conformation presents its hydroxyl and carbonyl moieties distinctively toward the membrane-water interface. The hydroxyls and carbonyls of the hunched conformation are much more shielded from the bulk water phase water and

https://doi.org/10.1021/acs.molpharmaceut.5c00580
Mol. Pharmaceutics 2025, 22, 4280−4292

oriented inward toward the other lipids of the membrane. This would of course facilitate hydrogen bonds between water and ceramides in the posturing conformation, with the hunched conformation favoring lipid−lipid hydrogen bonding with other headgroups at the membrane-water interface. Figure 9 further illustrates this by depicting ceramide NP molecules at the lipid−water interface from a hunched conformation to a posturing conformation, in the process of which the hydroxy groups of the ceramide gradually turn toward the bulk water phase, which is found to be in good agreement with the presented results.

While this hydrogen bonding pattern (more hydrogen bonds with the bulk water, less hydrogen bonds between lipids) may appear counterintuitive when one takes the permeability results into account, these findings agree with the results of the investigation of Mistry & Notman.[5] In their study into the mechanisms of permeation enhancer propylene glycol, skin lipid bilayers with a higher permeability for water in the presence of propylene glycol showed more lipid−lipid hydrogen bonding than those with a lower permeability. Furthermore, the only hydrogen bonds whose occurrence was associated with lower permeabilities were lipid−water hydrogen bonds, which mirrors our findings.

While our study was successful in illustrating the differences between SC lipid systems containing different ceramide species, one also has to note its limitations: First, while this study utilized lipid membranes comprising the SC lipids in the equimolar amount as found in human SC lipid matrix, multiple studies hint toward the fraction of cholesterol being overrepresented in simulations using equimolar amounts of lipids, as a significant portion of the cholesterol in the skin may exist in crystalline domains without mixing into the other lipids.[8,16,68] Second, this study aims primarily to compare the effects of different ceramide species in skin lipid mixtures. Thus, the total replacement of one ceramide species with the other was chosen to be able to observe potential changes more clearly as well as to better compare the results to literature values utilizing only one type of ceramide species in the skin lipid membrane. In reality, the shift from predominantly high ceramide NP concentrations to high ceramide NS concentrations in physiological and diseased stratum corneum is gradual and not absolute.[2,31,36] To add to this, other lipid species, in particular other ceramide species such as those with hydroxysphingosine or dihydrosphingosine as the LCB or alpha-hydroxylated fatty acid moieties, are present in the SC as well and not represented in this model.[3,31,36] Lastly, the simulation considered an SC lipid bilayer surrounded by a bulk water, which may only correspond to reality in the outermost layers of the SC lipids in very hydrated skin but otherwise would not be very common. While the SC in living skin is usually hydrated up to 50% of its dry weight, bulk free water domains in the intercellular regions are only present at extremely high hydration levels.[69] On the other hand, multiple studies have succeeded in modeling systems of the SPP as well as the complex LPP with lower degrees of hydration.[4,6,7,11,67] The SC lipid membranes with lower degrees of hydration show complex phenomena especially in regard to ceramide and lipid conformations in general, so a follow-up to this study using partially hydrated systems would allow for more insight into the interplay between the constituents of the SC and its barrier function.

CONCLUSION

This study investigated the influence of the type of ceramide species present in model bilayers of SC lipids on the permeability as well as the membrane structure: Utilizing constrained MD simulations, we were able to show a significantly lower water permeability of ceramide NP-containing membranes in comparison to that of ceramide NS-containing membranes. Structural investigations into the model systems revealed distinct conformational differences in the ceramide species mostly related to the different headgroups of the ceramides, which, in turn, then further changed the hydrogen bonding patterns and lipid tail conformation of the ceramides in the membrane. Our results agree well with findings from experiments as well as simulations from the literature and enable further investigations into the relation between the SC lipids and its unique diffusion barrier.

ASSOCIATED CONTENT

Supporting Information

The Supporting Information is available free of charge at https://pubs.acs.org/doi/10.1021/acs.molpharmaceut.5c00580.

Render of the bilayer membranes with inserted water molecules; Permeability comparison of systems using the modified and unmodified force fields; Detailed comparison and table of the hydrogen bonding patterns of ceramide NS and NP; APL over time for initial 300 ns runs as well as production 200 ns runs; Density graphs of the ceramide headgroup functional groups (PDF)

AUTHOR INFORMATION

Corresponding Author

Dominique J. Lunter − *Department of Pharmaceutical Technology, Faculty of Science, Eberhard Karls Universität Tübingen, 72076 Tuebingen, Germany*; Email: Dominique.Lunter@uni-tuebingen.de

Authors

Moritz Reuter − *Department of Pharmaceutical Technology, Faculty of Science, Eberhard Karls Universität Tübingen, 72076 Tuebingen, Germany*; orcid.org/0009-0009-7085-5462

Edwin Joseph − *Department of Chemical and Process Engineering, University of Surrey, Guildford GU27XH, U.K.*

Guoping Lian − *Department of Chemical and Process Engineering, University of Surrey, Guildford GU27XH, U.K.; Unilever R&D Colworth, Unilever, Sharnbrook MK441LQ, U.K.*

Complete contact information is available at: https://pubs.acs.org/10.1021/acs.molpharmaceut.5c00580

Notes

The authors declare no competing financial interest.

ACKNOWLEDGMENTS

The authors kindly thank the Boehringer Ingelheim Fonds (BIF) for supporting this project with a travel grant. The authors acknowledge support by the High Performance and Cloud Computing Group at the Zentrum für Datenverarbeitung of the University of Tübingen, the state of Baden-Württemberg through bwHPC, and the German Research Foundation (DFG) through grant no INST 37/935-1 FUGG.

■ ABBREVIATIONS

APL, area per lipid; SC, stratum corneum; PMcF, potential of mean constraint force; COM, center of mass; ACF, autocorrelation function, SPP, short periodicity phase; LPP, long periodicity phase; FFA, free fatty acids; LCB, long-chained base; TEWL, transepidermal water loss; RC, reaction coordinate; NVT, Constant Number, Volume, Temperature; NPT, Constant Number, Pressure, Temperature

■ REFERENCES

(1) van Smeden, J.; Janssens, M.; Kaye, E. C. J.; Caspers, P. J.; Lavrijsen, A. P.; Vreeken, R. J.; et al. The importance of free fatty acid chain length for the skin barrier function in atopic eczema patients. *Experimental Dermatology.* **2014**, *23* (1), 45−52.

(2) Sho, Y.; Sakai, T.; Sato, T.; Sonezaki, M.; Taima, H.; Taguchi, H.; et al. Stratum Corneum Ceramide Profiles Provide Reliable Indicators of Remission and Potential Flares in Atopic Dermatitis. *Journal of Investigative Dermatology.* **2022**, *142* (12), 3184−91.

(3) Rousel, J.; Năděban, A.; Saghari, M.; Pagan, L.; Zhuparris, A.; Theelen, B.; et al. Lesional skin of seborrheic dermatitis patients is characterized by skin barrier dysfunction and correlating alterations in the stratum corneum ceramide composition. *Experimental Dermatology.* **2024**, *33* (1), No. e14952.

(4) Wennberg, C.; Lundborg, M.; Lindahl, E.; Norlén, L. Understanding Drug Skin Permeation Enhancers Using Molecular Dynamics Simulations. *J. Chem. Inf Model.* **2023**, *63* (15), 4900−11.

(5) Mistry, J.; Notman, R. Mechanisms of the Drug Penetration Enhancer Propylene Glycol Interacting with Skin Lipid Membranes. *J. Phys. Chem. B* **2024**, *128* (16), 3885−97.

(6) Lundborg, M.; Narangifard, A.; Wennberg, C. L.; Lindahl, E.; Daneholt, B.; Norlén, L. Human skin barrier structure and function analyzed by cryo-EM and molecular dynamics simulation. *Journal of Structural Biology.* **2018**, *203* (2), 149−61.

(7) Piasentin, N.; Lian, G.; Cai, Q. In Silico Prediction of Stratum Corneum Partition Coefficients via COSMOmic and Molecular Dynamics Simulations. *J. Phys. Chem. B* **2023**, *127* (12), 2719−28.

(8) Shamaprasad, P.; Năděban, A.; Iacovella, C. R.; Gooris, G. S.; Bunge, A. L.; Bouwstra, J. A.; et al. The phase behavior of skin-barrier lipids: A combined approach of experiments and simulations. *Biophys. J.* **2024**, *123* (18), 3188−204.

(9) Lundborg, M.; Wennberg, C. L.; Narangifard, A.; Lindahl, E.; Norlén, L. Predicting drug permeability through skin using molecular dynamics simulation. *J. Controlled Release* **2018**, *283*, 269−79.

(10) Thomas, R.; Prabhakar, P. R.; Tobias, D. J.; von Domaros, M. Insights into Dermal Permeation of Skin Oil Oxidation Products from Enhanced Sampling Molecular Dynamics Simulation. *J. Phys. Chem. B* **2025**, *129* (6), 1784−94.

(11) Altun, D.; Larsson, P.; Bergström, C. A. S.; Hossain, S. Molecular dynamics simulations of lipid composition and its impact on structural and dynamic properties of skin membrane. *Chemistry and Physics of Lipids.* **2024**, *265*, 105448.

(12) Weerheim, A.; Ponec, M. Determination of stratum corneum lipid profile by tape stripping in combination with high-performance thin-layer chromatography. *Arch Dermatol Res.* **2001**, *293* (4), 191−9.

(13) Elias, P. M. Stratum corneum defensive functions: an integrated view. *J. Invest Dermatol.* **2005**, *125* (2), 183−200.

(14) Shamaprasad, P.; Frame, C. O.; Moore, T. C.; Yang, A.; Iacovella, C. R.; Bouwstra, J. A.; et al. Using molecular simulation to understand the skin barrier. *Prog. Lipid Res.* **2022**, *88*, 101184.

(15) van Smeden, J.; Janssens, M.; Gooris, G. S.; Bouwstra, J. A. The important role of stratum corneum lipids for the cutaneous barrier function. *Biochim. Biophys. Acta* **2014**, *1841* (3), 295−313.

(16) Mojumdar, E. H.; Gooris, G. S.; Bouwstra, J. A. Phase behavior of skin lipid mixtures: the effect of cholesterol on lipid organization. *Soft Matter.* **2015**, *11* (21), 4326−36.

(17) Mojumdar, E. H.; Kariman, Z.; van Kerckhove, L.; Gooris, G. S.; Bouwstra, J. A. The role of ceramide chain length distribution on the barrier properties of the skin lipid membranes. *Biochim. Biophys. Acta* **2014**, *1838* (10), 2473−83.

(18) Uche, L. E.; Gooris, G. S.; Bouwstra, J. A.; Beddoes, C. M. Increased Levels of Short-Chain Ceramides Modify the Lipid Organization and Reduce the Lipid Barrier of Skin Model Membranes. *Langmuir.* **2021**, *37* (31), 9478−89.

(19) Uche, L. E.; Gooris, G. S.; Bouwstra, J. A.; Beddoes, C. M. High concentration of the ester-linked ω-hydroxy ceramide increases the permeability in skin lipid model membranes. *Biochimica et Biophysica Acta (BBA) - Biomembranes.* **2021**, *1863* (1), 183487.

(20) Badhe, Y.; Schmitt, T.; Gupta, R.; Rai, B.; Neubert, R. H. H. Investigating the nanostructure of a CER[NP]/CER[AP]-based stratum corneum lipid matrix model: A combined neutron diffraction & molecular dynamics simulations approach. *Biochimica et Biophysica Acta (BBA) - Biomembranes.* **2022**, *1864* (10), 184007.

(21) Schmitt, T.; Lange, S.; Dobner, B.; Sonnenberger, S.; Hauß, T.; Neubert, R. H. H. Investigation of a CER[NP]- and [AP]-Based Stratum Corneum Modeling Membrane System: Using Specifically Deuterated CER Together with a Neutron Diffraction Approach. *Langmuir.* **2018**, *34* (4), 1742−9.

(22) Schmitt, T.; Lange, S.; Sonnenberger, S.; Dobner, B.; Demé, B.; Langner, A.; et al. The long periodicity phase (LPP) controversy part I: The influence of a natural-like ratio of the CER[EOS] analogue [EOS]-br in a CER[NP]/[AP] based stratum corneum modelling system: A neutron diffraction study. *Biochimica et Biophysica Acta (BBA) - Biomembranes.* **2019**, *1861* (1), 306−15.

(23) Gupta, R.; Dwadasi, B. S.; Rai, B. Molecular Dynamics Simulation of Skin Lipids: Effect of Ceramide Chain Lengths on Bilayer Properties. *J. Phys. Chem. B* **2016**, *120* (49), 12536−46.

(24) Gupta, R.; Rai, B. Molecular Dynamics Simulation Study of Skin Lipids: Effects of the Molar Ratio of Individual Components over a Wide Temperature Range. *J. Phys. Chem. B* **2015**, *119* (35), 11643−55.

(25) van Smeden, J.; Boiten, W. A.; Hankemeier, T.; Rissmann, R.; Bouwstra, J. A.; Vreeken, R. J. Combined LC/MS-platform for analysis of all major stratum corneum lipids, and the profiling of skin substitutes. *Biochim. Biophys. Acta* **2014**, *1841* (1), 70−9.

(26) Kawana, M.; Miyamoto, M.; Ohno, Y.; Kihara, A. Comparative profiling and comprehensive quantification of stratum corneum ceramides in humans and mice by LC/MS/MS. *J. Lipid Res.* **2020**, *61* (6), 884−95.

(27) Suzuki, M.; Ohno, Y.; Kihara, A. Whole picture of human stratum corneum ceramides, including the chain-length diversity of long-chain bases. *J. Lipid Res.* **2022**, *63* (7), 100235.

(28) Wang, E.; Klauda, J. B. Structure and Permeability of Ceramide Bilayers and Multilayers. *J. Phys. Chem. B* **2019**, *123* (11), 2525−35.

(29) Školová, B.; Janůšová, B.; Zbytovská, J.; Gooris, G.; Bouwstra, J.; Slepička, P.; et al. Ceramides in the Skin Lipid Membranes: Length Matters. *Langmuir.* **2013**, *29* (50), 15624−33.

(30) Janssens, M.; van Smeden, J.; Gooris, G. S.; Bras, W.; Portale, G.; Caspers, P. J.; et al. Increase in short-chain ceramides correlates with an altered lipid organization and decreased barrier function in atopic eczema patients [S]. *J. Lipid Res.* **2012**, *53* (12), 2755−66.

(31) Ishikawa, J.; Narita, H.; Kondo, N.; Hotta, M.; Takagi, Y.; Masukawa, Y.; et al. Changes in the ceramide profile of atopic dermatitis patients. *Journal of Investigative Dermatology.* **2010**, *130* (10), 2511.

(32) Das, C.; Olmsted, P. D.; Noro, M. G. Water permeation through stratum corneum lipid bilayers from atomistic simulations. *Soft Matter.* **2009**, *5* (22), 4549−55.

(33) Piasentin, N.; Lian, G.; Cai, Q. Evaluation of Constrained and Restrained Molecular Dynamics Simulation Methods for Predicting Skin Lipid Permeability. *ACS Omega.* **2021**, *6* (51), 35363−74.

(34) Shamaprasad, P.; Moore, T. C.; Xia, D.; Iacovella, C. R.; Bunge, A. L.; MCabe, C. Multiscale Simulation of Ternary Stratum Corneum Lipid Mixtures: Effects of Cholesterol Composition. *Langmuir.* **2022**, *38* (24), 7496−7511.

(35) Rivero, N.; Daza, M. C.; Doerr, M. Effect of the CER-[NP]:CER[AP] a ratio on the structure of a stratum corneum model

https://doi.org/10.1021/acs.molpharmaceut.5c00580
Mol. Pharmaceutics 2025, 22, 4280−4292

lipid matrix - a molecular dynamics study. *Chemistry and Physics of Lipids.* **2023**, *250*, 105259.
(36) Yokose, U.; Ishikawa, J.; Morokuma, Y.; Naoe, A.; Inoue, Y.; Yasuda, Y.; et al. The ceramide [NP]/[NS] ratio in the stratum corneum is a potential marker for skin properties and epidermal differentiation. *BMC Dermatology.* **2020**, *20* (1), 6.
(37) Uche, L. E.; Gooris, G. S.; Beddoes, C. M.; Bouwstra, J. A. New insight into phase behavior and permeability of skin lipid models based on sphingosine and phytosphingosine ceramides. *Biochim Biophys Acta Biomembr.* **2019**, *1861* (7), 1317−28.
(38) Reuter, M.; Schoenfelder, H.; Gaiser, A.; Volc, S.; Lunter, D. Emulsifier-induced changes to the human skin barrier − Connection to ceramide profiles and assessment as a skin lesion model. *Skin Pharmacology and Physiology.* **2025**, 1.
(39) Nădăban, A.; Frame, C. O.; El Yachioui, D.; Gooris, G. S.; Dalgliesh, R. M.; Malfois, M.; et al. The Sphingosine and Phytosphingosine Ceramide Ratio in Lipid Models Forming the Short Periodicity Phase: An Experimental and Molecular Simulation Study. *Langmuir.* **2024**, *40*, 13794.
(40) Gupta, R.; Sridhar, D. B.; Rai, B. Molecular Dynamics Simulation Study of Permeation of Molecules through Skin Lipid Bilayer. *J. Phys. Chem. B* **2016**, *120* (34), 8987−96.
(41) Wu, E. L.; Cheng, X.; Jo, S.; Rui, H.; Song, K. C.; Dávila-Contreras, E. M.; et al. CHARMM-GUI Membrane Builder toward realistic biological membrane simulations. *J. Comput. Chem.* **2014**, *35* (27), 1997−2004.
(42) Jo, S.; Kim, T.; Iyer, V. G.; Im, W. CHARMM-GUI: a web-based graphical user interface for CHARMM. *J. Comput. Chem.* **2008**, *29* (11), 1859−65.
(43) Lee, J.; Cheng, X.; Swails, J. M.; Yeom, M. S.; Eastman, P. K.; Lemkul, J. A.; et al. CHARMM-GUI Input Generator for NAMD GROMACS AMBER, OpenMM, and CHARMM/OpenMM Simulations Using the CHARMM36 Additive Force Field. *J. Chem. Theory Comput.* **2016**, *12* (1), 405−13.
(44) Abraham, M. J.; Murtola, T.; Schulz, R.; Páll, S.; Smith, J. C.; Hess, B.; et al. GROMACS: High performance molecular simulations through multi-level parallelism from laptops to supercomputers. *SoftwareX.* **2015**, *1*−*2*, 19−25.
(45) Pronk, S.; Páll, S.; Schulz, R.; Larsson, P.; Bjelkmar, P.; Apostolov, R.; et al. GROMACS 4.5: a high-throughput and highly parallel open source molecular simulation toolkit. *Bioinformatics.* **2013**, *29* (7), 845−54.
(46) Venable, R. M.; Sodt, A. J.; Rogaski, B.; Rui, H.; Hatcher, E.; MacKerell, A. D., Jr.; et al. CHARMM all-atom additive force field for sphingomyelin: elucidation of hydrogen bonding and of positive curvature. *Biophys. J.* **2014**, *107* (1), 134−45.
(47) Huang, J.; Rauscher, S.; Nawrocki, G.; Ran, T.; Feig, M.; de Groot, B. L.; et al. CHARMM36m: an improved force field for folded and intrinsically disordered proteins. *Nat. Methods.* **2017**, *14* (1), 71−3.
(48) Klauda, J. B.; Venable, R. M.; Freites, J. A.; O'Connor, J. W.; Tobias, D. J.; Mondragon-Ramirez, C.; et al. Update of the CHARMM All-Atom Additive Force Field for Lipids: Validation on Six Lipid Types. *J. Phys. Chem. B* **2010**, *114* (23), 7830−43.
(49) MacKerell, A. D., Jr.; Bashford, D.; Bellott, M.; Dunbrack, R. L., Jr.; Evanseck, J. D.; Field, M. J.; et al. All-Atom Empirical Potential for Molecular Modeling and Dynamics Studies of Proteins. *J. Phys. Chem. B* **1998**, *102* (18), 3586−616.
(50) Darden, T.; York, D.; Pedersen, L. Particle mesh Ewald: An N·log(N) method for Ewald sums in large systems. *Journal of Chemical Physics.* **1993**, *98* (12), 10089−92.
(51) Hess, B.; Bekker, H.; Berendsen, H. J. C.; Fraaije, J. G. E. M. LINCS: A linear constraint solver for molecular simulations. *J. Comput. Chem.* **1997**, *18* (12), 1463−1472.
(52) Bussi, G.; Donadio, D.; Parrinello, M. Canonical sampling through velocity rescaling. *J. Chem. Phys.* **2007**, *126* (1), 014101.
(53) Bernetti, M.; Bussi, G. Pressure control using stochastic cell rescaling. *J. Chem. Phys.* **2020**, *153* (11), 114107.
(54) Lee, C. T.; Comer, J.; Herndon, C.; Leung, N.; Pavlova, A.; Swift, R. V.; et al. Simulation-Based Approaches for Determining Membrane Permeability of Small Compounds. *Journal of Chemical Information and Modeling.* **2016**, *56* (4), 721−33.
(55) Berendsen, H. J. C.; Marrink, S.-J. Molecular dynamics of water transport through membranes: Water from solvent to solute. *Pure Appl. Chem.* **1993**, *65* (12), 2513−20.
(56) Marrink, S.-J.; Berendsen, H. J. C. Simulation of water transport through a lipid membrane. *Journal of Physical Chemistry.* **1994**, *98* (15), 4155−68.
(57) Diamond, J. M.; Katz, Y. Interpretation of nonelectrolyte partition coefficients between dimyristoyl lecithin and water. *J. Membr. Biol.* **1974**, *17* (2), 121−54.
(58) Kubo, R. The fluctuation-dissipation theorem. *Rep. Prog. Phys.* **1966**, *29* (1), 255.
(59) Marrink, S. J.; Berendsen, H. J. C. Permeation Process of Small Molecules across Lipid Membranes Studied by Molecular Dynamics Simulations. *Journal of Physical Chemistry.* **1996**, *100* (41), 16729−38.
(60) Humphrey, W.; Dalke, A.; Schulten, K. VMD: visual molecular dynamics. *J. Mol. Graph.* **1996**, *14* (1), 33−8.
(61) Wickham, H. *ggplot2: Elegant Graphics for Data Analysis*; Springer-Verlag: New York, 2016. DOI: 10.1007/978-3-319-24277-4
(62) R Core Team R: A Language and Environment for Statistical Computing. *R Project*; R Foundation, **2023**.
(63) Školová, B.; Kováčik, A.; Tesař, O.; Opálka, L.; Vávrová, K. Phytosphingosine, sphingosine and dihydrosphingosine ceramides in model skin lipid membranes: permeability and biophysics. *Biochimica et Biophysica Acta (BBA) - Biomembranes.* **2017**, *1859* (5), 824−34.
(64) Wang, E.; Klauda, J. B. Models for the Stratum Corneum Lipid Matrix: Effects of Ceramide Concentration, Ceramide Hydroxylation, and Free Fatty Acid Protonation. *J. Phys. Chem. B* **2018**, *122* (50), 11996−2008.
(65) Del Regno, A.; Notman, R. Permeation pathways through lateral domains in model membranes of skin lipids. *Phys. Chem. Chem. Phys.* **2018**, *20* (4), 2162−74.
(66) Notman, R.; Anwar, J. Breaching the skin barrier — Insights from molecular simulation of model membranes. *Adv. Drug Delivery Rev.* **2013**, *65* (2), 237−50.
(67) Nădăban, A.; Rousel, J.; El Yachioui, D.; Gooris, G. S.; Beddoes, C. M.; Dalgliesh, R. M.; et al. Effect of sphingosine and phytosphingosine ceramide ratio on lipid arrangement and barrier function in skin lipid models. *J. Lipid Res.* **2023**, *64* (8), 100400.
(68) Mojumdar, E. H.; Groen, D.; Gooris, G. S.; Barlow, D. J.; Lawrence, M. J.; Deme, B.; et al. Localization of Cholesterol and Fatty Acid in a Model Lipid Membrane: A Neutron Diffraction Approach. *Biophys. J.* **2013**, *105* (4), 911−8.
(69) Bouwstra, J. A.; de Graaff, A.; Gooris, G. S.; Nijsse, J.; Wiechers, J. W.; van Aelst, A. C. Water Distribution and Related Morphology in Human Stratum Corneum at Different Hydration Levels. *Journal of Investigative Dermatology.* **2003**, *120* (5), 750−8.